MODELING AND ANALYSIS OF ASYNCHRONIZED INTERFERENCE IN WIRELESS NETWORKS

Sam Darshi

MODELING AND ANALYSIS OF ASYNCHRONIZED INTERFERENCE IN WIRELESS NETWORKS

A

Thesis Submitted

in Partial Fulfilment of the Requirements

for the Degree of

DOCTOR OF PHILOSOPHY

by

Sam Darshi

Department of Electronics and Electrical Engineering
Indian Institute of Technology Guwahati
Guwahati - 781 039, INDIA.
August, 2015

To my grand mother and parents...

Certificate

This is to certify that the thesis entitled "**MODELING AND ANALYSIS OF ASYNCHRONIZED INTERFERENCE IN WIRELESS NETWORKS**", submitted by **Sam Darshi** (09610203), a research scholar in the *Department of Electronics & Electrical Engineering, Indian Institute of Technology Guwahati*, for the award of the degree of **Doctor of Philosophy**, has been carried out by him under my supervision and guidance. The thesis has fulfilled all requirements as per the regulations of the institute and in my opinion has reached the standard needed for submission. The results embodied in this thesis have not been submitted to any other University or Institute for the award of any degree or diploma.

Prof. Ratnajit Bhattacharjee
Deptt. of Electronics & Electrical Engg.
Indian Institute of Technology Guwahati
Guwahati - 781039, Assam, India.

Acknowledgements

First and foremost, I feel it as a great privilege in expressing my deepest and most sincere gratitude to my supervisor *Prof. Ratnajit Bhattacharjee*, for his excellent guidance. His kindness, dedication, friendly accessibility and attention to details have been a great inspiration to me. My heartfelt thanks to my supervisor for the unlimited support and patience shown to me. His constant emphasis on clear communication helped me a lot. He has enriched my life in many significant ways. I thank him from the bottom of my heart for always being there with me during all kinds of distress.

I would like to thank my present doctoral committee members: Prof. S. Nandi, Dr. Tony Jacob, and Dr. B.K. Rai for sparing time out of their busy schedule to evaluate my progress and enrich this work with their invaluable suggestions and feedbacks. I would also like to thank some of previously associated members of my committee: Prof. A. Mahanta, Dr. A. Mitra and Dr. P.R. Sahu for their significant suggestions. I would like to thank other faculty members for helping me with my research work in innumerable ways.

My special thanks to Mr. Sanjib Das, Mr. Utpal and Mrs. Jharna to extend their untiring help and support for various activities. I thank to Mr. Nanu A. Kachari, Mr. Bhriguraj Borah and Mr. Raktajit Pathak from CSE department for maintaining an excellent computing facility and providing various resources useful for the research work. I would also like to thank everyone in High Frequency Lab, Image & Signal Processing Lab and Communication Lab-I, II who made these years really enjoyable.

I am really fortunate to find (now Dr.) Samar Shailendra accepting my friendship. I enjoyed all my discussions, technical as well as non-technical with him. His personality and unique skills were a great help to me during my research phase. Our many discussions, often at the expense of his time, let me to better ideas and corrected problems. I cherish our continuing friendship. One more person I would like to mention here is Mr. Sumit agarawal. His positive approaches towards any problem inspired me a lot.

I have no words to express my thanks to some important friends especially, Gaurav, Anurag, (now Dr.) Syantan and Mr. Ramesh mishra. My work in this place definitely would not be possible without their love and care that helped me to enjoy my stay in IIT Guwahati, the place where I

lived for almost six long years and the place which I love and call my second home.

I thank all my fellow research scholars for their co-operation. During these years at IITG, I have had several friends that have helped me in several ways, I would like to say a big thank you to all of them for their friendship and support.

I also extend my thanks to the staff of EEE office and Academic Office for helping me out with all sorts of academic activities during my stay at IITG. Last but not the least, I thank everyone who have made my stay here wonderful and memorable.

My deepest gratitude goes to my family for their continuous love and support throughout my studies. The opportunities that they have given me and their unlimited sacrifices are the reasons where I am and what I have accomplished so far.

Finally, I believe this research experience will greatly benefit my career in the future.

(Sam Darshi)

Abstract

This research deals with various aspects of modeling and analysis of asynchronized co-channel interference in wireless networks. We investigate infrastructure-less networks which is assumed to have negligible co-ordination among nodes and infrastructured networks with some practical constraints. The absence of co-ordination and presence of practical constraints in frequency reuse scenarios make the interference asynchronous in nature. In this work, we model the asynchronous co-channel interference and analyze its effects on different system performance parameters. The analytical insight helps a system designer to set-up the network in an environment where interference is present, while maintaining the desired Quality of Service.

We propose two models for quantifying the asynchronous interference in un-coordinated wireless networks. First model is to calculate the effective overlap experienced by a bit of the desired frame due to interfering frames. Then, by introducing an energy based metric EINR and with the help of the proposed model, we calculate the outage probability of the network node at the bit level in the presence of asynchronous interference.

Second model is an amplitude based model which gives the index and overlap of bit(s) of interfering frames. Using this model, bit error rate has been calculated for a network node having interference as the bottle-neck. This bit error rate analysis takes sign of the bit of interfering frame into account. The probability density function of fractional overlap variable and amplitude of effective interference have also been derived. Effect of interference range on performance of network node has also been investigated.

We have also discussed interference management strategies in heterogeneous wireless networks which comprise of femtocells operating within the coverage area of a cellular base station. For asynchronous interference management in such networks, an optimum subband selection method has been proposed, taking some practical constraint into account.

Contents

List of Figures

List of Tables

Glossary

EINR	signal Energy to Interference energy plus Noise spectral density ratio Ratio
SINR	Signal Power to Interference power plus Noise Ratio
AWGN	Additive White Gaussian Noise
MAC	Medium Access Control
PDF	Probability Density Function
CDF	Cumulative Distribution Function
QoS	Quality of Service
CCI	Co-channel Interference
ACI	Adjacent Channel Interference
PLP	Power Law Propagation
GMM	Generalized Moment Matching
CSI	Channel State Information
BER	Bit Error Rate
ABER	Average Bit Error Rate
$ABER_N$	Average Bit Error Rate with noise considered
ABSR	Average Bit Success Rate
AOPNN	Average Outage Probability of Network per Node
AIVS	Average Interference Variance Sum
BPSK	Binary Phase Shift Keying
i.i.d.	Independent and Identically Distributed
i.n.i.d.	Independent and Non-Identically Distributed
CLT	Central Limit Theorem
TS	Timing Synchronization
TO	Timing Offset

List of Publications

Journal Publications

1. S. Darshi and R. Bhattacharjee, "Outage analysis of asynchronized wireless networks in interference limited environment," *Vehicular Technol. IEEE Transaction on*, vol. 62, Issue 8, pp. 3863-3874, Oct. 2013.

2. S. Darshi and R. Bhattacharjee, "BER Analysis of Asynchronised Wireless Network in Presence of Non-Identically Distributed Interferers, "in *Wireless Personal Communication, Springer*, Vol. 82, Issue 4, pp. 2583-2600, June 2015.

International Conferences

1. S. Darshi and R. Bhattacharjee, "Interference Analysis of Subband Allocation for Femtocells in Fractional Frequency Reuse Based OFDMA Networks, "in *International Conference on Signal Processing and Communications (SPCOM)*, pp. 1-6, July 2014.

2. S. Darshi and R. Bhattacharjee, "Subband Allocation for Femtocells in Presence of Asynchronous Interference in Fractional Frequency Reuse Based OFDMA Networks,"in *IEEE TENCON*, pp. 1-6, October 2014.

1

Introduction

Contents

Wireless communication has seen an unprecedented growth in recent years. Spectrum available currently for wireless services is limited as the technologies to utilize the huge spectrum available at higher frequencies are not yet fully developed. Therefore, frequency reuse in different forms is inevitable for accommodating the huge demands for capacity and providing variety of services. Because of the inherently broadcast nature of the wireless channels, frequency reuse results in co-channel interference (CCI) which affects the Quality of Service (QoS) of wireless systems. Apart from CCI, another form of interference called adjacent channel interference (ACI) results due to leakage of signal power to neighbouring channels. In this thesis, we focus our attention mainly on CCI and we assume that ACI can be taken care of by proper filtering. Specifically, we investigate the scenarios where CCI is asynchronous in nature. One such scenario can be found in the networks which operate in unlicensed spectrum. Unlike the networks which operate in licensed spectrum and have a central entity to govern the various activities, networks in unlicensed spectrum operate in distributed manner. This leads to independent transmission activities by user nodes which resulted into asynchronous interference. Networks with central entity also, may be having such possible scenarios of asynchronous interference, if some practical constraints are considered.

We take such scenarios for further investigation in this thesis work to model and analyze the asynchronous interference.

1.1 Spectrum Reuse from an Interference Perspective

The necessity to utilize the available spectrum more efficiently has always been a matter of concern in design of wireless communication systems. Frequency reuse is considered to be an effective mean of fulfilling the demands for higher data rates and capacity which is becoming unrelenting with the increasing number of (wireless/mobile) users and advancements in technologies in recent years.

However, as already mentioned, spectrum reuse causes the problem of CCI. From receiver point of view, any signal, other than the one originated from desired transmitter, on the same frequency band is termed as CCI. CCI, if not properly accounted for, might severely affect the system performance parameters such as throughput, capacity, outage probability and bit error rate (BER). CCI decides the lower constraint on the level of frequency reuse that can be implemented while designing various wireless systems [4]. The incorporation of frequency reuse in network deployment

may be found in various forms of wireless networks including different kinds of infrastructured, infrastructure-less and heterogeneous systems. Therefore, the problem of CCI can be observed in almost all kind of wireless networks which employ frequency reuse. This research work analyzes asynchronous interference in some scenarios of infrastructured, infrastructures-less and heterogeneous systems. In this chapter, subsequent sections elaborate the problem of asynchronous interference in infrastructures-less as well as infrastructured systems along with the brief introduction of available models for interference analysis. The limitation of existing models to address issues of asynchronous interference is also outlined. Moreover, it is worth mentioning here that the interfering sources for a given receiver are intended sources for other receivers. Therefore, while system design should ensure that enhancement of signal quality for a given link, at the same time, it should not be at the cost of signal strength deterioration at nearby locations where same frequency is reused.

1.2 Asynchronous Co-channel Interference in Wireless Networks

CCI in the wireless networks is investigated by several researchers [5–8]. The study of pernicious effects of CCI is carried out in a large number of existing literature. But, most of the modeling and analysis of interference scenarios are centered around the infrastructured networks like cellular network [4, 9, 10], since they are well developed and widely spread wireless networks. System evaluation is performed under the assumption of perfect synchronization for these networks.

However, in recent times use of infrastructure-less ad-hoc type networks are increasing (in unlicensed band) because of the ease in their deployment and operability. Since, such ad-hoc wireless networks are localized and decentralized in nature, they are generally independent to each other in the absence of any central entity. As they cover relatively small geographical areas, many of such networks may be found in vicinity of each other [11]. Moreover, regular arrival of various new advancements and technologies in the market makes the simultaneous presence of more than one technologies in the vicinity of one another inevitable. This scenario of co-existence makes the interference more detrimental. The operation of different infrastructure-less (ad hoc) independent wireless networks in the vicinity of one another makes the interference asynchronous in nature, since, there may not be any level of co-ordination among them. Such appearance of different networks in the vicinity makes the co-ordination among various networks difficult to

achieve and maintain. Achieving co-ordination among nodes of a large network is also difficult. In large wireless networks, such as widely spread sensor networks, the problem of asynchronous interference exist, since achieving and maintaining synchronization in such large networks also are very challenging. However, through local control packet exchanges before actual communication, some level of synchronization between intended transmitter-receiver node pairs can be achieved.

The presence of asynchronous interference is also reported in case of large infrastructure based wireless networks, such as cellular system, WIMAX and orthogonal frequency division multiplexing/orthogonal frequency division multiple access (OFDM/OFDMA) based cellular systems with femtocells [12, 13]. These recent research works have pointed out that the nature of CCI may be asynchronous if some practical constraint are considered while analyzing infrastructured wireless networks. There may be other reasons also for the asynchronization in such networks. For example, keeping in view the increased capacity demand due to the emerging next generation wireless networks, deploying cells with smaller size is a typical practice to achieve high capacity [10]. However, this approach is not cost effective and feasible as well since, it involves more access points (base station) deployment with in the network. Moreover, studies show a huge amount of data and voice traffic originate from indoor users [14]. Therefore, the aim of the network designer is to achieve high capacity along with proper QoS to the indoor users. In such scenario, femtocells can be considered as an effective mean to achieve both the requirements. Since, mostly these femtocells are user driven, they remain independent of the central control [15]. Therefore, the conventional network planning and radio resource management techniques can not be applied to such hybrid kind of networks. Thus, the network architecture, interference management and synchronization are some of the challenges for such hybrid network with femtocells despite the above mentioned advantages [16]. The independency among femtocells as well as among base stations and femtocells results in negligible co-ordination among these entities. It further leads to the problem of asynchronous interference when the scenarios are coupled with some practical constraints.

The asynchronous interference may be the outcome of timing asynchronization and/or uncoordination among users in large (infrastructure-less) networks [17,18] or propagation delays and/or timing offsets in infrastructure based wireless networks. The problem of asynchronous interference might not be eliminated completely possibly due to inherent properties of wireless channel, but can be addressed upto certain level by proper and robust system design and use of interference

management schemes. The robust network design and interference management schemes against such asynchronous interference calls for proper insight of the interference mechanism which take place in such networks as well as accurate analysis and modeling of the same.

1.3 Various Available Models for Interference Analysis

While quantifying the (effects of) interference, the key question to be answered is how the interference would affect the reception of any desired signal at the receiver. Taking this into consideration, available works for interference modeling can be classified into two groups based on the strategies used to quantify the unintended signals:

- **Collision Based model** : In early works, interference is modeled using collision theory [19]. This collision theory works on '*all or nothing*' phenomenon [1]. This theory is primarily based on the assumption that if more than one signals are transmitted at the same time using same frequency band, all signals are lost at the receiver, regardless of power levels of the individual transmitted signals. Most of the works on random access techniques are based on this collision theory.

- **Capture Effect Based Model** : Models in this group consider capture effect to quantify the interference. According to the capture effect, if two or more signals appear simultaneously at the receiver (access point) on the same frequency, the stronger signal captures the channel and subdues the weaker (interfering) signals [20]. The strength of the signal can be decided by signal to interference plus noise ratio (SINR). Therefore, out of all incoming signals at receiver, the signal with the highest SINR may be correctly received unlike the collision model in which all simultaneously received signals are considered lost. So, with capture model (radio capture phenomenon) under consideration, a transmission is successfully received at receiver terminal even in the presence of interfering signals if any (desired) transmission is sufficiently stronger than the other signals. Intuitively, it can be pointed out that models based on capture phenomenon are more realistic than the models based on collision effect.

Out of various available models, additive model (physical interference model [7]) is based on the capture effect. Other interference models, such as capture threshold model, protocol model, interference range model take collision effect into consideration while modeling the interference for

a communication link. Models based on capture effect are more complex than the models based on collision theory. However, the simplified interference models might be useful in some specific application scenarios [21]. For example, to show the interference relationship between pair of links or pairs of terminals [22, 23], graphs can be constructed using protocol interference model. This alternate representation of interference (relation) using graphs (also known as interference graphs) under the protocol interference model has an important role in graph theory in the field of wireless network modeling. Graph based models are very useful for solving problems in the context of frequency assignments [24], transmission scheduling, resource allocation and topology control. A detailed discussion on available models and their classifications is carried out in chapter 2.

1.4 Status of Existing Models in Dealing with Asynchronous Scenarios

In order to have efficient interference management/avoidance schemes for asynchronous scenarios in wireless networks, a proper and accurate model is necessary for the same. The existing models developed for the synchronized scenarios (infrastructured networks) may not be directly applicable for the asynchronized scenario found in infrastructure-less as well as infrastructured networks due to the characteristic differences between the two scenarios. Here, we point out few such differences between the two scenarios of wireless networks which suggest the further modifications that are required in existing models to make them more suitable for the asynchronous scenarios.

- In most of the cases, as mentioned before, synchronization among users (networks) is primarily due to advantageous presence of the centralized control in the infrastructured networks. This central entity takes care about all the (control) signaling issues and protocols for such networks. In asynchronous scenarios found in infrastructure-less networks, the absence of central node makes the distributed implementation of several algorithms and protocol favourable.

- Nodes in infrastructured networks communicate through base station or access point for most of the time, while infrastructure-less networks work on direct peer to peer communication principle.

- In order to reduce the overall interference in infrastructured wireless networks, power level adjustments might be implemented for various transmitters according to the fading and path

loss conditions. In such scenario, the transmit power of a user node becomes a function of its distance relative to the serving base station. This situation might create a quite different scenario in terms of interference compared to the networks having uniform/no power control for transmit power of various user nodes, generally the case when there is no central node.

The above discussion indicates the few possible differences in the two scenarios of wireless networks. Thus, even though these two types of network may operate in the same wireless environment, the characteristics of the interference found in them can be fairly different. Therefore, same interference model can not be applicable when two dissimilar interference scenarios exist. In the next section, we will look into some of the potential issues which need to be taken care while developing a model to address interference for asynchronous environment.

1.5 Issues Related to Modeling and Analysis of Asynchronous Interference

Some works are available in literature which deals with the problem of interference in various wireless networks [1]. But, most of works are carried out under the assumption of global synchronization within the network. The physical interference model, which takes capture effect into account, gives better characterization of interference in practical conditions, is also based on the perfect synchronization assumption [25]. With synchronization assumption, desired and interfering frames are considered to have complete overlap. The assumption of global synchronization might be justified upto certain extent for infrastructure based networks like cellular system where a centralized control tries to maintain the network-wide synchronization. For those networks, which do not have any central entity, assumption of synchronization if considered while modeling the systems, it may lead to inaccurate evaluation of performance parameters. In the absence of a central entity, user nodes can have independent transmission schedules which will result into the asynchronous arrival of interfering signals at the receiver node [2]. Asynchronous arrival of frames will result into partial overlap of frames and interference modeling with such partial overlap is more general as complete overlap representing synchronized transmission becomes a special case.

The infrastructured systems such as cellular network generally have some sort of regular (fixed) network deployment/geometry. Regular deployment of nodes makes the information gathering process relatively deterministic. For example, the number of co-channel interferers and their locations

may easily be calculated for a cellular network with minimal amount of prior information [5]. On the other hand, the information gathering process might not be easy for asynchronous environment in infrastructure-less systems due to absence of any central entity. With the irregular deployment of nodes in such type of networks, the calculation of the number of co-channel interferers and their locations is a difficult task. Additional complexity is introduced due the uncertainty associated with the wireless medium. In such scenario, a probabilistic model for effective number of interferers and other required parameters should be developed first to model this scenario.

The independent nature of the networks hinders the application of any planned interference avoidance scheme (for example frequency reuse concept of cellular system) for asynchronous networks. Therefore, these infrastructure-less ad-hoc wireless networks require some dynamic, light-weight and localized interference avoidance scheme [21]. The design of such interference avoidance schemes require proper insight of the interference mechanism happening in the network in order to model and analyze the same. We take some of the above mentioned aspects/issues of asynchronous CCI for further study in this thesis work.

1.6 Motivation of the Present Work

As discussed in the previous sections, the problem of CCI exists for both, infrastructured as well as infrastructure-less wireless networks, if they employ frequency reuse. However, the advantageous presence of central entity in infrastructured network makes it easy to deal with the interference problem with proper interference management schemes such as (optimum) reuse factor based network deployment in cellular network [26]. For infrastructure-less networks, the absence of central entity advocates the distributed implementation of various schemes which further hinders the application of any planned interference avoidance scheme for such networks.

Moreover, the existing models developed for the synchronized environment, generally found in infrastructured networks, require some additional modeling aspects to be incorporated to become applicable for the asynchronized environment found in infrastructure-less and infrastructure-based networks as well. One of the major issue needs to be incorporated arises due to the lack of co-ordination among nodes. Unlike the infrastructured networks, where co-ordination can be easy to achieve with the help of central entity, obtaining co-ordination in infrastructure-less networks can be a difficult task. As mentioned before, absence of co-ordination in the later type of network

leads to the problem of asynchronous arrival of frames at receiver. With asynchronous arrival of interfering frames, every bit of the desired frame may experience different amounts of interference. Since, the total amount of interference plays an important role while deciding the node (network) performance, this asynchronous arrival of frames needs to be investigated with utmost care up to the bit level. Existing works [2, 27–30] in literature do not address this issues adequately. In this context, one of the main objectives of this thesis is to include the various aspects of asynchronous arrival while modeling the interference scenario at the bit level.

In addition, available works are based on some simplified assumptions while modeling various interference scenarios. One of such assumption is considering the transmission/reception range of a node as circular. While this assumption makes the analysis simple, it does not reflect the true shape of either of the ranges. In a wireless communication, due to the uncertainty of medium, a nearby interfering node may not create much interference at a given receiver, while a distant interferer may produce more interference for the same receiver. This aspect needs to be considered while modeling since, the overall interference is a function of number of interferers also.

Guard zone also plays an important role to decide the number of interferers. Depending upon the medium access control (MAC) protocol, it restricts the nearby nodes (strong interferers) from transmission. An optimum value of interference range further affects the overall interference power. To the best of author's knowledge, the various aspects of MAC as well as interference range are not effectively addressed in existing works while analyzing asynchronous interference in wireless environment.

A proper insight of the effects of various network parameters might be crucial while designing a network least affected by the interference. Various such network parameters plays an important role in analyzing the effects of asynchronous interference. The effects of various network parameters such as antenna height, deployment area, frame size, node density, interference range factor etc. on the asynchronous interference have not been investigated in detail. This is another dimension which is not exploited in the available works.

As already mentioned, infrastructured networks are generally assumed to be (globally) synchronized from interference perspective in existing works [4, 25, 31, 32]. However, recent literature claims that considerable degree of asynchronization exists if some of the practical constraint are taken into account [33, 34]. Propagation delays and timing offsets are some of the practical con-

straints that can affect the synchronization of arrival of frames at the receiver. Ideal scenarios are usually assumed instead of these practical conditions while analyzing the network performance in an interference environment.

Moreover, in the present scenario, the current technologies are expected to deliver an improved QoS to the users under various interference conditions. In obtaining such strict QoS requirements, an accurate modeling of those interference environment conditions plays an important role. An accurate modeling further demands for a precise evaluation of various network parameters in order to reflect a better representation of those conditions. For example, to achieve high data rates and enhanced spectrum efficiency, next generation communication standards such as Long Term Evolution (LTE), WiMAX employ OFDMA. The efficient operation of OFDMA requires a lot of information regarding various network parameters such as channel state information (CSI), user and path loss condition related parameters. Assuming idealistic conditions does not provide accurate evaluation of network parameters. Taking this into consideration, an efficient interference management/avoidance scheme is need to be developed for infrastructured networks also, with proper incorporation of various practical constraints that can make the interference asynchronous.

The discussion presented above opens up some of the potential areas which require further investigation. The assumption of perfect synchronization among transmissions in many of the existing models leave room for the development of a generic model to address the partial overlap in asynchronized environment. Several phases of the design and deployment of wireless networks, such as capacity evaluation, error analysis, outage performance and analysis of performance degradation due to interference require proper model of asynchronous interference. An appropriate model of such interference can also be useful in designing appropriate signal processing techniques and protocols capable of reducing the effects of interference.

1.7 Thesis Contribution

This thesis aims at addressing the modeling issues of asynchronous CCI which may appear due to the lack of proper co-ordination among user nodes or/and due to some of the practical constraints. Some modeling approaches have been proposed for analyzing asynchronous CCI for infrastructure-less as well as infrastructured wireless networks. In particular, the following are the main contributions of this thesis. This thesis

(a) analyzes various aspects of infrastructure-less and infrastructured wireless networks from asynchronous interference perspective.

(b) proposes two approaches for analyzing different scenarios of asynchronous interference in wireless networks.

(b.1.1) The first approach is an energy based method which introduces a parameter *EINR* (signal *E*nergy to *I*nterference energy plus *N*oise spectral density *R*atio) and using the same, develops a model to analyze asynchronous interference at bit level in wireless networks. The proposed model is general enough and applicable to various kind of wireless networks. The model includes the existing models as special cases.

(b.1.2) Proposes a modeling approach for outage analysis using *EINR* metric in asynchronous interference-limited environment.

(b.2.1) Proposes a method for calculating the index and overlap made by a bit of interfering frame to the bit of desired frame.

(b.2.2) Proposed another bit level approach which uses an (scaled) amplitude metric based method and considers the sign of bit(s) of interfering frames while modeling the asynchronous interference.

(b.2.3) Determines the probability density function (pdf) of interference in an asynchronous environment as a function of basic parameters of the network. BER performance has been evaluated using the second (scaled) amplitude metric based approach.

(b.2.4) The effects of node density, antenna height, interference range and deployment area on the network performance have been analyzed in an asynchronous interference-limited environment.

(c) As an interference management/avoidance approach, the thesis proposes a distributed resource selection method for femtocells in OFDM/OFDMA based cellular network in an environment where interference is asynchronous in nature due to some practical considerations. The thesis

(c.1) analyzes the issues affecting the selection of optimum subband, suitable for femtocell communication considering asynchronous nature of interference. The proposed method takes some of the practical constraint into account while analyzing the suitable subband.

(c.2) For suitable subband selection, two methods have been proposed based on different considerations.

1.8 Thesis Organization

This thesis is organized as follows. A structural organization of this thesis is shown in Figure 1.1.

- **Chapter 1**, the current chapter, describes the problem statement and the motivation behind them. This chapter highlights the basics of wireless systems from interference perspective as well as the types of interference. A brief introduction of the problem of asynchronous interference in infrastructure-less as well as in infrastructured wireless networks is also presented here. This chapter also summarizes the thesis contribution and provides a brief outline of the thesis organization.
- **Chapter 2**, presents a literature survey of related works in the area of modeling and analysis of interference, asynchronous interference, MAC and interference range factor. The chapter

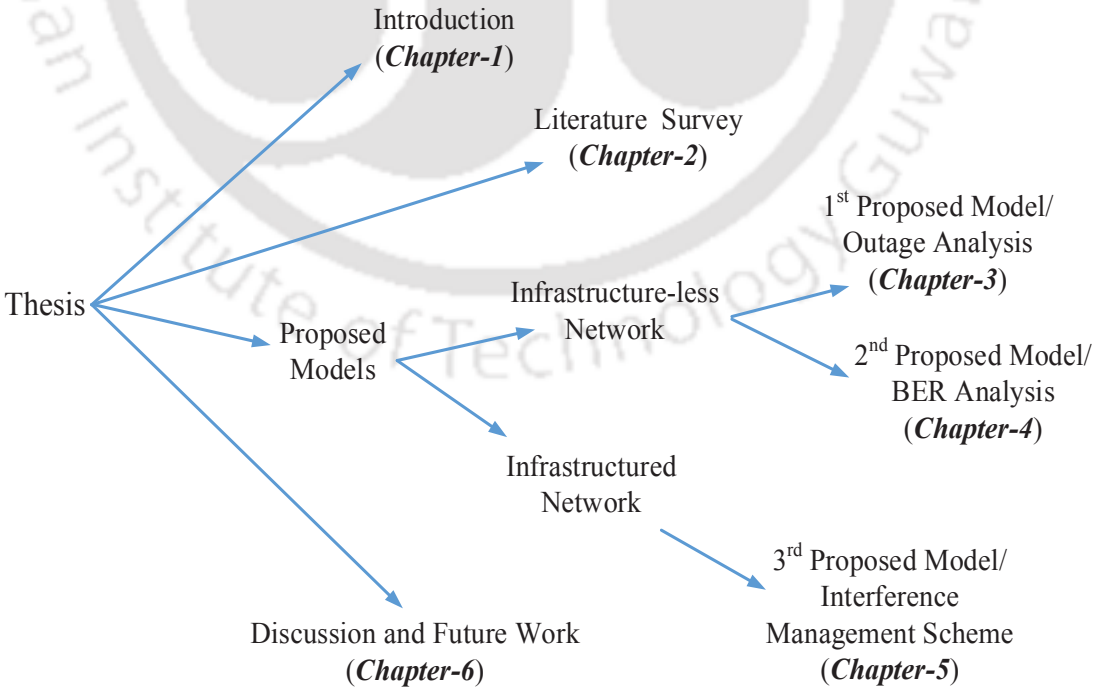

Figure 1.1: Thesis organization.

also elaborates some issues related to asynchronous interference, introduced in chapter 1. It also covers the survey related to the resources allocation in heterogeneous/overlaid wireless networks.

- **Chapter 3**, proposes an energy based approach to model the interference, which is asynchronous in nature, for wireless networks. The model is general enough to address the interference in synchronized networks also. Here, we introduce a metric *EINR* to address the asynchronized interference. Using the *EINR* metric, the network performance is evaluated in terms of outage probability along with some other performance parameters. The effects of antenna height are also discussed.

- **Chapter 4**, proposes a (scaled) amplitude based method to analyze the error performance of wireless network in the presence of asynchronized interference. The proposed method takes the sign of bit(s) of interfering frame into account while addressing the partial overlap scenario. Along with this, this chapter also provides pdf of partial overlap term and amplitude of asynchronous interference in closed form. The effects of interference range factor and signal phase are also analyzed here.

- **Chapter 5**, introduces an interference management/avoidance approach for wireless networks. To explore further, heterogeneous wireless network is considered for analysis purpose. We take OFDM/OFDMA based cellular networks which employ femtocells to fullfill the high data rate/capacity requirement of users. Cellular systems, based on OFDM/OFDMA technique, instead of traditional frequency reuse methods, use fractional frequency reuse (FFR) methods to further ameliorate the high data rate/capacity requirements [35]. From femtocell point of view, FFR can further be used as a technique to combat against CCI by selecting a subband which is least affected by the interference. Here, we analyze the frequency subband allocation for femtocells deployed in OFDMA based cellular networks from the perspective of asynchronous interference in the network.

- **Chapter 6**, concludes this thesis with a summary of the work done and includes some suggestions that may be investigated in future research.

2

Literature Survey: Review of Related Work

Contents

In last few decades, tremendous growth in wireless networks and devices can be witnessed. Different applications of wireless communications and networks are becoming ubiquitous and sophisticated. The number of users of wireless systems are also continuing to increase at higher rate. With the current spectrum allocation strategies as well as due to the fact that the communications at higher frequencies are still challenging, the spectrum is presently scarce. Therefore, current and future wireless systems are expected to operate in a challenging scenario of spectrum availability in order to fulfill the various kind of needs of users.

Keeping in view the limited spectrum availability, frequency reuse comes as a viable mean to manage the scarcity of spectrum. It allows distant users to use the same frequency. But, this scheme of frequency scarcity management does not come at free of cost due to the broadcast nature of wireless medium with omnidirectional antennas[†]. Reuse of frequency results in CCI that can not be avoided completely due to broadcast nature of wireless medium. In order to have a proper avoidance/management of CCI, which arises due to the frequency reuse, general and accurate models are necessary to get an insight of interference mechanism. Some models are available in the literature to quantify different interference scenarios. But, most of the available models and approaches are developed by assuming that the network is centrally synchronized. This assumption is not tenable with infrastructure-less ad-hoc kind of networks having limited power and processing capability constraints. Processes, like achieving and maintaining synchronization around the network requires a lot of overhead resulting into additional power consumption and reduces the life span of the device (network). Taking recent interest of research community in ad-hoc networks into account, it will be meaningful to analyze the networks under practical scenarios in which power consuming processes are not accounted. Out of many consequences of taking practical scenarios into account, one possibility is the asynchronized communication in a network. As discussed in the chapter 1, models/approachs used for the synchronized networks may not be suitable for asynchronized scenario. Asynchronized scenario requires models which are general enough to take into account various situations. This chapter further elaborates some aspects of modeling and analytical approaches for the interference in an asynchronized environment.

In this chapter, first, we elaborate on different models for interference based on various classifications. Some of the problems associated with the interference modeling are also discussed. Issues related to asynchronized interference are also pointed out. Finally, concept of overlaid/heterogeneous

[†]Antennas are assumed to be omnidirectional for this work. Directional antennas are not being considered here.

networks along with interference management approaches are discussed from user's different QoS related requirements point of view.

2.1 Interference Modeling

CCI is one of the primary bottle-neck in wireless networks which employ frequency reuse. Broadcast nature of wireless channel hinders the complete removal of the detrimental effects of CCI but those effects can be compensated upto certain extent with proper insight of interference mechanism happening in the network.

An accurate modeling of interference provides such valuable insights to the system designer. A lot of interference models, with different intended applications, level of details and form of describing interference are proposed in literature to quantify the effects of interference in wireless networks. The main objective of this thesis work is to model and analyze the asynchronous interference. Before delving deeper into that topic, first a brief summary of available models is presented to get a feel of existing approaches for interference analysis.

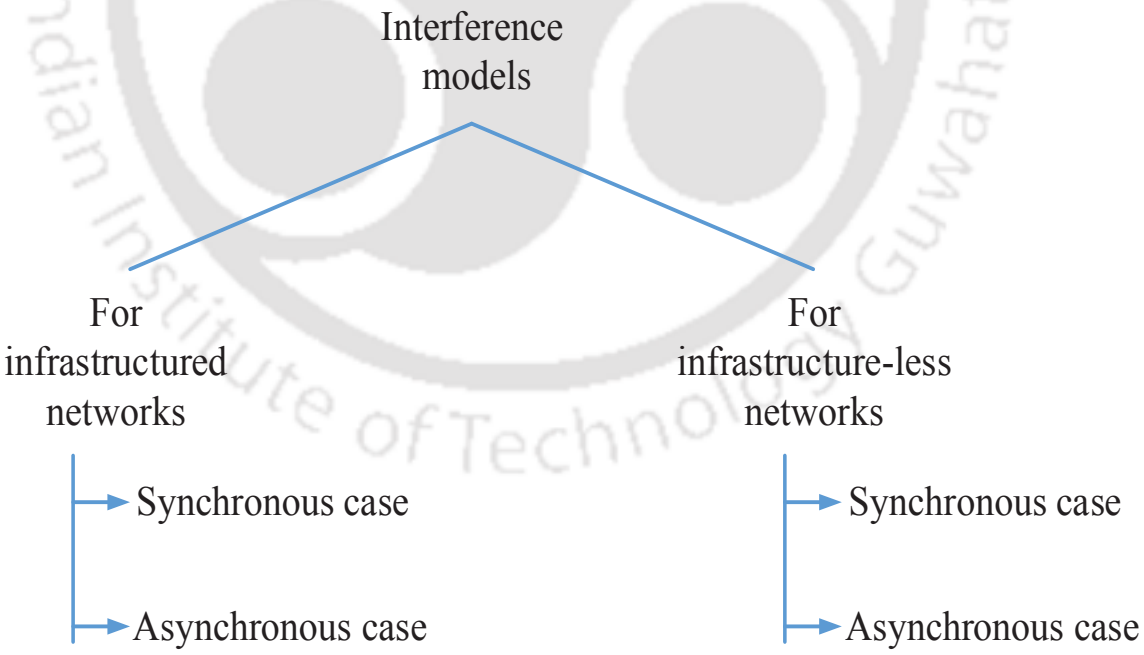

Figure 2.1: Classification of various available models of interference.

As shown in Figure 2.1, various available models of interference for wireless network can be classified under two large groups:

(i) models for infrastructured networks

(ii) models for infrastructure-less networks

The fundamental differences between the two kind of networks justifies the classification. As mentioned before, the major difference between infrastructured networks and infrastructure-less networks is the absence of any central entity in later class of networks. For infrastructure-less networks, the absence of central entity makes the synchronization/co-ordination difficult to achieve. In the absence of proper co-ordination, the level of synchronization among user nodes of same network or different wireless networks can be negligible. Consequently, distributed implementation of several network protocols and algorithms in infrastructure-less networks remains useful since most of the time, nodes in such networks are restricted to operate using limited or no information on the status of whole network. Nodes in the infrastructured networks, on the other side, often have sufficient information about the network through the central node (*e.g.* base station in cellular networks). The presence of central entity in infrastructure based networks, makes it easy to achieve and maintain synchronization/co-ordination among user nodes of (different) networks. Moreover, due to absence of any central entity, nodes operate directly on a peer to peer basis in infrastructure-less networks, while the presence of central entity makes the direct communication possible among nodes and base station most of the time. These characteristic differences indicate the necessity of different treatment for interference analysis/modeling in these two kind of networks.

The models, developed for these networks, can be further divided into two classes for this thesis work:

(a) for synchronized scenario

(b) for asynchronized scenario

Most of the modeling approaches in literature assume a centrally synchronized scenario for both infrastructure based as well as infrastructure-less networks. As discussed in chapter 1, for infrastructure based networks, this assumption is reasonable due to the presence of a governing node but for infrastructure-less networks, this assumption is not tenable and if used, lead to impractical representation of the real systems. Achieving global synchronization, without any central node is a difficult task to perform. This process is also highly energy consuming due to large number of packet exchanges and therefore can not be termed as efficient for energy/power constrained

ad-hoc and sensor kind of networks. However, works are available that points out the problem of asynchronization in both kind of networks. But, they do not address various interference related issues adequately up to the bit level [2]. Various issues related to asynchronous interference modeling along with inapplicability of models/approaches developed for synchronous scenario in asynchronous scenario are discussed in Sec. 2.2.1. Here, a brief introduction of some widely used interference models is given. There exist a fair degree of trade-off among interference models in terms of simplicity and accuracy. These models differ in the way they treat the interfering signal while evaluating the system performance. Some of the important models available in literature to quantify the interference are as follows:

- **Protocol model** : Let $\{M_i\,;\, i \in \urcorner\}$ be the subset of nodes concurrently transmitting over a particular sub channel. Given that the transmitter node is in reception range of receiver node, i.e. $|M_i - M_j| \leq R_C$, protocol model gives the condition for a transmission, originated by node M_i towards another (receiver) node M_j, $j \in \urcorner$, to be successful in frequency reuse scenario as

$$|M_k - M_j| \geq (1+\Delta)|M_i - M_j| \tag{2.1}$$

where M_k, $k \in \urcorner$ can be any other node of the network transmitting on the same frequency and R_C denotes the reception range. The parameter $\Delta > 0$ incorporates the effects of guard

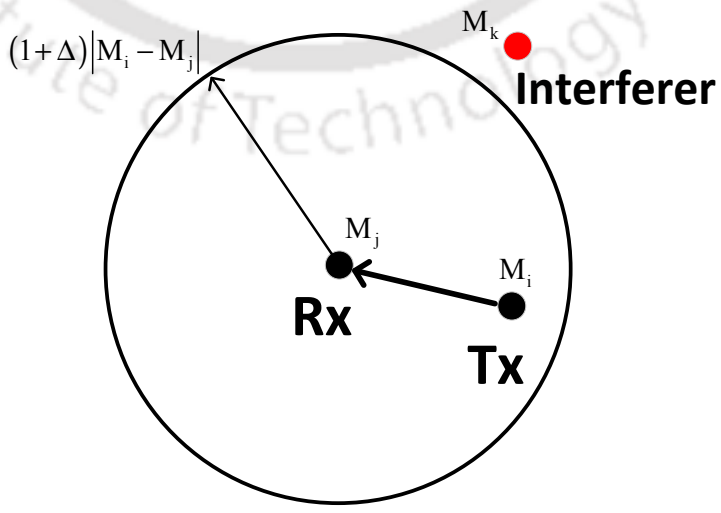

Figure 2.2: Geometric interpretation of Protocol model [1].

zone around the communicating pair. This model checks the condition in (2.2) for each ongoing transmission. Therefore, as per protocol model, if the distance of receiver from the intended transmitter is lesser than the distance from each interferer by a given quantity, than the ongoing transmission will be considered as successful [7]. Figure 2.2 shows a possible scenario of protocol model in which for a successful reception at M_j, interfering terminal M_k is outside the reception range of M_j.

- **Interference Range Model** : This model works on the concept of interference range [36]. In a frequency reuse scenario, given that the transmitter node is in reception range of receiver node, i.e. $|M_i - M_j| \leq R_C$, a transmission is considered to be successful if

$$|M_k - M_j| \geq R_I \tag{2.2}$$

where R_I denoted the interference range.

Authors in [21] show that if we consider $R_I = R_C(1+\Delta)$, interference range model becomes a simplified version of protocol model. As per protocol model, the interferer - receiver separation should be proportional to transmitter - receiver separation, while interference range model needs this separation to be greater than the interference range. Figure 2.3 depicts a possible case of interference range model.

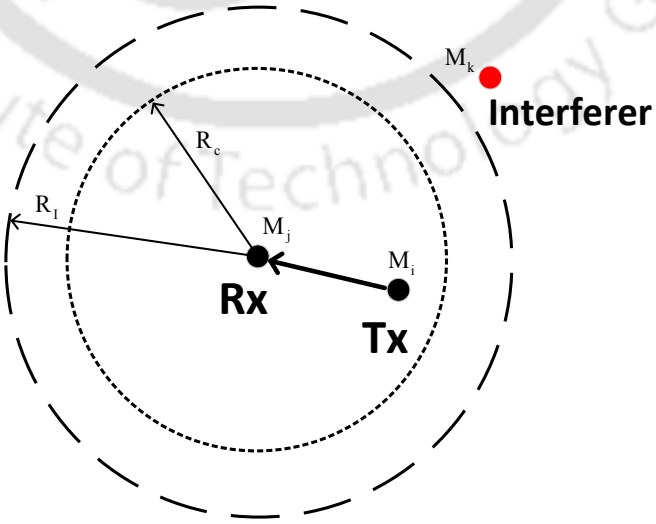

Figure 2.3: Geometric interpretation of Interference range model.

◆ **Capture Threshold Model** : This interference model is based on the capture effect. According to the capture threshold model[†], a transmission from a node M_i is successfully received by a node M_j if

$$\frac{P_i \left|M_i - M_j\right|^{-\eta}}{P_k \left|M_k - M_j\right|^{-\eta}} \geq CpThresh \qquad \forall\, k,\, k \neq i \qquad and \tag{2.3}$$

$$P_i \left|M_i - M_j\right|^{-\eta} \geq RxThresh \tag{2.4}$$

where P_i and P_k are the transmitted power used by the desired and interferer node, respectively, and η is the path loss exponent. *CpThresh* and *RxThresh* denote capture and receiver threshold, respectively. It may be noted that this model considers one interferer at a time while calculating the decision metric. If the ratio of the received power from the desired and interfering transmitter is above *CpThresh*, then the frame is assumed to be unaffected by that particular interfering transmission. While using this model, one has to check the condition for successful reception for all active links [21].

◆ **Physical model** : This model may be considered as an accurate, developed but more complex version of the capture threshold model. Many wireless physical layer technologies consider the addition of all other ongoing transmissions and noise as undesired signal for the massage to be decoded. Motivated by the above fact, the physical model of interference works on the SINR thresholding concept. If SINR remains above a certain threshold for the entire duration of the frame transmission, the transmission is assumed to be successful. Then, the SINR for a transmission from node M_i towards the (receiver) node M_j, considering the effects all concurrently active links, may be written as

$$\text{SINR} = \frac{P_i \left|M_i - M_j\right|^{-\eta}}{N \;+ \sum\limits_{k \in \urcorner;\, k \neq i} P_k \left|M_k - M_j\right|^{-\eta}} \tag{2.5}$$

where N is the thermal noise power in the frequency band of operation. With physical model under consideration, a frame is considered received successfully, only if the following condition

[†]Modules can be easily found in *ns*2 network simulator. Available : http://www.isi.edu/nsnam/ns/.

remains valid for entire frame duration :

$$\text{SINR} \geq \beta \tag{2.6}$$

where β is the threshold depending on the coding and modulation scheme [7].

It may be noted that various models use different assumptions while modeling to keep the analysis simple. Some of such assumptions may be listed as : considering single interferer at a time, interferer - receiver separation greater than the transmitter - receiver separation or interferer - receiver separation proportional to a fixed quantity (interference range) for successful packet reception, etc. The models based on simplified assumptions reduce the calculations involved by considerable amount at the cost of accuracy. For example, taking single interferer at a time (pairwise interference modeling) does not reflect the practical conditions of decoding. Considering the broadcast nature of wireless medium, a better strategy would involve the accumulation of all undesired transmissions at receiver while evaluating the performance metric.

Interference model proposed by Gupta *et.al.* in [7] takes the sum of all other ongoing transmissions (and noise) as undesired signal while calculating the signal to interference (plus noise) ratio. Thus, the physical model (additive interference model) in [7] gives relatively accurate representation of interference statistics and better insight to the interference mechanism from system designing perspective.

Based on the above discussions, these models may also be categorised as member of the family in which models describe the effects of interference. They emphasize on some aspect of the network behaviour or any particular network performance metric that is affected by CCI. There exist some more interference models which can be considered as the part of another family in which models describe the characteristics of interference itself. Models that belong to the later family, emphasize on the statistical characteristics of interference such as, cumulative distribution function, probability density function, moments of different orders. Such knowledge about the statistical nature of interference may be helpful in lower layers related issues like detection/estimation analysis, correlation analysis, etc. Statistical interference models primarily deal with the stochastic nature of various factors that affect the interference such as, pattern of the data traffic, location of randomly distributed interferers, wireless channel. Some approaches taken for the models of this family can be listed as: considering the distribution of interference as α-*stable* [37] or as a shot noise [38],

assuming distribution of node terminals as homogeneous Poisson Point Process (PPP) [39, 40], Binomial point process (BPP) [41] or Matern Point Process (MPP) [42, 43]. However, distributions are unknown for interference based on these point processes.

2.1.1 Graph Based Approaches for Interference Modeling

There are some key elements of interference analysis that may be described efficiently by mean of graphs [44] in wireless networks. Link scheduling and network topologies are some of the key elements of interference analysis in wireless networks. A proper link scheduling and robust topologies also play an important role in designing a network, which is least affected by the CCI. The typical problems such as scheduling [45], frequency assignment problems [46] and topology control [47], can be efficiently handled by graphs which is another important form of describing the effects of interference. Graphs are primarily used to model two scenarios in a wireless network : interference and connectivity. Interference graphs may be used to analyze the interference. To analyze the connectivity related issues, connectivity graphs may be utilized [48].

Table 2.1: Various models for interference analysis

Interference model	***Principle on which model is developed***	***Remark***
Protocol model [7]	Successful reception requires the interferer-receiver separation greater than the transmitter-receiver separation with transmitter-receiver separation must be less than the communication range.	Considers link by link interference while calculating the distance metric.
Interference range model [36]	Frame reception on a link is successful if the interferer-receiver separation greater than the interference range with transmitter-receiver separation must be less than the communication range.	Link by link interference consideration at the time of distance metric calculations.
Capture threshold model [21]	For successful packet reception, the desired signal as well as a ratio of desired to interference signal must be above certain thresholds.	Takes one interferer at a time while calculating the SIR metric.
Physical model [7]	In order to decode the wireless signal, treats the sum of all other on going transmissions and environmental disturbances as undesired signal.	Based on the *capture effect*.
Graph based model	Model the interference as pairwise relationship between terminals or links. However, models based on aggregate interference have also been proposed [48].	Based on the *graph theory*.

Using graphs, a network may be represented by $G = (V, E)$, where V and E denote the set of vertices and set of edges joining two vertices, respectively. Independent sets, matching, spanning tree, vertex coloring, conflict graphs [49] and flow contention graphs are some of the important tools in graph theory which can be very useful while carrying out the interference analysis.

To the best of author's knowledge, the concept of graph theory is not exploited in asynchronous interference analysis. However, a considerable amount of work is available for interference analysis in synchronous scenarios [50–53]. A comparative study of some important interference models is presented in Table 2.1.

2.2 Asynchronous Interference Modeling and Analysis

In previous section, we have discussed various available models and approaches to quantify the interference in wireless networks. However, those models are based on the assumption that the network is synchronized. Therefore, those models (in the current form) can not be utilized to properly analyze the asynchronous scenarios. Before moving towards the development of models which can efficiently address the asynchronous interference scenarios, first various issues related to asynchronous scenario needs to be pointed out. This section elaborates some important issues related to modeling of interference in asynchronous environment. Some of the analysis aspects of wireless network from interference perspective are also pointed out.

2.2.1 Modeling Issues

The CCI in the scenarios, where the level of synchronization among user nodes of (different) network(s) is negligible, can not be accurately addressed with the models existing for synchronized networks. Generally, in networks where some central authority remains active for the network (user) nodes to take decisions like what optimum transmission power level to use, which channel to be utilized for communication and when to transmit, a considerable level of co-ordination among the nodes can be observed. Such networks are assumed to be synchronized. In case of the synchronized (coordinated) networks, the transmissions of various nodes are perfectly synchronized, since transmission schedules are supposed to be decided by the central authority. Various nodes transmit in the predefined time slots. Figure 2.4 depicts a possible interference scenario in a wireless network where perfect synchronization is assumed to exist with propagation delay neglected for short distances and considering the frame duration much larger. It may be observed that the

starting point of reception is same for both the desired as well as undesired (interfering) frames due to the synchronization assumption. Entire undesired frame is responsible for creating interference at receiver node. Therefore, the interference scenario experienced by all the bits of desired frame is almost similar (with slow fading assumption).

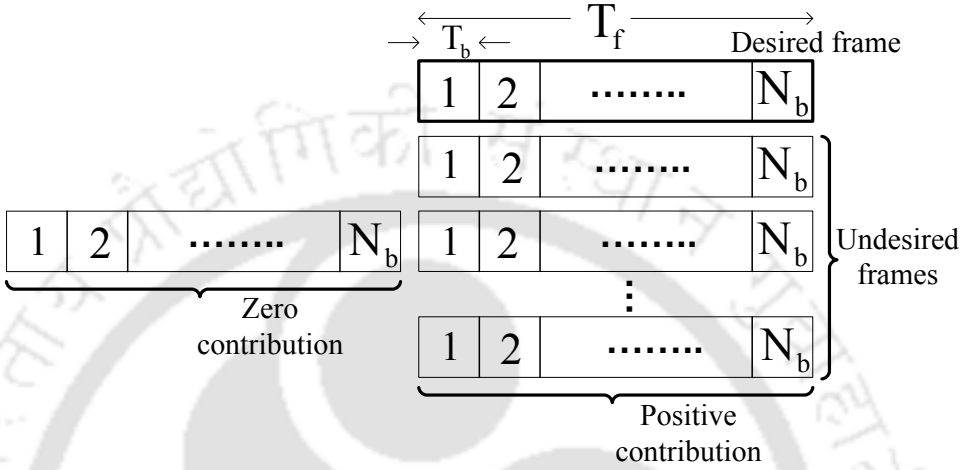

Figure 2.4: Frames overlap in a perfectly synchronized wireless network.

On the contrary, nodes of the networks, having no central authority, works in an autonomous fashion. Based on the local information available, nodes take decision to give a best possible value of desired QoS. Since, nodes (or group of nodes) take decisions locally, level of co-ordination remains negligible among the nodes. Such networks are assumed to be asynchronized. It may be noted that a significant amount of synchronization may still be achieved in such networks by some (periodic) information exchange among nearby (group of) nodes. But, this incurs large cost in terms of energy and resources, which further increases with growing network size. Therefore, by designing nodes (devices) to work independently, the requirement of any central entity might be neglected. In such un-coordinated networks, the lack of synchronization among different transmitter nodes results in un-coordinated transmission schedules which leads to the asynchronized arrival of frames at the receiver nodes. With asynchronized arrival of undesired frames, the complete frame may not be responsible for the interference but a part of it. Figure 2.5 delineates one such possible scenario in an un-coordinated wireless network. In this case, it might be noted that due to partial overlap, the interference scenarios observed by all the bits of desired frame are not similar.

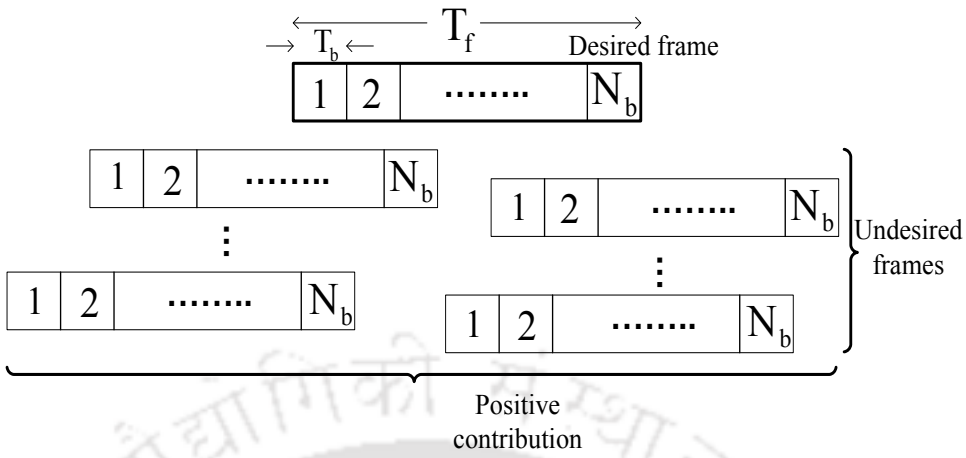

Figure 2.5: Frames overlap in an asynchronized wireless network.

2.2.2 Issues Related to Performance Metrics

In order to obtain the system performance for environments where asynchronous interference is present, irrespective of the model used to quantify the effects of interference, any performance metric must include the resultant interference. As discussed earlier, the performance metric, which takes the effects of all ongoing transmissions into account (additive approach) can give a better characterization of synchronous networks in an interference environment. Considering this, the SINR may be taken as a useful measure for observing the detrimental effects of interference, since it takes the summation of all ongoing undesired transmissions in to account. The number of interferers is not a deterministic quantity in an (non-centralized) wireless network due to the uncertainty of wireless medium and availability of data to be sent (*eg.* in event driven scenarios), therefore, the total interference power also becomes a random quantity. The randomness in interference power along with variable desired power in fading scenarios makes overall SINR parameter fluctuating.

In previous section, we have discussed that in an asynchronous environment, the interference experienced by different bits of a frame might not be same. Therefore, analysis at bit level can be more insightful than the packet level analysis. Various performance metrics may be found in literature to evaluate the network performance. Out of various available metrics, Outage probability, BER, throughput are some of the important ones that give a meaningful insight to the system performance.

In this section, we discuss some of the above mentioned metrics from interference perspective to figure out the effect of interference on network performance. Existing works related to these

metrics will also be discussed along with some inadequately addressed issues.

2.2.2.1 Performance Evaluation Using Outage Probability

For a specific QoS requirement, the SINR must be above some predefined threshold. Outage probability is a useful measure for observing the SINR variation with respect to the overall interference or total number of interferers. It gives meaningful insight to systems operating over fading channels. Outage probability is defined as the probability that the SINR (SNR) is below certain threshold or equivalently, error rate exceeds some specified value [54]. To the best of authors knowledge, outage probability computation considering asynchronous interference at bit level is not addressed in literature.

However, some packet level approaches to calculate the outage probability can be found in [55, 56]. In their work in [55], authors have considered a spectrum sharing scenario in which a primary network co-exists with a secondary network, such scenario may be found in cognitive radio networks to meet the demands for frequency spectrum. Authors in [55] investigated the outage probability of the secondary network in the scenario in which primary and secondary networks are not synchronized.

Another packet level approach to deal with interference is proposed in [2]. A general framework for interference analysis is presented and the same is used to find the closed form expression for network throughput. To validate the proposed framework, a heterogeneous system consisting of one IEEE 802.11b network and multiple Bluetooth networks is analyzed. For the sake of completeness, the network scenario is reproduced in Figure 2.6. Since, devices are operating in an unlicensed frequency band, it is assumed that there is no central point of control. Various networks/devices have to share the spectrum in a fair way and they must be designed to cope with interference. In the absence of any central control, the interfering packet arrival is modeled in an asynchronous manner. However, the study is carried out under the assumption of static channel (no fading) and without considering the effects of MAC protocol on interference.

A interference power calculation framework is proposed by Hekmat *et.al.* in [30]. In their work in [30], authors have presented a method to calculate the expected interference power and its distribution function in infrastructure-less wireless networks, such as ad-hoc and sensor network. However, instead of directly addressing the ad-hoc kind of networks, authors have estimated the

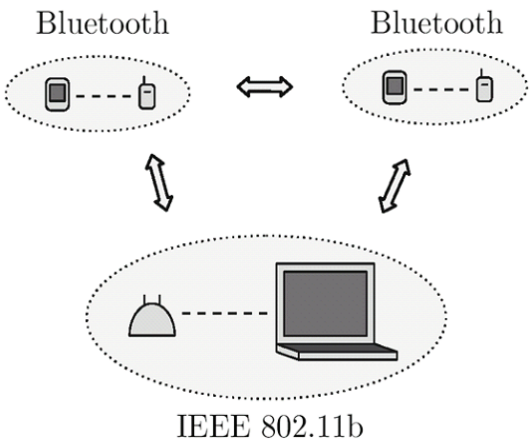

Figure 2.6: Example of asynchronized interfering wireless networks [2].

interference statistics for fixed topology networks first and then added required aspects to make it suitable for infrastructure-less topologies. While calculating the interference power statistics, MAC protocol characteristics, density of nodes and traffic load per node are some of the important parameters that are included into the analysis. Authors have shown that the proper selection of MAC protocol plays an important role in deciding the interfering node density. However, the work carried out in [30] is based on the perfect synchronization assumption.

2.2.2.2 Performance Evaluation Using Bit Error Rate

Apart from outage probability, BER is also considered to be an accurate measure for system performance. BER calculations may be an insightful and interesting way to observe the effects of interference on system performance. Variety of works can be found in literature for BER calculations in interference environment [57–63]. But, mostly, these work also are carried out under the assumption of perfect synchronization. To the best of author's knowledge, very limited work is available evaluating system performance in an asynchronous interference environment. BER performance of Binary Phase Shift Keying (BPSK) in presence of multiple co-channel interferers is presented in [64]. Authors have assumed that there is no synchronization between desired and interfering signals. In their work, authors have pointed out that one has to deal with the number of active interferers very carefully while determining the protection ratio (minimum SIR) to obtain a specified bit error probability. Simulation results for Gaussian Minimum Shift Keying (GMSK) are also presented in this study. This study is carried out for static channel (no fading) conditions.

An analytical framework for interference analysis for packet radio networks employing BPSK modulation is presented in [65]. It is assumed that the system under consideration is unslotted. Therefore, interference level does not remain constant over the packet duration. In his approach towards dealing this scenario, author has quantified the performance of the unslotted system by considering an equivalent slotted system that experiences the same short term average interference.

An expression for the exact bit error probability for the detection of a coherent BPSK signal experiencing a number of asynchronous interferers in Rayleigh fading channels is derived in [66]. However, the final expression requires the use of numerical methods to get the final values. In his study, author has shown that Gaussian approximation is accurate even in the case of a single interferer when all the signals are Rayleigh faded.

A similar result is obtained in [67] also. For the BER calculations, the validity of Gaussian approximation in case of asynchronous CCI is discussed in [67]. The result of this investigation shows that in addition to the case of large number of interferers, Gaussian approximation is accurate in case of smaller number of interferers also, provided the desired signal is subjected to fading. Authors have shown that when the desired signal is Rayleigh faded, even in the presence of only one unfaded interferer, the Gaussian approximation gives acceptable results.

For ALOHA type networks that employ BPSK (or QPSK) in Rayleigh fading environment, a packet error analysis is presented in [68]. Throughput performance is also investigated for different local area environments. Closed form expressions for packet error rates, taking bit to bit error dependence into account, are derived based on the concept of the equivalent SINR.

The closed form expressions for pdf, cumulative distribution function (cdf) and characteristic function are obtained for co-channel interferers in [69] for L-level amplitude shift keying (L-ASK) modulation scheme. Expressions for error-floor for an L-ASK system with one co-channel interferer, considering transmission over an undistorted channel and matched filter reception, are also derived.

BER analysis of coherent BPSK in the presence of co-channel interferers with desired and interfering signals experiencing Nakagami fading is presented in [70]. The analysis is carried out under the assumption of slow fading, timing asynchronization and independent fading gains. However, final expressions require numerical methods for evaluation.

A probabilistic treatment for the performance of the bluetooth piconet under CCI from other bluetooth piconets is presented in [28]. Author has investigated an upper bound on the packet

error rate (PER) as well as lower bound on aggregated throughput of collocated piconets. In his work, author has assumed asynchronized piconets. Capture effect has not been taken into account.

A comparative study of some important available works are presented in Table 2.2.

Table 2.2: Summary of available works for infrastructure-less wireless networks in exiting literature.

Reference	***Summary of the work presented***	***Remark***	***Network set-up***	***MAC consideration***
Stranne *et al.* [2]	Throughput analysis of system consisting of 802.11b and Bluetooth networks	Packet level approach	Asynchronized infrastructure-less	No
Jang *et al.* [56]	Outage analysis of cognitive radio network	Packet level approach	Asynchronized cognitive network	No
Hekmat *et al.* [30]	Interference power calculation framework for ad-hoc/sensor networks	packet level approach	Synchronized ad-hoc networks	Yes
Panichpapiboon *et al.* [58]	BER calculations for sensor networks in Rayleigh fading	Packet level approach	Synchronized infrastructure-less	Yes
Mckay *et al.* [62]	Error probability and SINR analysis in Rician fading	Packet level approach	Synchronized infrastructured	No
Lavric *et al.* [63]	PER analysis for coexisting sensor, 802.15.4 and bluetooth networks	Packet level approach	Synchronized infrastructure-less	Yes
M. Chiani [64]	BER analysis of BPSK and GMSK with multiple interferes for static channel	Bit level approach	Asynchronized infrastructure-less	No
K. Hamdi [66]	BEP in presence of asynchronous co-channel interferers	Bit level approach	Asynchronized infrastructure-less	No
Giorgetti *et al.* [67]	BER calculations using Gaussian approximation in case of asynchronous co-channel interferers	Bit level approach	Asynchronized infrastructure-less	No
Hamdi *et al.* [68]	PER for ALOHA type network using bit-to-bit error dependence	Bit level approach	Slotted packet random access network	No
Sivanesan *et al.* [70]	BER analysis for coherent BPSK in Nakagami fading	Bit level approach	Asynchronized network	No
Amre El-Hoiydi [28]	Upper bound on PER and lower bound on throughput for collocated piconets without capture effect	Packet level approach	Asynchronized bluetooth network	No

2.3 Interference Analysis and Management in Heterogeneous/ Overlaid Wireless Network

This section presents the analysis and discusses the issues related to management of interference in hetrogeneous/overlaid[†] wireless network. Current demand for high data rate, efficient spectrum usage, better coverage and capacity increases the relevance of such kind of hybrid wireless networks. Out of many possible solutions, having transmitter and receiver closer to each other is one of the simplest and surest way to achieve good quality links, more spatial reuse, high capacity and coverage [14]. The most common technique used to achieve this in existing wireless networks is deployment of more infrastructure, possibly in terms of the hot spots, base stations and relays. However, these approaches may not economical. In this scenario, the recent concept of femtocells (home base stations) can be a less expensive alternative [16]. Femtocell is a cellular network low power ($10 \sim 100$ mw) access point, based on mobile technology, providing wireless voice and broadband services to customers in home or office environment [71]. These short range ($10 \sim 30$ m) base stations are installed by consumers for better indoor voice and data reception. Femtocell connects mobile devices to a mobile operator network via standard consumer broadband connection, including ADSL, optical fibers, wireless last mile technologies or separate radio frequency (RF) backhaul channel. Femtocell or femto access points are developed to provide cost effective and high bandwidth services in next generation wireless communication systems. A femtocell networks may be considered as a wireless overlaid networks, that runs (almost) independently on top of the existing (cellular) network, although supported (to an extent) by its infrastructure. Femtocells are expected to offer new services and offload traffic from existing networks [72] when properly coupled with FFR in OFDMA based cellular networks [73, 74].

2.3.1 Interference Scenarios

In overlaid networks, the (large scale) deployment of secondary network over the parent network gives rise to many technical challenges. Interference is one of the major challenge to be dealt with. In case of macrocell-femtocell network, the two-tier architecture allows us to classify the interference in two main classes [16]:

- ✦ **Cross-tier interference** : Interference among the network elements of different tiers/layers

[†]Wireless overlaid networks are heterogeneous networks, which built on top of an existing network with the purpose to implement network services that are not available in the existing network.

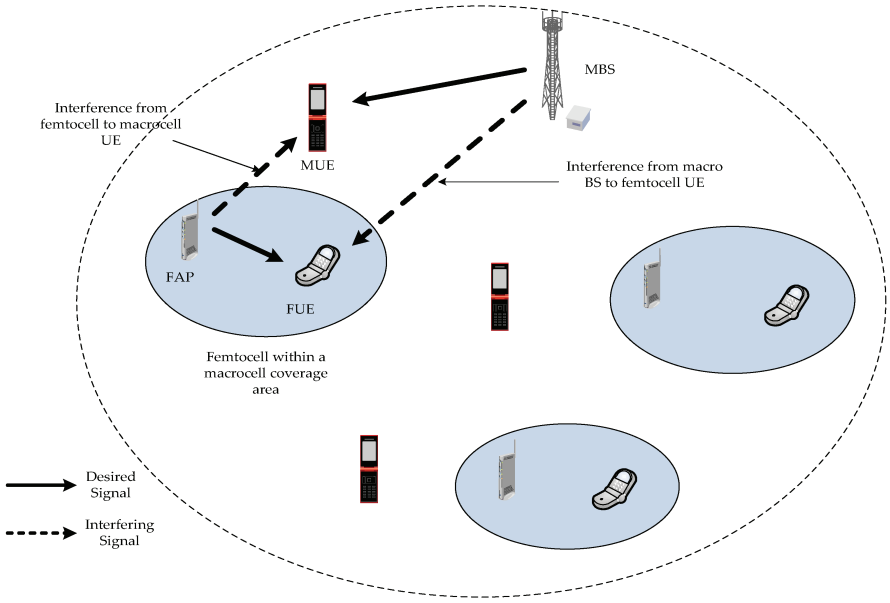

Figure 2.7: Cross-tier interference between neighbouring femtocells in a two-tier network [3].

is known as *cross-tier interference*. In case of OFDMA based femtocell network, cross-tier interference occurs between the elements of femtocell tier and macrocell tier. A possible scenario of such interference is reproduced in Figure 2.7 for the sake of completeness [3], where a femtocell access point (FAP) may cause interference to downlink of macrocell user equipment (UE). Also, a macrocell UE may cause interference at the uplink of nearby FAP. Cross-tier interference occurs only if source and victim both use the same sub channel.

- **Co-tier interference** : Interference among the network elements of same tier/layer is known as *co-tier interference*. In case of OFDMA based femtocell network, co-tier interference occurs between neighbouring femtocells. Since, femtocells use considerably low transmit power for communication purposes, co-tier interference is prominent between immediate neighbours. A possible co-tier interference scenario can be found in apartments among femtocells which are randomly deployed as per user's convenience. Some other examples of such interference may be found in between femtocell UE and neighbouring femtocell base station, where UE creates uplink interference to BS as reproduced in Figure 2.8. A femtocell BS may also act as a downlink interferer to UEs. However, these cases of interference might appear only if the two femtocells are operating with same sub channel. A proper subband allocation can be an efficient way to mitigate co-tier interference in OFDMA based femtocell networks.

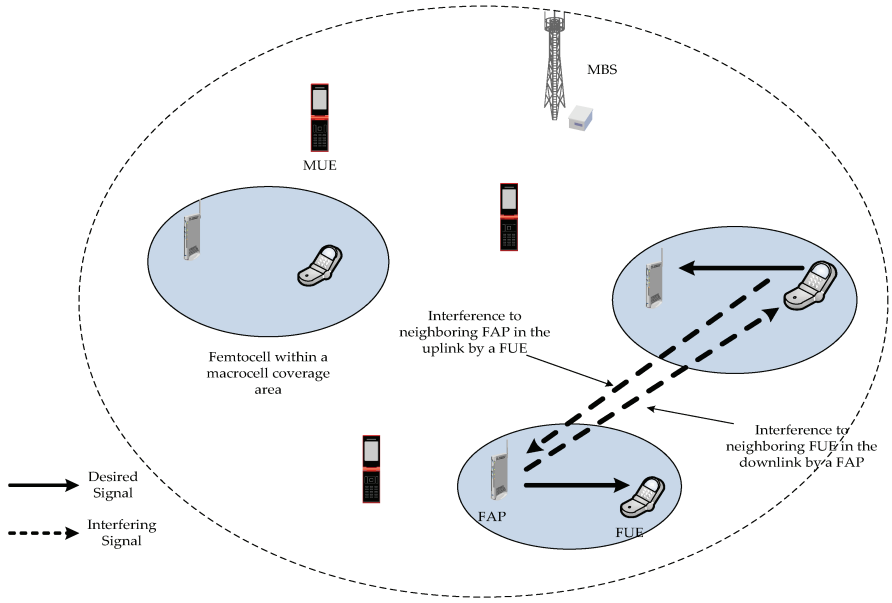

Figure 2.8: Co-tier interference between neighbouring femtocells in a two-tier network [3].

2.3.2 Issues Related to Interference Management

Before developing the strategies for the management of interference, it is important to have proper knowledge of the factors that affect the interference in overlaid wireless networks. There are many factors having critical impact on interference. Out of those factors, methods of spectrum allocation along with the techniques used to access the femtocells play a key role in deciding the impact of interference on network performance.

2.3.2.1 Spectrum Allocation Methods : Contribution to Interference

Some portion of spectrum is needed for the proper operation of these overlaid networks. This portion can be a separate part of spectrum allocated by the system designer/operator or the same portion of spectrum as used by the parent network. For example, in case of OFDMA based macrocell-femtocell two tier network, spectrum can be allocated to femtocells in two ways :

- **Separate-channel Allocation mode** : In this allocation mode, a separate channel is allocated to femtocell which is not used by the parent macrocell. Such allocation strategy helps in reducing the interference between macrocell and femtocell at the cost of spectrum. This mode is also known as *split spectrum mode* [75].

- **Co-channel Allocation mode** : Femtocell shares the same sub channel as used by the

parent macrocell. This allocation mode (also called *shared spectrum mode*) is efficient from spectrum point of view but creates excessive amount of interference. However, this mode might be favoured by the operators as assigning a separate sub channel to femtocells may be too expensive keeping the scarcity of spectrum in view. This allocation mode results in considerable increment in system capacity also, along with the higher amount of risk of femtocell and macrocell users causing interference to each other [3].

Thus, it can be observed that interference issue exists in both kind of allocation modes. A robust and efficient interference management scheme is necessary for satisfactory operation of femtocell as well as cellular networks.

2.3.2.2 Access Methods : Effects on Interference

One of the main objectives of femtocell networks is to share the load (traffic) with cellular network in order to provide better services to users. By performing this offloading, femtocell helps those users to get better QoS parameters as well as cellular BS in terms of reduced load. Strategies or methods which decide whether offloading can be executed or not, i.e. if a particular user may allowed to join a specific femtocell network, known as *access methods*. Based on the access permissions, there can be following types of access methods :

- ✧ **Closed Access** : Only a subset of users, which are registered with femtocell owner, can access the femtocell. Only owner has the right to decide as to which user can access the femtocell. This access method is referred to as closed subscriber group (CSG) by the Third Generation Partnership Project (3GPP) [76].

- ✧ **Open Access** : All users are allowed to use any nearest femtocell. This mode does not require any pre-registration with femtocell owner.

- ✧ **Hybrid Access** : This mode of access allows all users to use some limited amount of femtocell resources, while members of CSG can access all the facilities [77].

Interference in the network may dramatically get affected by the selection of access method in femtocells. In case of closed access mode, which is generally preferred by home users, any outside user near the femtocell will get excessive amount of interference if both are using the same sub channel (co-channel deployment of femtocell). The situation becomes even worse for cell edge users.

At edge locations, SINR drops drastically due to weaker signal from distant MBS but comparatively stronger interfering signal from nearby femtocell. However, closed access mode is preferable from security and privacy point of view.

Open access mode on the other hand, does not contribute much in the network interference, since it allows the near by cell user to connect with the femtocell. Therefore, minimizes the negative impact of femtocell tier on macrocell tier. Since, users are (always) authorised to connect to the near by femtocell, they positively remain connected with the strongest server and thus resulted in the improved throughput of network. Nevertheless, open access mode has some shortcomings also. For example :

- ✗ In case of mobile users, number of handovers may be significantly high which imposes burden on macrocell and femtocell as well.
- ✗ The high number of handover processes by a user moving between one femtocell to another femtocell or macrocell increases the signaling overhead as well as probability of call dropping.
- ✗ Sharing of the femtocell resources with non CSG users may reduce the performance of femtocell owner.
- ✗ Security and privacy issues may arise.

Thus, it can be observed that access methods have direct impact on the interference and hence, network designer need to select it very intelligently. Keeping in view the pros and cons of closed and open access modes, one intuitive solution comes out as hybrid access, an intermediate approach. Hybrid access method provides a compromise between the extent of access granted to non-CSG members and the impact on the performance of CSG members. This access method allows certain (outside) non-CSG members to access the limited resources of femtocell [3]. Access rules for this method must be finely and intelligently tuned, since it directly affects the performance of subscribed users. An improper access rule can lead subscribed members to think that they are paying for a services that is exploited by others also [77]. A comparative study of the three access methods is given in Table 2.3.

Table 2.3: Comparison of access methods for femtocells.

Closed Access	*Open Access*	*Hybrid Access*
Suitable for home users	For open places like cafe, hotspots, stations	For business purposes
Better service to subscribers	Nearby non-CSG members may also get benefitted	Full service to CSG and limited service to non-CSG members
Owner is responsible for billing	Place owner may charge members	Owner may nominally charge non-CSG members
Lower network throughput	Increased overall network throughput	Values in between closed and open access
Privacy and security assured	Privacy and security issues	Values in between closed and open access
No handovers	Frequent handovers	Values in between closed and open access
Higher interference	Negligible interference	Values in between closed and open access

2.3.2.3 Interference Management : Comparison with Cellular Network

Approaches for interference management for a overlaid (two-tier) network and traditional cellular (macrocell) network are quit different. In traditional macrocell networks, usually users at the cell edge get affected severely by the interference, while in overlaid networks, due to the random deployed locations of femtocells within macrocells [78], effects of interference become visible throughout the cell and no more limited to the edges only. Secondly, better spectrum utilization along with range extension are two main benefits that can be gained by femtocell deployment [79]. However, due to extended coverage, macrocell users at the edge face performance degradation due to higher interference. This shows that femtocell deployment makes interference scenarios different and complex to deal. This further advocates the importance of efficient interference management/avoidance schemes in heterogeneous/overlaid wireless networks.

2.3.3 Interference Management Strategies

As pointed out earlier that broadcast nature of wireless medium does not allow the complete removal of CCI in wireless networks, effects of interference can only be reduced with effective management schemes. Several interference management schemes are reported in the literature. A general classification can be performed as follows :

- **Cooperation based Approaches** : This approach tries to manage interference cooperatively. It involves resource coordination among interfering base stations and UE. Some of the important techniques in this category are enhanced inter-cell interference coordination (eICIC) [80], coordinated multipoint communications, joint power control [81] and slowly-adaptive interference management [78].

- **Distributed Approaches** : The other category of approaches are distributed in nature. These approaches do not require any kind of cooperation/coordination among cells and therefore, do not incur any additional overhead. Some techniques in this category are static resource partition [35], distributed power control [82], receivers with advanced functions, adaptive femtocell access [83], fractional frequency reuse, subband allocation [84] and hybrid frequency assignments [75].

2.3.3.1 Appropriate Strategies for Interference mitigation

Suitability of any approach vastly depends on various environmental/network factors. Base stations in different locations may have dissimilar infrastructure support in terms of power, backhaul connection capabilities, protocols and processing capabilities. Since, IP based backhaul connection are generally provided by third parties, femtocells also can have different connections (in terms of capacity, load, delay) towards the cellular BS. Given such scenarios, both cooperation based as well as distributed approaches for interference management might be fruitful in two-tier heterogeneous wireless networks.

Particularly, the efficiency of cooperation based approaches depends upon the ability of network to handle the inter-cell information sharing overhead which is inevitable to bring certain level of coordination among BSs and FBSs in cells. Cooperation based approaches can even perform unsatisfactory in heterogeneous networks if the way of overhead sharing is not optimized [80].

Distributed interference management approaches, on the other hand, do not rely on the overhead sharing factor. But, the performance of these schemes can be suboptimal in cases, since the optimization is local only.

2.3.4 Motivation for Our Work

Previous sections elaborate on the usefulness of two-tier overlaid wireless network as a potential solution for attaining larger coverage, high data rate, capacity and better (re)use of spectrum. As

an example, macrocell - femtocell two tier network is discussed. However, the femtocell technology is still in development phase and therefore, requires proper addressing of several issues such as interference, power control, access methods, security and hand-off. Out of these issues, we have taken the critical issue of interference which acts as a limiting factor in achieving desired outcome, for further investigation. Different aspects of interference are studied in detail such as, possible sources of interference, types of interference and some interference management approaches.

It may be observed that the problem of interference exist for both kind of deployment modes, separate as well co-channel. However, a proper allocation/selection of sub band can minimize the detrimental effects of interference up to certain extent. Keeping this in view, the optimum selection of sub band is taken for further detailed discussion. Moreover, while discussing the subband selection, we will try to address some more practical issues which are not properly touched upon in the existing available works.

2.3.5 Interference management by optimum Subband Allocation : A Practical View

An optimum subband allocation in two-tier femtocell network can be crucial from following considerations :

- ✓ Interference minimization between different femtocells as well as femtocells and macrocell.
- ✓ Smooth hand-off process for a user switching between macrocell and femtocell (or vice-versa) [75].
- ✓ Efficient (re)use of spectrum.

However, in a heterogeneous (two-tier) network, implementation of conventional frequency planning/allocation schemes is very difficult and less efficient due to random and opportunistic placement of femtocells by end user. Further, in overlaid network of femtocells, the assumption of absence of coordination/cooperation among femtocells and macrocell BS looks reasonable due to security, limited availability of backhaul bandwidth and scalability issues [84].

Few works are available on the analysis of subband allocation, frequency assignment, resource partitioning [75, 85, 86] for femtocell two-tier networks. In [85], a subband allocation analysis for FFR based OFDMA femtocells is presented along with the optimal power allocation. The study assumes a static channel scenario. Authors have concluded that optimality of a subband

for femtocell is highly dependent on the location of femtocell within the macrocell. A frequency assignment strategy is proposed in [75] for femtocells considering practical issues like hand-off, coverage and interference. In his work in [75], in order to get an optimal frequency assignment, authors have divided the macrocell into two regions : inner and outer. Co-channel operation is then allowed only in the outer region for more efficient cell search. Femtocells in inner region are not allowed to use the same subband which is used by macrocell. Different frequency planning schemes for OFDMA based cellular networks are discussed in [87]. A decentralized subband allocation scheme is proposed in [84] for two-tier network. Another decentralized algorithm for joint subband, rate and power allocation in OFDMA based two-tier femtocell network is reported in [88]. The resource allocation scheme in [88] is based on conventional FFR (also known as soft FFR) and assumes that femtocells are operating in closed access mode. A dynamic clustering based subband allocation scheme using (weighted) interference graph is investigated in [89]. Authors in [89] has provided a cognitive subband self-management mechanism to allocate the subband for the newly added femtocells. As opposed to closed access, open access may be an efficient way to mitigate cross-tier interference in femtocell networks. A resource allocation method for OFDMA femtocells is proposed in [90], assuming femtocells are operating in open access mode. The resource allocation method in [90] ensures QoS in neighboring macrocell user (MU) in dead zone as well as limits cross-tier interference to other MUs.

However, these works are carried out under the assumption of ideal network environment and perfect coordination among the femtocells and macrocell. This assumption resulted in the synchronized interference scenario, as discussed in Sec. 2.2.1. Such assumptions make the modeling simple and bring tractability from mathematical aspects but do not reflect the true practical conditions in the analysis of various network parameters and metrics. It has been recently pointed out that timing asynchronization issues often appears among various users due to practical constraint like propagation delays and timing offsets [34, 91].

Timing asynchronization issues become even more imperative in subband allocation analysis, since it consists of channel sensing to predict the level of interference present. In order to decide the optimum subband for communication purposes in an interference limited/affected environment, femtocell unit must check the level of interference present in each subband. As discussed earlier in Sec. 2.2.1, the total interference depends on the overlap mechanism of frames also. Therefore, to get

an accurate statistics about subband selection, the asynchronization issues must be included in the analysis as they result in partial overlaps of frames, which ultimately affects the total interference.

Table 2.4: Summary of available works for heterogeneous/overlaid wireless networks in exiting literature.

Reference	***Work summary***	***Resource allocation***	***Scenario***	***Propagation & timing offsets***
Guvenc *et al.* [75]	Proposed frequency assignment method for femtocells	Sub-band	Synchronized	Not considered
Chandrasekhar *et al.* [81]	Proposed a distributed utility based SINR adaptation for femtocells	Power	Synchronized	Not considered
Han *et al.* [82]	Proposed power control strategies for interference mitigation in femtocells	Power	Synchronized	Not considered
Choi *et al.* [83]	Discussed tradeoffs relating to access policies for femtocells	None	Synchronized	Not considered
Chandrasekhar *et al.* [84]	Proposed decentralized spectrum allocation policies for two-tier networks	Sub-band	Synchronized	Not considered
Lee *et al.* [85]	Sub-band and optimal power allocation for OFDMA based femtocell networks	Sub-band power	Synchronized	Not considered
Jeon *et al.* [86]	proposed a downlink radio resource partitioning scheme for two-tier cellular networks	Frequency band	Synchronized	Not considered
Salati *et al.* [88]	Proposed decentralized algorithm for joint subband, rate and power allocation	Sub-band, rate and power	Synchronized	Not considered
Li *et al.* [89]	Proposed a dynamic clustering-based sub-band allocation scheme	Sub-band	Synchronized	Not considered
Tarasak *et al.* [91]	Capacity and symbol error rate evaluations under interference and timing misalignment	None	Asynchronized	Considered
Li *et al.* [90]	Proposed a resource allocation method for open access OFDMA femtocells	Sub-band	Synchronized	Not considered

Some of the important existing works are summarized in Table 2.4.

2.3.6 Some More Issues to Address

Further, for the networks with perfect synchronization possibly due to a central entity, most of the parameters, needed for network performance evaluation, are (conditionally) deterministic in nature. While for the asynchronized networks, in the absence of centralized control, one has to develop probabilistic models to estimate those parameters for network evaluation. For example, the number of effective co-channel interferers and their location can be easily calculated for a cellular like synchronized/systemetic networks, given that how many tiers have been considered and the reuse factor. If only first tier or first and second tier or first, second and third tier of nodes are to be taken into account, respectively, then one can easily figure out that the effective number of interferers would be 6 or (6+12) or (6+12+18), respectively. But in an asynchronized scenario, randomly located nodes can have independent transmission schedules. Therefore, at any given time, the number of co-channel interferers becomes random. To estimate the number of interferers, one has to develop a probabilistic model. Moreover, there may be other independently operating network near by with no co-ordination among them. For such interfering networks also, one has to opt for a proper modeling approach since very limited data is available about them apriori.

2.4 Summary

This chapter provides an exhaustive review of works related to interference modeling that have been reported in literature. This chapter discusses the scenarios where the interference is asynchronous in nature and also highlights why existing methods cannot model properly the interference in an asynchronous network. The needs for new modeling approaches are emphasized and issues that are required to be addressed in such model(s) are also discussed. Interference Analysis and Management in Heterogeneous/ Overlaid Wireless Network has been discussed in considerable details. This chapter also sets the basis and the motivations for the analysis that are carried out in the subsequent chapters.

3

Outage Analysis of Asynchronous Interference Limited Wireless Network

Contents

In this chapter, performance of interference limited wireless networks in asynchronized environment is analyzed. Working towards one of the main objective of this thesis work, a modified model is proposed for addressing interference at bit level in un-coordinated/asynchronized wireless networks. The model calculates precisely the amount of interference by carefully addressing the overlap of transmissions which results due to frequency reuse in the network. This model lays the foundation also for our work in subsequent chapters. For the proposed model, taking MAC constraints into account, the probability of a node being in the guard zone as well as effective number of interferers are calculated. Closed form expressions are derived for a specific case. Here, rather than using unit disc model, we use link probability based model. Two-slope path loss model is used to account for path loss conditions. Finally, as a performance evaluation metric, we analyze outage performance of the network using the proposed interference model. Height of antennas also plays a key role in determining the network performance, as it affects the line of sight component. Some simulation results are presented to reflect the effects of antenna height on the network performance.

3.1 Introduction

In wireless networks, spatially distributed nodes communicate with each other over multipath fading channels. For such networks, mutual interference among links becomes a bottle-neck unless appropriate measures are taken. In licensed spectrum, however, the impact of interference on network performance can be controlled up to a considerable extent by applying interference aware topologies and robust policies by a central entity. But, the absence of a central entity among various networks and sharing of same spectrum, make the situation difficult to handle for the unlicensed case. In unlicensed spectrum, robust system design is a good option to deal with network interference [92]. Hence, an accurate interference model is required to be developed.

In recent years, interference modeling has gained a lot of interests [6, 25, 27, 29]. In the context of such interference limited wireless networks, several terminologies are used in literature which have different interpretations. Till date, physical interference model is considered to be an efficient and accurate model for analyzing interference due to its additive nature [1, 7, 21].

In large wireless networks, synchronization is difficult to achieve in the absence of central control. Being a high energy requiring process, synchronization remains a less favourable option for energy constrained networks. In this chapter, we analyze energy constrained interference limited

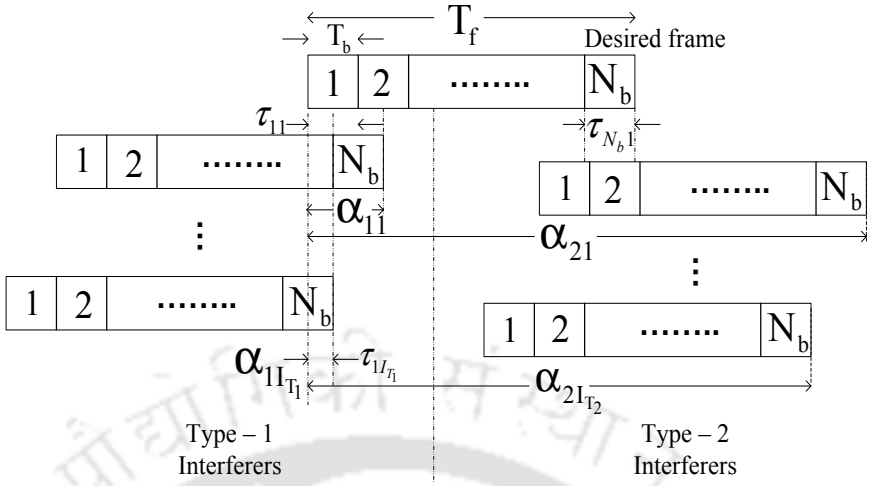

Figure 3.1: Frame overlap in an asynchronous network.

networks, in which no synchronization is assumed to exist among (groups of) the nodes. The network is considered to have independent and non-identically distributed (i.n.i.d.) interfering nodes. No assumptions have been made explicitly regarding the locations of interfering nodes such as, first/second tier of interfering nodes, equidistant interfering nodes etc. Therefore, at any desired receiver node, randomly and independently distributed interfering nodes result in interfering signals having different means and variances. In practice, such an interference scenario can be found in ad-hoc and sensor networks. Under such circumstances, independently scheduled transmission of any node can result into random frame overlap. Figure 3.1 shows the possible frame overlaps in such an asynchronized network. Frames are of duration T_f and consist of N_b bits of duration T_b. It is assumed that frame size is same throughout the network. The assumption of perfect synchronization among transmissions in many of the existing models leaves room for the development of a generic model to address the partial overlap in asynchronized environment. We propose a generic metric that addresses the partial overlap case in an asynchronized network which can also take care of the complete overlap in a synchronized network. Outage analysis for such network, is carried out using generalized moment matching (GMM) method to validate the proposed metric.

In our proposed model, for defining transmission / reception range of a node, we use a link probability based range instead of commonly used unit disk model (UDM) [29, 93]. A two-slope model [10] is used to account for distance dependent path loss and antenna height effects are also considered. Table 3.1 summarizes the notations used in this chapter.

Table 3.1: Summary of Notations

Symbol	***Description***
I_{T_1}, I_{T_2}	number of type-1, type-2 interferers
$\alpha_{1\mathrm{j}}$, $\alpha_{2\mathrm{j}}$	relative position of first bit of desired frame to last bit of jth interferer frame
τ_{ij}	extent of overlap of ith bit due to bit(s) of jth interfering frame
$P(i_{co})$, $P(i_{po})$	probability for ith bit to be completely, partially overlapped
r_z	guard zone
r_{zRx}	receiver's guard zone
$P^i_{r_{zRx}}$, $P^i_{r_{zTx}}$	probability for ith node to be in r_z of receiver, transmitter
$Tx_{r_{zRx_o}}$, $Tx_{r_{zTx_o}}$	number of transmitters inside the r_z of intended receiver, transmitter
$Rx_{r_{zRx_o}}$, $Rx_{r_{zTx_o}}$	number of receivers inside the r_z of intended receiver, transmitter

Main contributions of this chapter can be summarized as follows :

✎ This chapter proposes a classification of undesired users as type-1 and type-2 interferers from modeling perspective.

✎ It proposes a method to calculate the fractional overlap experienced by a bit of desired frame due to bit(s) of interfering frame in an asynchronous environment,

✎ It proposes an energy based metric *EINR* to quantify the ratio of desired and undesired signal energies in an asynchronous environment,

✎ Calculates the effective number of interferers taking MAC protocol into consideration,

✎ Estimates interference by taking link probability based ranges into account and analyzes the effects of number of interferers along with other important system parameters on the network outage performance.

3.2 System Model

3.2.1 Network Organization

We consider an interference limited network, where K nodes (homogeneous) are randomly distributed over an area of size $A_r \times A_r$ m^2, having the node density of $D = K/(A_r \times A_r)$ $nodes/m^2$.

At any time instant, K_s number of nodes are expected to have data to send. Under favourable conditions, these nodes may become transmitters and K_s $(\geq 1)^{\dagger}$ node pairs are assumed to be asynchronously communicating over the wireless channel. As there are more than one transmitter - receiver node pairs communicating over the same channel, each receiver node experiences interference from nearby nodes. A guard zone exists around each transmitter and receiver. With large randomly deployed network, it is important to consider average behavior of network rather than per node fairness. Therefore, network edge effects are neglected throughout the study. Node mobility is also not being considered here. In this work, rectangular pulses (in time domain) are assumed for the modelling purpose.

3.2.2 Proposed Model for Representing Interference

As discussed earlier, for analysis of interference limited network, models such as physical interference model [7] or additive interference model [21], protocol interference model [1], capture threshold model and interference range model [21] are employed under the assumption of perfect synchronization. Physical interference model calculates SINR for the network combining all incoming signals, other than the desired one, as interfering signals, whereas other models consider pairwise interference modeling for each link.

In an asynchronized network, since the transmission of a node may start at any point of time, it results into partial overlap of frames, as shown in Figure 3.1. As already pointed out, existing models do not have flexibility of addressing such partial overlap of frames effectively, up to the bit level. Taking this into consideration, we propose a new metric signal **E**nergy to **I**nterference energy plus **N**oise spectral density **R**atio (*EINR*) for analysis of interference limited wireless network at bit level as follows

$$EINR = \frac{E_d}{N_o + E_I} \tag{3.1}$$

where E_d is the bit energy of desired signal frame, N_o is noise power spectral density and E_I is the total amount of energy contributed in a bit duration T_b by all unintended frames and is given by

$$E_I = \sum_{j=1}^{K_s-1} E_j \tag{3.2}$$

where E_j is the interference energy due to jth interferer's frame. It can be shown that SINR is a specific case of *EINR* for $R_b = W$, where R_b and W are the bit rate and the bandwidth of the

†At least one node pair is assumed to be operational.

system, respectively.

Assuming bit by bit decoding, for the correct reception of ith bit, SINR corresponding to that bit should be above some predefined threshold for synchronized systems. However, in an asynchronized system, the bit of desired frame may also experience partial overlap from bit of jth interferer frame. Considering this partial overlap, we define two kind of interferers (frames) with respect to desired node (frame).

(i) Type-1 : Those unintended transmitters, whose transmission are being received by the desired receiver before the reception of first bit of the desired frame.

(ii) Type-2 : Those unintended transmitters, which initiate their transmissions some time later than the reception of the first bit of the desired frame.

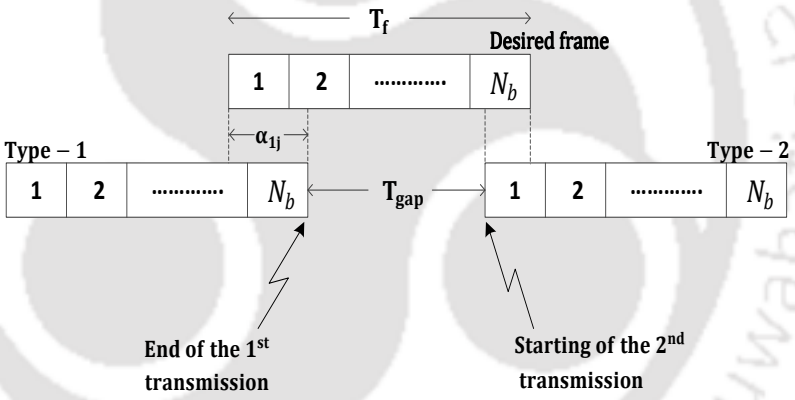

Figure 3.2: Event of simultaneous occurrence of type-1 and type-2 interferers.

For the sake of simplicity, we assume that a node cannot become a type-1 and a type-2 interferer, simultaneously. However, there may be a situation where a node becomes type-1 and type-2 interferer simultaneously. For example, in wireless networks where transmissions are event driven, if the condition $T_{gap} < (T_f - \alpha_{1j})$ becomes true, where T_{gap} is the delay between the end point of one transmission and the starting point of successive transmission, as shown in Figure 3.2, then type-1 interferers will also be called type-2 interferers.

To deal with both types of interferers, we introduce two parameters α and τ. α is uniformly distributed in range $[0,\ 2N_b]$ and τ takes on values within range $[0,\ 1]$. The range of α can be further split into $[0,\ N_b)$ and $[N_b,\ 2N_b]$, that corresponds to type-1 (α_{1j}) and type-2 (α_{2j}) interferers,

respectively, and τ_{ij} corresponds to the ith bit of frame, $i = 1, 2,.., N_b$. α_{1j} (α_{2j}) represents the relative position of first bit of desired frame with respect to the last bit of jth interferer frame, τ_{ij} gives the extent to which ith bit of desired frame is overlapped by the bit(s) of jth interferer's frame. The amount of total interfering energy depends upon received power of interfering bit(s) as well as the extent of overlap (τ_{ij}). Thus, total interfering energy (incoherent sum) for ith bit, E_{iI}, can be calculated as

$$E_{iI} = \sum_{j=1}^{I_{T_1}} P_j \, \tau_j \, T_b + \sum_{m=1}^{I_{T_2}} P_m \, \tau_m \, T_b \tag{3.3}$$

where I_{T_1} and I_{T_2} are the number of type-1 and type-2 interferers, respectively, also $I_{T_1} + I_{T_2} = K_s$-1[†] . $P_j(P_m)$ is the average power of jth(mth) interfering frame received during ith bit of desired frame. With reference to Figure 3.1, depending on the value of α_{1j} (α_{2j}), τ_{ij} can be calculated as :

$$\text{for} \quad \alpha_j < N_b : \qquad \tau_{ij} = \begin{cases} 0 & ; i > \lceil \alpha_j \rceil \\ 1 & ; i < \lceil \alpha_j \rceil \\ 1 + \alpha_j - \lceil \alpha_j \rceil & ; i = \lceil \alpha_j \rceil \end{cases} \tag{3.4}$$

$$\text{and} \quad \alpha_j \geqslant N_b : \qquad \tau_{ij} = \begin{cases} 0 & ; i < \lceil \alpha_j - N_b \rceil \\ 1 & ; i > \lceil \alpha_j - N_b \rceil \\ \lceil \alpha_j \rceil - \alpha_j & ; i = \lceil \alpha_j - N_b \rceil \end{cases} \tag{3.5}$$

where $\lceil . \rceil$ is ceiling of the argument and (3.4) and (3.5) correspond to type-1 and type-2 interferers, respectively.

Thus, *EINR* parameter based model gives us the flexibility to deal with all possible frame overlaps and hence, it gives more accurate measure of interference at a particular node.

Two important parameters of interest in the proposed model are mean overlap of the ith bit of desired frame and the expected number of effective type-1 and type-2 interferers. These statistics

[†]Under worst case assumption, all interfering transmitters are active (activity probability = 1).

will be needed in Section 3.3. Next, we develop the mathematical framework for the same :

3.2.2.1 Characterization of Overlap

- **Type-1 interferers :** The pdf of uniformly distributed random variable (RV) α is (dropping the subscript $\{j,1\}$ on α)

$$f_{\alpha}(x) = \frac{1}{N_b} \tag{3.6}$$

Assuming bitwise detection, probability that ith bit of desired frame is completely overlapped ($P(i_{co})$) by type-1 jth interferer's frame, conditioned on α

$$\begin{aligned} P(i_{co}|\ \alpha) &= P(\alpha\ \geqslant i) \qquad ;1 \leqslant i < N_b \\ &= \int_{i}^{N_b} f_{\alpha}(x)\,dx \\ &= \frac{N_b - i}{N_b} \end{aligned} \tag{3.7}$$

Also, the probability of partial overlapping ($P(i_{po})$), for given α is

$$\begin{aligned} P(i_{po}|\ \alpha) &= P((i-1) \leqslant \alpha \leqslant\ i) \qquad ;1 \leqslant i < N_b \\ &= \int_{i-1}^{i} f_{\alpha}(x)\,dx \\ &= \frac{1}{N_b} \end{aligned} \tag{3.8}$$

Therefore, the overlap of the desired ith bit due to type-1 jth interferer ($\tau_{ij}^{T_1}$), in terms of α, can be written as

$$\tau_{ij}^{T_1} = \begin{cases} 1 & \text{with} \quad P = \dfrac{N_b - i}{N_b} \\ 1 + \alpha - \lceil \alpha \rceil & \text{with} \quad P = \dfrac{1}{N_b} \\ 0 & \text{with} \quad P(\alpha < (i-1)) \end{cases} \tag{3.9}$$

Hence, the mean value of $\tau_{ij}^{T_1}$ conditioned on α becomes, $\mathrm{E}[\tau_{ij}^{T_1}|\alpha]$ = Possible values of $\tau_{ij}^{T_1}$, weighted by corresponding probabilities, where E[.] is the expected value of the argument.

$$\begin{aligned} E\left[\tau_{ij}^{T_1}|\alpha\right] &= \sum_{k=1}^{2} \tau_{ijk}^{T_1}\ P\left[\tau_{ij}^{T_1} = \tau_{ijk}^{T_1}\right] \\ &= \frac{N_b - i}{N_b} + \frac{(1 + \alpha - \lceil \alpha \rceil)}{N_b} \end{aligned} \tag{3.10}$$

Removing the condition on α, we get

$$E\left[\tau_{ij}^{T_1}\right] = \int_0^{N_b} E\left[\tau_{ij}^{T_1}|\alpha\right] f_\alpha(x)\, dx = \frac{N_b - i}{N_b} + \frac{1}{2N_b} \tag{3.11}$$

◆ **Type-2 interferers :** Probability that ith bit of desired frame gets completely overlapped by type-2 interferer's frame, conditioned on α, is given by (dropping the subscript $\{j, 2\}$ on α)

$$P(i_{co}|\ \alpha) = P(\lceil \alpha - N_b \rceil < i) \tag{3.12}$$

For type-2 interferers, $\alpha \in [N_b, 2N_b]$. So, $\lceil \alpha - N_b \rceil$ becomes a discrete uniform RV which takes integer values within the interval $[0, N_b]$ with probability mass function (pmf) $= \frac{1}{N_b+1}$. Now, (3.12) becomes

$$P(i_{co}|\ \alpha) = \sum_{j=0}^{i-1} \frac{1}{N_b+1} = \frac{i}{N_b+1} \tag{3.13}$$

Also, for a given α, the probability for partial overlapping of ith bit comes out as

$$P(i_{po}|\ \alpha) = P[\lceil \alpha - N_b \rceil = i] = \frac{1}{N_b+1} \tag{3.14}$$

Therefore, due to type-2 jth interferer, the overlap of desired ith bit, $\tau_{ij}^{T_2}$, in terms of α, can be written as

$$\tau_{ij}^{T_2} = \begin{cases} 1 & \text{with} \quad P = \dfrac{i}{N_b+1} \\ \lceil \alpha \rceil - \alpha & \text{with} \quad P = \dfrac{1}{N_b+1} \\ 0 & \text{with} \quad P(\lceil \alpha - N_b \rceil > i) \end{cases} \tag{3.15}$$

Hence, the mean value of $\tau_{ij}^{T_2}$, conditioned on α becomes

$$E\left[\tau_{ij}^{T_2}|\alpha\right] = \frac{i}{N_b+1} + \frac{(\lceil \alpha \rceil - \alpha)}{N_b+1} \tag{3.16}$$

Removing the condition on α, we can write

$$E\left[\tau_{ij}^{T_2}\right] = \frac{i}{(N_b+1)} - \frac{N_b}{2(N_b+1)} + \frac{1}{2} \tag{3.17}$$

Figure 3.3 shows the variation of expected overlap for bit of the desired frame due to type-1 (3.11) and type-2 (3.17) interferers.

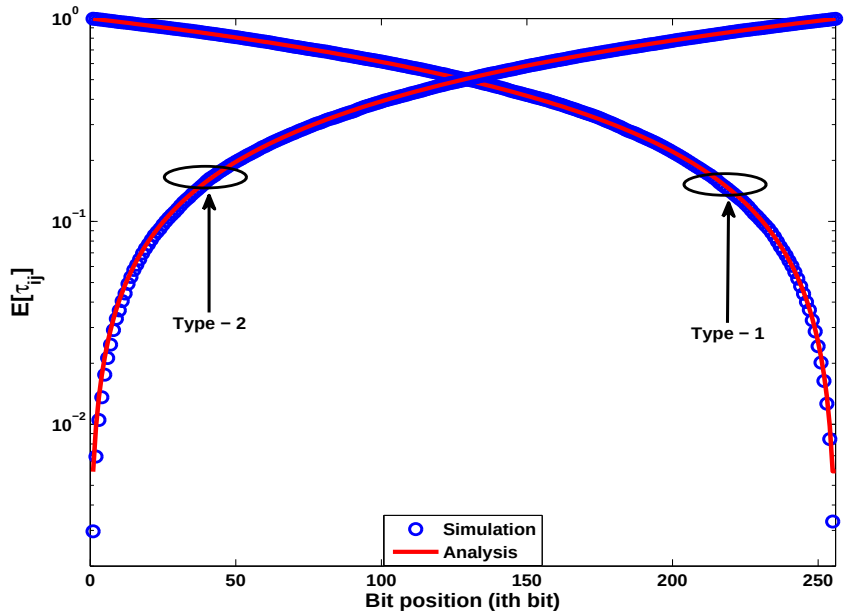

Figure 3.3: Expected overlap of ith bit of desired frame due to type-1 and type-2 interferers.

3.2.2.2 Expected Numbers of Type-1 and Type-2 Interferers

Unlike [31], where only first tier of nodes are considered as effective interferers, this work does not take any assumption while calculating effective number of interferers. A generic solution is presented here to calculate the effective number of interferers, outside the guard zone, r_z. However, assumption as in [31] may be useful in case of less dense network with high path loss exponent, where only few nodes outside the r_z act as effective interferers.

At any time instant, the effective number of interferers in the network are all transmitters except those barred by MAC protocol (lie within r_z), i.e.

$$\text{effective interferes} = K_s - \text{desired transmitter} - \text{transmitters barred by MAC protocol} \quad (3.18)$$

In a randomly deployed network, a transmitter node can be categorized as a potential interferer if the received power (P_r) from that node at receiver of interest, Rx_o, is considerably high (assuming links are reciprocal).Therefore, probability for ith transmitter node to be within the guard zone

around a receiver ($P^i_{r_{zRx}}$), conditioned on r is given by

$$\begin{aligned} P^i_{r_{zRx}}\,|\,r \;&=\; P\left[i \in r_{zRx}|\,r\right] \;=\; P\left[P_r \geqslant \Psi P_{th}|\,r\right] \\ &= \int_{\Psi P_{th}}^{P_T} f_{P_r}(p)\; dp \end{aligned} \tag{3.19}$$

where r_{zRx}, P_{th}, P_T, r and $f_{P_r}(p)$ are receiver's guard zone, detection threshold, transmitted power, distance between receiver node and interfering node and the pdf of received power, respectively[†]. The radius of guard zone can be adjusted with $\Psi \in (0, 1]$. Here, a trade-off exists between network capacity and interfering users. Large value of Ψ results in high interference energy, but the sum capacity also increases. A small value of Ψ restricts more users from transmitting, thereby keeping interference energy low but sum capacity is also reduced. To solve (3.19) further, it is assumed that the received power is lognormally distributed in shadowing environment. Using the pdf of lognormal RV in (3.19), we find

$$\begin{aligned} P[i \in r_{zRx}|\,r] &= \int_{\Psi P_{th}}^{P_T} \frac{4.343}{p\sqrt{2\pi\sigma^2}}\, \exp\left[-\frac{((p)_{dB} - m)^2}{2\sigma^2}\right] dp \\ &= \frac{1}{2}\left[erf\left(\frac{m - (\Psi P_{th})_{dB}}{\sqrt{2}\sigma}\right) - erf\left(\frac{m - (P_T)_{dB}}{\sqrt{2}\sigma}\right)\right] \end{aligned} \tag{3.20}$$

where m and σ are mean and standard deviation of corresponding Gaussian distribution. Calculations for estimated number of effective interferers are based on average signal strength which is lognormally distributed. Considering r as a uniformly distributed RV which takes values in the range $[\lambda_o, \sqrt{2}A_r]$, where λ_o and $\sqrt{2}A_r$ are signal wavelength and the diagonal distance of deployment area, respectively, removing the condition on r, we get

$$\begin{aligned} P^i_{r_{zRx}} \;&=\; P\left[i \in r_{zRx}\right] \\ &= \int_{\lambda_o}^{\sqrt{2}A_r} P\left[i \in r_{zRx}|\,r\right]\; f_r(r)\; dr \end{aligned} \tag{3.21}$$

In the absence of closed form expression for the general case of (3.21), a closed form expression is given for the special case of path loss exponents, $\eta_1 = \eta_2 = \eta$ in Appendix A.1. It is enough to say, the event that a node falls in the guard zone r_z, follows Bernoulli distribution with $P^i_{r_{zRx}} = P\left[i \in r_{zRx}\right]$. Also, if N and N_r represent the total number of nodes in the network

[†] P_T is used as the upper limit as maximum received power cannot exceed P_T, even if the transmitter is in close proximity of the receiver.

and in the guard zone, respectively, then N_r follows binomial distribution with $P[N_r = N_o] = C^N_{N_o} \left(P^i_{r_{zRx}}\right)^{N_o} \left(1 - P^i_{r_{zRx}}\right)^{N-N_o}$.

Now the number of (interfering) transmitters inside the r_z of Rx_o can be written as

$$\begin{aligned} Tx_{r_{zRx_o}} &= (K_s - 1)\, P^i_{r_{zRx_o}} \\ &= (K_s - 1) \left(\frac{\Re}{\sqrt{2}A_r - \lambda_o}\right) \end{aligned} \tag{3.22}$$

where $\Re$ is a part of the solution of (3.21) and a function of deployment area width as well as wavelength[†].

As class-2 MAC protocol (CSMA/CA with reservation)[‡] of [30] is used, transmitters having associated receivers in r_z of Rx_o do not contribute to effective interference, hence, they are considered as barred. In case of randomly distributed nodes, a node is assumed to have equal probability to become either transmitter or receiver. So, the number of receivers in the r_z (of intended transmitter / receiver) can be assumed to be proportional to the number of transmitters in the same r_z. Here, we assume the number of such receivers in the r_z of Rx_o can be given by

$$Rx_{r_{zRx_o}} = \psi_1\, (K_s - 1)\, P^i_{r_{zRx_o}} \tag{3.23}$$

where $Rx_{r_{zRx_o}}$ is also equal to the number of those transmitters, whose corresponding receivers are in r_z of Rx_o. Suitable practical value of proportionality constant ψ_1 is obtained through simulation. Therefore, the effective number of interferers from receiver's perspective ($I^{Rx_o}_{eff}$) becomes

$$I^{Rx_o}_{eff} = (K_s - 1) - \left[Tx_{r_{zRx_o}} + Rx_{r_{zRx_o}}\right] \tag{3.24}$$

Again due to MAC protocol under consideration, transmitter nodes having good link with Tx_o (intended transmitter) are also not able to transmit because of exposed node phenomenon. The number of such transmitters can be calculated as

$$Tx_{r_{zTx_o}} = I^{Rx_o}_{eff}\, P^i_{r_{zTx_o}} \tag{3.25}$$

Receiver nodes having good link probability with Tx_o are also not been able to receive the data from their corresponding transmitters. Hence, they are effectively barred and do not contribute in

[†]For comparison purpose in Figure 3.4, standard numerical techniques can be used to obtain $\Re$ in (3.22) in the absence of closed form.

[‡]Other examples of class-2 MAC protocol are MARCH [94] and S-MAC [95].

effective interference. Same as (3.23), such receivers can be calculated as

$$Rx_{r_{zTx_o}} = \psi_2 \, I_{eff}^{Rx_o} \, P^i_{r_{zTx_o}} \tag{3.26}$$

where $Rx_{r_{zTx_o}}$ also gives the number of those transmitters, whose corresponding receivers are in r_z of Tx_o. Suitable practical value of proportionality constant ψ_2 also is obtained through simulation.

Now, the number of effective interferers becomes

$$\begin{aligned} I^*_{eff} &= I_{eff}^{Rx_o} - \left[Tx_{r_{zTx_o}} + Rx_{r_{zTx_o}} \right] \\ &= (K_s - 1) \left[1 - (1 + \psi_1) \, P^i_{r_{zRx_o}} \right] \left[1 - (1 + \psi_2) \, P^i_{r_{zTx_o}} \right] \end{aligned} \tag{3.27}$$

Under the assumption of homogeneity and reciprocal links, to make situation symmetric from transmitter and receiver point of view, we take $\psi_1 = \psi_2$ and $P^i_{r_{zRx_o}} = P^i_{r_{zTx_o}}$. Under the assumptions, (3.27) simplifies to

$$I^*_{eff} = (K_s - 1) \left[1 - (1 + \psi_1) \, P^i_{r_{zRx_o}} \right]^2 \tag{3.28}$$

In case of other MAC protocols (class-1, class-3) of [30], a slight modification will be required accordingly.

Considering the worst case scenario of random transmission slots, where all transmitters outside the combined guard zone $r_{z_{Rx_o+Tx_o}}$ transmit (activity probability = 1) and create interference, it may be considered as a valid assumption that $I^*_{eff}/2$ will be of type-1 and $I^*_{eff}/2$ will be of type-2 interferers. So, $\mathrm{E}[I_{T_1}] = \mathrm{E}[I_{T_2}] = I_{eff} = \lfloor I^*_{eff}/2 \rfloor$. In practical scenario, the actual number of interferers will be even less than that of calculated in (3.28), as some of them will be further barred by the other transmitters as well. In an asynchronous environment, it is extremely difficult to account for such interferers and are not included in our analysis as well as simulation.

Figure 3.4 shows the effective number of type-1 (type-2) interferers w.r.t. total number of interferers (transmitters). Analytical results are in good agreement with simulation results. Simulation model is discussed in Section 5.4 in detail.

3.2.2.3 Exposed Node Phenomenon : A different View

In literature, exposed node phenomenon is considered as a channel capacity wasting event. But, this same event may become advantageous if looked from the interference perspective. Suppose, transmitter T_{X_1} and receiver R_{X_1} are in communication phase. Another transmitter T_{X_2}, lying

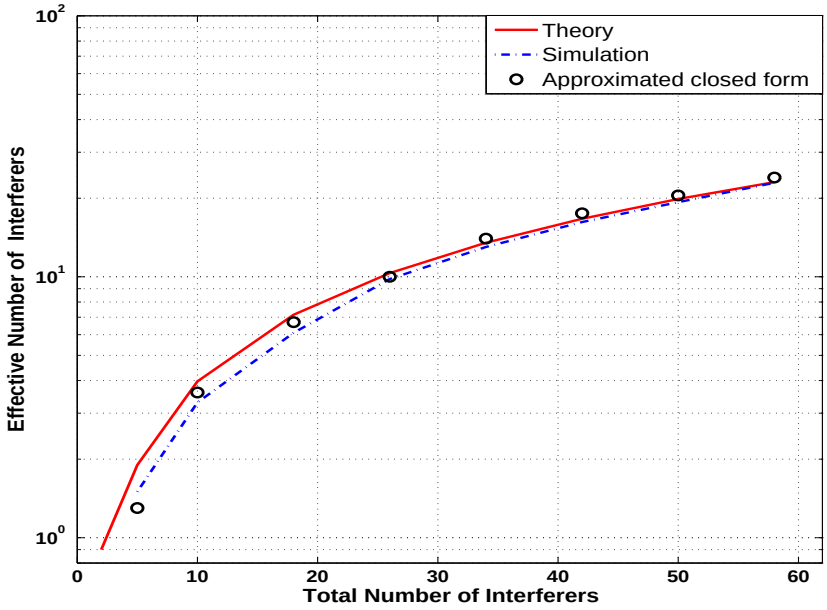

Figure 3.4: Effective number of type-1(type-2) interferers ($\psi_1 = \psi_2 = 0.8$).

within the transmitting range of T_{X_1} (R_{Tx_1}) but outside the interference range of R_{X_1}, is associated with receiver R_{X_2}. For general network, T_{X_2} may be allowed to transmit if R_{X_2} remains unaffected from transmission of T_{X_1} (class-3 MAC protocol [30]). But in interference limited network, transmission of T_{X_2} will interfere in the reception of R_{X_1}. Interfering energy received at R_{X_1} from T_{X_2} (and other such nodes) may actually lower the *EINR* (depending upon link condition). Therefore, exposed node phenomenon is actually beneficial in networks, where interference is a bottle-neck.

3.2.3 Path loss Model

In order to include distance dependent path loss exponent variation, we use two-slope (TS) path loss model [10], [96].

$$P_r = \frac{K_o}{r^{\eta_1}\left(1+\frac{r}{g}\right)^{\eta_2}} P_T \tag{3.29}$$

Two-slope model works with two path loss exponents. In shorter distances, the path loss exponent is mainly decided by η_1 (approximately 2) and for larger distances, path loss exponent primarily depends upon η_2 (values may vary from 2 to 6 depending upon channel conditions). K_o

is a system dependent constant, P_T is the transmitted power in Watt, r is the distance between transmitter and receiver in meter and g is the turning point (break point) of attenuation curve given by $g = (4h_T h_R)/\lambda_o$, where h_T and h_R are the transmitter and receiver antenna heights, respectively and λ_o is the signal wavelength. It may be noted that (3.29) is not applicable for near field region. This issue is addressed by assuming no reception within $r < \lambda_o$ [97]. A modified model has also been proposed for near field transmission [98]. For $r < g$, TS model behaves like free space propagation model and for $r \geq g$, it exhibits high signal attenuation as compared to free space.

3.2.4 Received Signal Model

Effect of shadow fading is included in our model using lognormal shadowing model [99].

$$10\log_{10}\left[P_r\right] = 10\log_{10}\left[P_r^m\right] + \varepsilon \tag{3.30}$$

where P_r and P_r^m are the received power and average power, respectively of mth node at r distance from transmitter node. P_r^m is given by (3.29). In (3.30), ε is the zero mean normal distributed RV (in dB) with standard deviation σ (in dB).

3.2.5 Link Probability Based Range and Guard Zone

As stated earlier, UDM is often used in representing the Guard zone. In practical networks, an ongoing transmission may get affected by the transmission of interfering nodes lying outside the circular guard zone, while due to shadowing effects, it may be unaffected by the transmission of some nodes lying within the range. UDM assumption [21], [93] does not take this fact into account. In our model, for a pair of nodes, if the received power is above a predefined threshold, two nodes are considered visible to each other. To incorporate the same into analysis, we take help of link probability concept [99]. In [99], the expression for link probability is calculated for power propagation path loss model. As we are using two-slope model for path loss modeling, so link probability expression under two-slope model is derived as

$$P\left(r\right) = \frac{1}{2}\left[1 - erf\left(-7.07\log_{10}\left(H^{\frac{1}{\sigma}} r^{-\frac{\eta_1}{\sigma}} \left(g+r\right)^{-\frac{\eta_2}{\sigma}}\right)\right)\right] \tag{3.31}$$

where $H = R^{\eta_1}\ (g+R)^{\eta_2}$, $R =$ limiting range to be in outage.

To control the strong interfering signals generated due to simultaneous transmissions from nearby nodes, guard zone around the communicating pair is created. This guard zone results due

to use of MAC protocols [29].

3.2.6 Channel Model

In our analysis, we are considering an asynchronized system with frequency-flat fading. Only receiver node is assumed to have complete CSI. Regarding the signals x_i transmitted by a transmitter node to the corresponding receiver, we assume that E(x_i) = 0 and E($|x_i|^2$) = 1, for i = 0, 1, 2,$\cdots$ K_s-1.

For this direct transmission setup, we define the system model by following set of equations :

$$y(t) \;=\; \sqrt{E_{sd}}\, a_{sd}\, x_o(t) \;+\; Z_{Id} \tag{3.32}$$

Here Z_{Id} includes the effect of interference from all other sources and noise term. Z_{Id} is given by

$$Z_{Id} \;=\; \sum_{j=1}^{I^*_{eff}} \sqrt{E_{jd}}\, a_{jd}\, x_j\left(t'\right) \;+\; n\left(t\right) \tag{3.33}$$

where $y(t)$ is the received signal at the destination terminal, $x_o(t)$ is the desired transmitted signal from corresponding source and $x_j(t')$ is the signal received from jth interferer, where $t \leq t' \leq (t + T_b)$, a_{sd} (a_{jd}) denotes the channel coefficient between source (interferer) and destination, modeled as zero mean circularly symmetric complex Gaussian RV with unit variance, $|a_{jd}|$ is Rayleigh distributed and $|a_{jd}|^2$ is exponentially distributed. E_{sd} (E_{jd}) is the average signal energy received at the destination terminal over one symbol duration including path loss and shadowing. In (3.33), $n(t)$ denotes system noise modeled as AWGN with power spectral density N_o.

3.3 Performance Analysis

The interference models are classified into two groups in [1]. Our model falls in the second group, which deals with the network performance affected by the interference. Based on the proposed metric *EINR* (3.1), correct reception of desired frame in terms of type-1 and type-2 interferers is possible only if

$$\frac{E_{id}}{N_o + \left(E_{I_{T_1}} + E_{I_{T_2}}\right)} \;\geqslant\; \beta \qquad ;\forall\; i \;=\; 1, 2, 3.....N_b \tag{3.34}$$

Using, (3.3), (3.29) and $E_{id} = P_{ir}\, T_b$, desired as well as interference signal energy can be written

as

$$E_{id} \;=\; P_{ir}\, T_b \;=\; \frac{K_o}{r^{\eta_1}\left(1+\frac{r}{g}\right)^{\eta_2}}\, P_T\, e^{\lambda\varepsilon}\, T_b |a_{id}|^2 \tag{3.35}$$

$$E_{I_{T_t}} \;=\; \sum_{j=1}^{I_{T_t}} P_j\, \tau_j\, T_b \;=\; \sum_{j=1}^{I_{T_t}} \frac{K_o}{r_j{}^{\eta_1}\left(1+\frac{r_j}{g}\right)^{\eta_2}}\, P_T\, e^{\lambda\varepsilon} \tau_j\, T_b |a_{jd}|^2 \tag{3.36}$$

where P_{ir}, P_j and r_j are the desired signal power, power received from jth interferer at the destination node and the distance between that interferer and destination node, respectively and t $\in$ {1, 2}. The constant λ is given by $\frac{\ln(10)}{10}$.

Using (3.35) and (3.36) in (3.34), we get

$$EINR_i = \frac{\frac{K_o}{r^{\eta_1}\left(1+\frac{r}{g}\right)^{\eta_2}} P_T e^{\lambda\varepsilon}\, T_b |a_{id}|^2}{N_o + \sum\limits_{j=1}^{I_{T_1}} \frac{K_o}{r_j^{\eta_1}\left(1+\frac{r_j}{g}\right)^{\eta_2}} P_T e^{\lambda\varepsilon_j} \left(\tau_{ij}^{T_1} T_b\right) |a_{ijd}|^2 + \sum\limits_{m=1}^{I_{T_2}} \frac{K_o}{r_m^{\eta_1}\left(1+\frac{r_m}{g}\right)^{\eta_2}} P_T e^{\lambda\varepsilon_m} \left(\tau_{im}^{T_2} T_b\right) |a_{imd}|^2} \tag{3.37}$$

which gives the accurate expression of *EINR* parameter in an asynchronized interference limited environment and for the channel model considered here.

3.3.1 Analysis Under Approximation

It is difficult to calculate pdf of *EINR*, having (3.37) in the current form. To modify (3.37), we replace I_{T_1} and I_{T_2} by their expected values E[I_{T_1}] and E[I_{T_2}] respectively[†], as derived in Section 3.2.2.2 where this is denoted as I_{eff}. With the approximation and some further modifications, (3.37) becomes

$$EINR_i = \frac{\frac{K_o}{r^{\eta_1}\left(1+\frac{r}{g}\right)^{\eta_2}} P_T e^{\lambda\varepsilon}\, T_b |a_{id}|^2}{N_o + T_b \sum\limits_{j=1}^{I_{eff}} \frac{K_o}{r_j{}^{\eta_1}\left(1+\frac{r_j}{g}\right)^{\eta_2}} P_T e^{\lambda\varepsilon_j} |a_{ijd}|^2 \left(\tau_{ij}^{T_1} + \tau_{ij}^{T_2}\right)} \tag{3.38}$$

Even in this modified form, use of (3.38) for calculation of *EINR* pdf requires the distribution of sum of lognormally distributed RVs (interference power element) with one sided random weights. To the best of our knowledge, no closed form expression for such kind of distribution is known.

[†]Justification concerning this replacement can be found in Appendix A.2.

However, in [4, 9, 100, 101] another lognormal distribution is used as an approximation for sum of lognormal RVs. To compute the mean and variance (or even higher moments) of resulting distribution, several approaches are proposed in literature [102,103]. As the present case deals with lognormal RVs with one sided random weights, so, in order to solve (3.38), we use GMM method for linear combination of lognormal RVs [31,32]. To apply GMM method, we modify (3.38) as

$$EINR_i = \frac{|a_{id}|^2}{\left(\frac{r^{\eta_1}\left(1+\frac{r}{g}\right)^{\eta_2} N_o}{K_o P_T T_b}\right) e^{-\lambda\varepsilon} + \sum_{j=1}^{I_{eff}} \left(\frac{r}{r_j}\right)^{\eta_1} \left(\frac{g+r}{g+r_j}\right)^{\eta_2} |a_{ijd}|^2 \left(\tau_{ij}^{T_1} + \tau_{ij}^{T_2}\right) e^{\lambda(\varepsilon_j-\varepsilon)}} \tag{3.39}$$

which can further be written in compact form as

$$EINR_i = \frac{|a_{id}|^2}{\Upsilon_o e^{-\lambda\varepsilon} + \sum_{j=1}^{I_{eff}} \Upsilon_{ij}\ e^{\lambda(\varepsilon_j-\varepsilon)}} \tag{3.40}$$

where

$$\Upsilon_o = \left(\frac{r^{\eta_1}\left(1+\frac{r}{g}\right)^{\eta_2} N_o}{K_o P_T T_b}\right)$$

$$\Upsilon_{ij} = \left(\frac{r}{r_j}\right)^{\eta_1} \left(\frac{g+r}{g+r_j}\right)^{\eta_2} |a_{ijd}|^2 \left[\tau_{ij}^{T_1} + \tau_{ij}^{T_2}\right]$$

Denominator of (3.40) is a combination of lognormal RVs weighted by one-sided RVs. Here, we take a lognormal approximation for the denominator as

$$\Upsilon_o e^{-\lambda\varepsilon} + \sum_{j=1}^{I_{eff}} \Upsilon_{ij}\ e^{\lambda(\varepsilon_j-\varepsilon)} = e^{\lambda\hbar_i} = \widetilde{N} \tag{3.41}$$

where $\hbar$ is a Gaussian RV, whose mean and variance can be calculated through GMM method (details are given in Appendix A.3) and $\widetilde{N}$ is the combination of $(I_{eff}+1)$ RVs with random and independent weights. Now, the $EINR_i$ can be re-written as

$$EINR_i = \frac{|a_{id}|^2}{e^{\lambda\hbar_i}} \tag{3.42}$$

i.e., in form of a ratio between two RVs, the numerator is a unit mean exponential RV and denominator is a lognormally distributed RV.

3.3.2 Outage Probability Calculation

This section calculates the outage probability to observe the effects of interference on network performance using EINR parameter. The outage probability is defined as the probability that received SINR (in our case *EINR*) falls below some specified threshold β. Outage probability, P_{out} can be written as

$$P_{out} = P\left(EINR < \beta\right) \tag{3.43}$$

If the received *EINR* for a bit falls below the threshold β, bit is considered lost. Threshold β is a dimensionless quantity, depends on the specific application's QoS. It may be noted that while dealing with *EINR* parameter, we essentially talk of outage at the bit level. Using (3.42) and (3.43), P_{out} for ith bit can be written as

$$P_{out}^{bit_i} = P\left[\frac{|a_{id}|^2}{e^{\lambda h_i}} < \beta\right] \tag{3.44}$$

Using corresponding pdf expressions, The pdf of *EINR* can be written as [104]

$$f_{EINR_i}(w) = \int_0^{\infty} \frac{1}{\sqrt{2\pi}\sigma_{\lambda h_i}} \exp\left(-\frac{\left(\ln \widetilde{N} - m_{\lambda h_i}\right)^2}{2\sigma_{\lambda h_i}^2}\right) \exp\left(-w\,\widetilde{N}\right) d\widetilde{N} \tag{3.45}$$

Therefore, the outage probability expression becomes

$$P_{out}^{bit_i} = \int_0^{\beta} f_{EINR_i}(w)\, dw \tag{3.46}$$

In the absence of closed form expression for (3.46), standard numerical techniques [105] can be used to obtain outage probability.

With the outage probability calculated above, the probability of success can also be estimated as

$$P_{suc}^{bit_i} = 1 - P_{out}^{bit_i} \tag{3.47}$$

Therefore, the total number of bits received throughout the network is given by, total received bits $= K_s \times \mathrm{F}_T \times \mathrm{N}_b \times P_{suc}^{bit_i}$, where F_T represents the total number of frames sent by a user node.

The probability of packet (frame) outage can be easily obtained where transmission of bits can be assumed to be independent. If the transmission of bits are not independent, more rigorous

treatment is needed, which is not considered here. However, simulation results are presented for packet outage probability, interference energy per packet and packets received successfully.

Table 3.2: Simulation parameters

Parameter	***Value***
Number of nodes (K)	1000
Area ($A_r \times A_r$)	2000×2000
Transmission power (P_T)	0 dBm
Transmission range	400 m
Frame length (B/F)	128, 256 bits[†]
Bandwidth	4 MHz
Path loss exponents (η_1, η_2)	3, 4
Sigma (σ)	0, 9
Threshold (β)	$-20dB, -60dB$

3.4 Numerical Results

In this section, various numerical results are presented for validating the proposed model and use of GMM method for ad-hoc and sensor network scenario. Simulation results are compared with analytical results for some representative cases. To check the performance of our model, we have simulated the complete network with the parameters given in Table 3.2. K nodes are generated randomly over an area of $A_r \times A_r$ m^2. Randomly selected K_s transmitter nodes are then paired with receiver nodes based on the transmission (reception) range criteria. Following the class-2 MAC protocol, r_z is defined around the communicating pairs using link probability $P(r)$. Under the assumption of no central synchronization, nodes outside the r_z are free to schedule their transmissions at any time. A bit is declared in outage if the calculated $EINR$ metric is below the threshold.

Outage probability related results are presented first. Numerically, we have estimated the *A*verage *O*utage *P*robability of *N*etwork per *N*ode (P_{AOPNN}), defined as,

$$P_{AOPNN} = \frac{\text{Total lost frames / Total sent frames}}{\text{Number of users}} \tag{3.48}$$

Along with outage probability, number of frames received by individual nodes as well as for the

[†]We have observed that frame length has a huge impact on simulation time with the resources available. Therefore, to complete the simulation within feasible time, relatively smaller number of bits are considered here for illustration purpose for the frame length.

network will also be discussed. Further, behavior of interference energy will also be presented. The effect of antenna height on network performance is studied through simulation.

3.4.1 Effect of Number of Interferers

Figure 3.5 shows the P_{AOPNN} w.r.t increasing number of concurrent transmissions for two threshold values. It can be observed that as the number of concurrent transmissions increases, outages probability approaches some limiting value. Intuitive explanation comes from the interference averaging effect [106, 107], which states that when the number of users are very large, variance reduces noticeably due to law of large numbers [104].

For comparison purpose, performance of power law propagation model (PLP model, $P_r = P_o\ (r_o\ /\ r)^{\eta}$, [6]) is also given with $\Psi_{TS} < \Psi_{PLP}$ and $\Psi_{PLP_{-60}} < \Psi_{PLP_{-20}}$. In interference free environment, where performance becomes independent from number of concurrent transmissions, PLP model is found to underestimate the performance due to distance-independent path loss exponent. Two-slope model takes care of the path loss exponent variation with distance which results into higher outage. In interference limited environment, PLP model gives higher values of outage probability than TS model for large threshold value. This behavior is again due to constant path loss exponent, that results into very high interference energy from other transmitting nodes in the network, which in turn gives very low *EINR* values. With TS model, interference energy keeps on decreasing for distant interfering nodes hence, it provides higher *EINR*. However, the behavior of approaching some limiting value due to law of large numbers can be observed in both the models. It may be noted that the PLP model behavior is different at lower value of threshold due to larger r_z.

Analytical results closely follow the simulation results for bit level calculations as shown in Figure 3.5(a). Minor differences in the results are due to the approximations used in the analytical formulation and the dispersion of random weights [31].

Reduction of variance in interference energy for the case of large number of interferers under high interference regime can be observed in the form of saturation in Figure 3.6. Again, it is apparent that PLP overestimates the interference energy. The effect of frame size can also be observed from the results. Small frames perform better as compared to large frames as they are less prone to errors. It may be noted that if shadowing effect is not included, both TS and PLP model underestimate the network performance.

Increasing the number of concurrent transmissions has the effect of reducing the average number

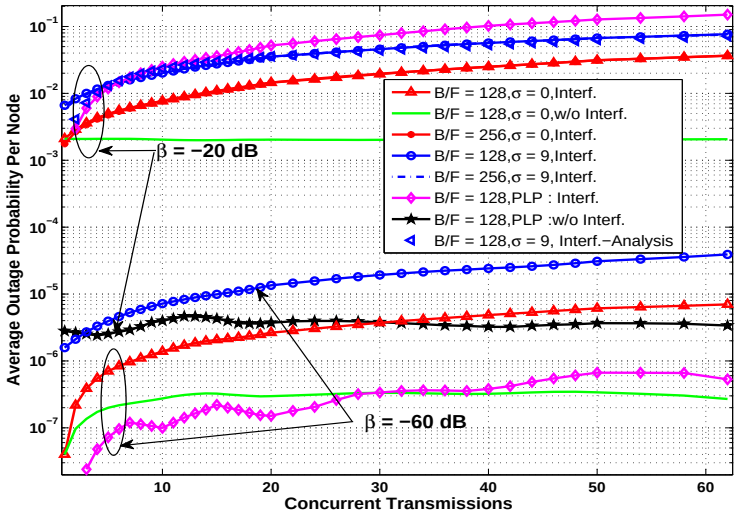

(a) Bit-wise

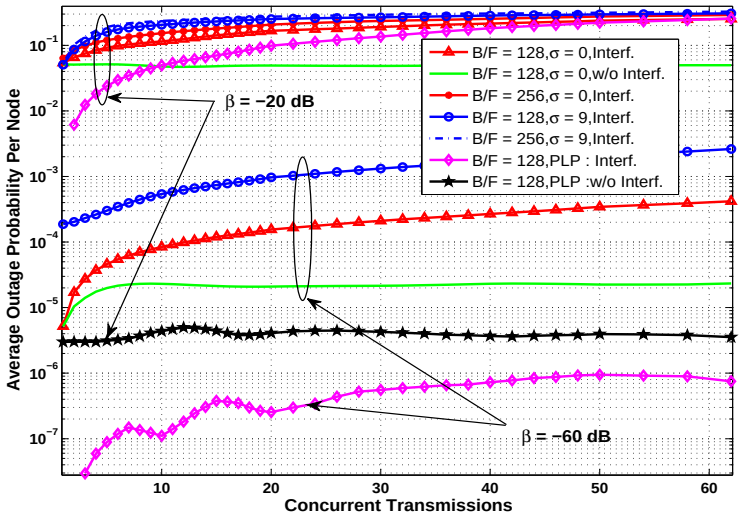

(b) Frame-wise

Figure 3.5: Outage performance (a) bit-wise (b) frame-wise under interference (Interf.) limited asynchronous environment. For β = -60 dB, $P^{PLP}_{AOPNN,w/o\ interf.} \approx 0$ (not shown in the curve).

of successfully received frames for the individual nodes, but considering network as a whole, the total number of successfully received frames increases. This can be observed from Figure 3.7 and Figure 3.8. Figure 3.7 delineates the variation of number of successfully received frames per node with increasing number of cuncurrent transmissions. Figure 3.8 shows the total number of correctly received bits and frames over the entire network as a function of increased number of concurrent

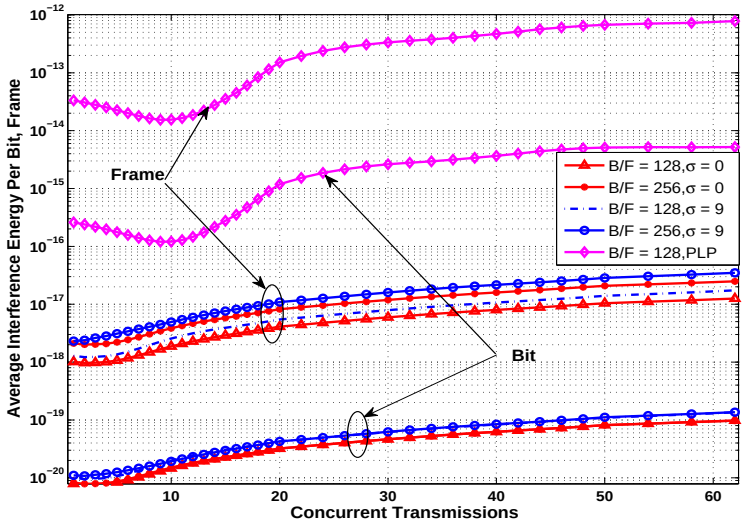

Figure 3.6: Average interference energy per bit, frame (β = -20 dB).

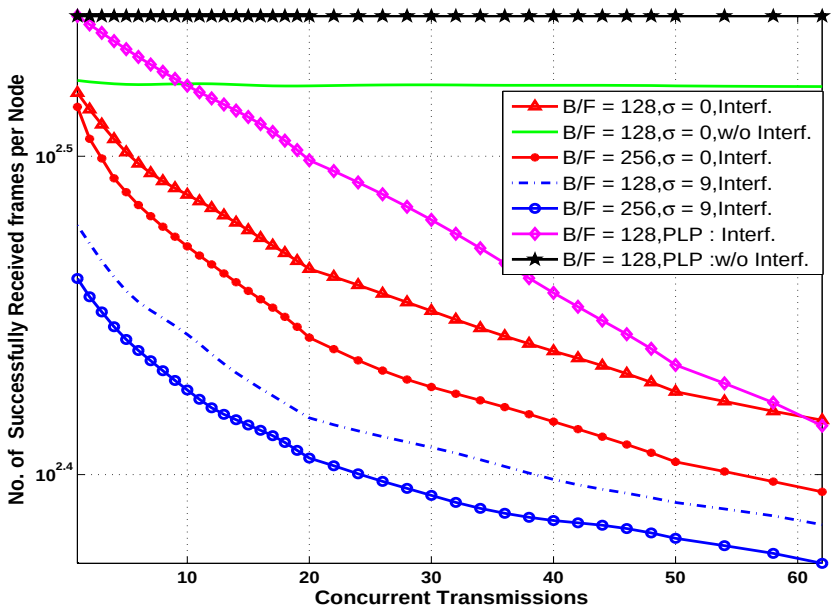

Figure 3.7: Successful frames reception per node in interference (Interf.) limited asynchronous environment.

transmissions. Results related to correctly received bits are compared with analytical results also.

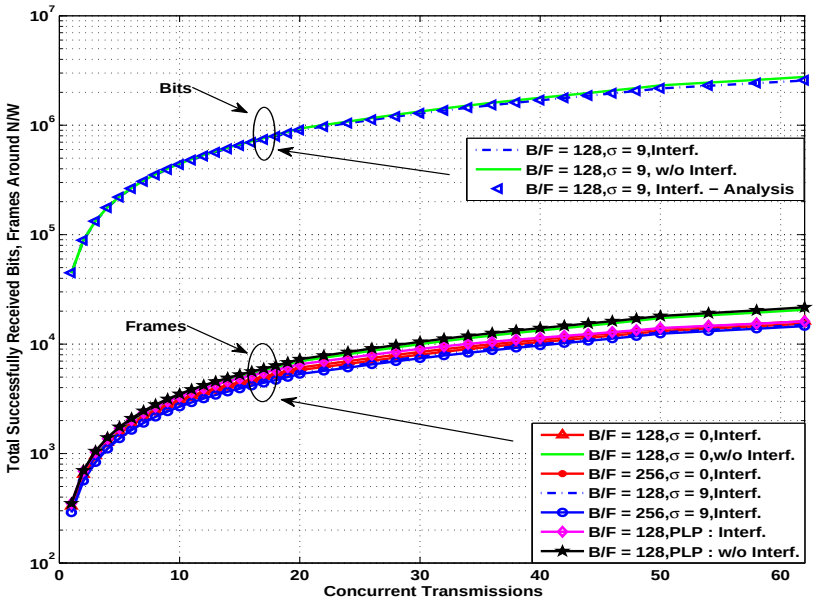

Figure 3.8: Successful reception of bits, frames throughout the network in interference (Interf.) limited asynchronous environment.

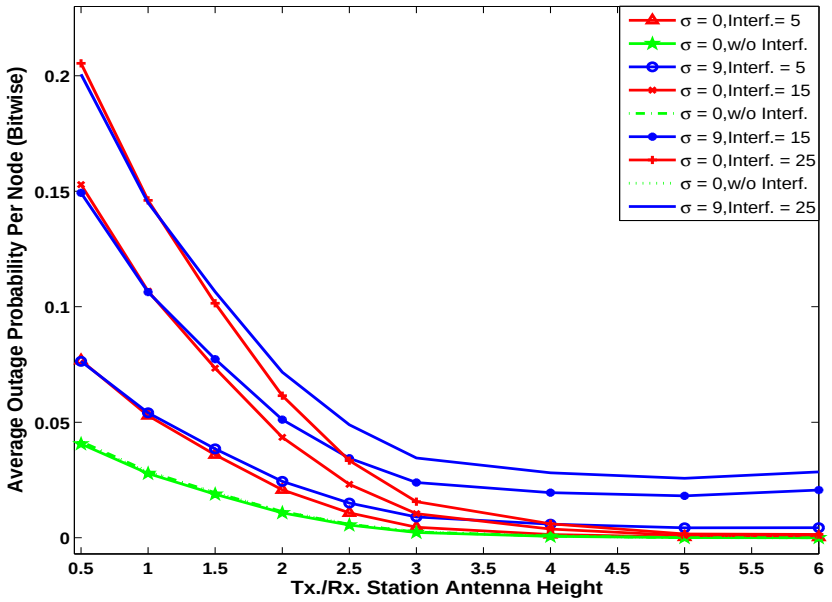

Figure 3.9: Bit-wise average outage performance for different number of interferers (Interf.) under interference limited asynchronous environment .

3.4.2 Effect of Antenna Height

This section discusses the effect of antenna height on the network performance for the same network considered in the previous section. For simulation purpose, it is assumed that antenna heights of transmitter and receiver node are same, *i.e.* $h_T = h_R$. Figure 3.9 shows the bit-wise P_{AOPNN} with variable antenna heights. Figure 3.10 gives the number of total successfully received frames throughout the network with variable antenna heights. Both, the shadowing as well as non-shadowing environment cases are considered for the sake of comparison. It can be seen from the simulation results that improved outage performance is obtained under shadowing environment at low antenna heights.

Figure 3.11 shows the average frames received per network node with variable antenna heights for different number of interferers. Unlike the last section (observation w.r.t. variable number of interferers), here network-wide as well as single user performance improves with increase in antenna height. In this figure, two regions can be seen : the interference limited region (low antenna heights) and transmission capacity limited region (large antenna heights).

It may be noted that keeping the antenna very low results in performance degradation due to poor *EINR* but after a certain height, the amount of improvement becomes marginal. So, this study also provides an insight into the practical height at which a node is to be placed, for a given set of network parameters.

3.5 Comparison with Existing works

To the best of our knowledge, the scenario and the modeling approach reported in the chapter is not available in any literature. Therefore, direct comparison of our results with any existing work is not feasible. As we have already mentioned, the works which are very close to ours [2, 65] used different approach for modeling. However, the model proposed in this thesis can also address the synchronous case, for which the results are available in the existing literature. Therefore, we present a comparison of the performance of our model for this specific case with results available in existing literature. For a given number of interferers, interference experienced by a bit of desired frame will always be greater in a synchronous case as compared to the asynchronous case. The number of interferers creating interference to the desired bit are equal to the effective number of interferers in synchronous case, where as asynchronous case consists of number of interferers always

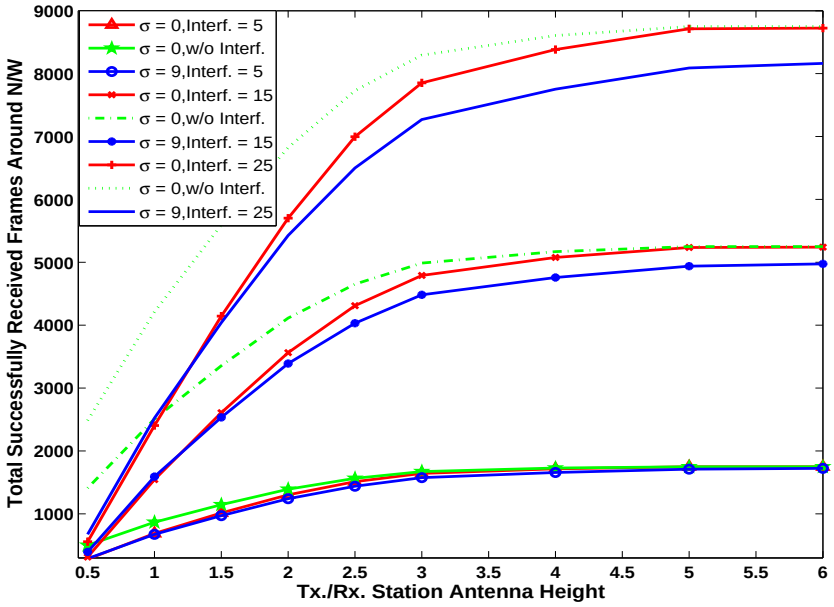

Figure 3.10: Successfully received frames around the network for different number of interferers (Interf.) under interference limited asynchronous environment .

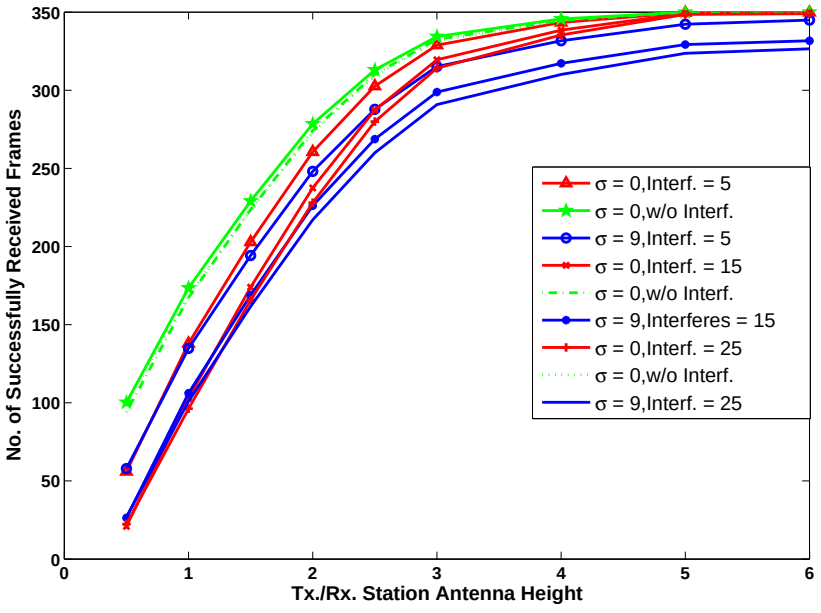

Figure 3.11: Average number of frames received per node for different number of interferers (Interf.) under interference limited asynchronous environment.

less (or equal to) than the effective number of interferers.

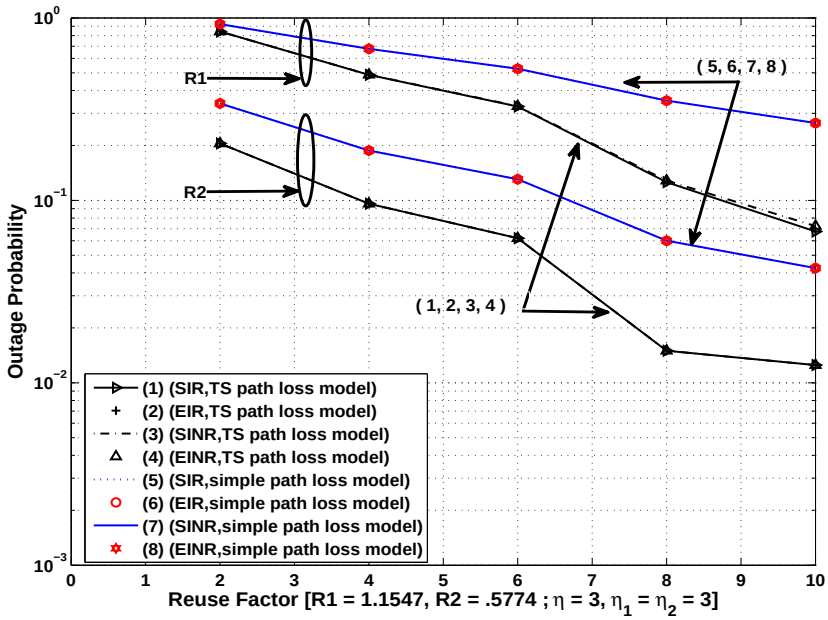

Figure 3.12: Outage performance versus reuse factor (R1, R2) for $\eta = 3$.

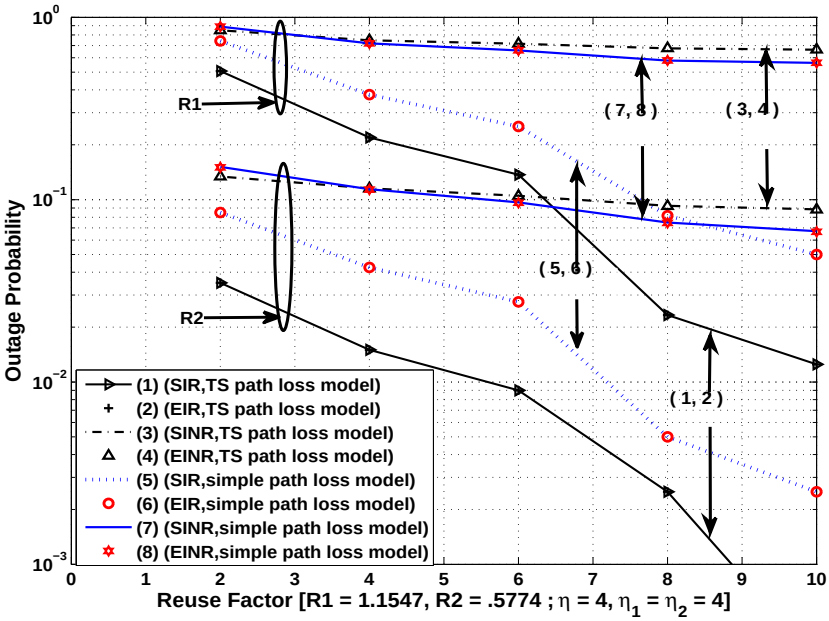

Figure 3.13: Outage performance versus reuse factor (R1, R2) for $\eta = 4$.

Figure 3.12 and Figure 3.13 show the comparison results for outage probability of cellular network with complete overlap of undesired frames. SIR plots represents the performance given

in [31], Figure 2(a). We have also obtained the outage performance for the same scenario with our EINR based model. The performance with EINR (SINR) and EIR (SIR) for both simple path loss model and with two-slope model have also been provided. EIR, SIR and EINR, SINR plots are in good agreement. For path loss exponent 3, interference power (energy) dominates. Outage performance with EIR (SIR) and EINR (SINR) are similar. However, for higher path loss condition (= 4), interference power becomes small compared to noise power. Even under such conditions, outage performance based on our model, EIR and SIR [31] are similar. Same observations can be made for outage performance based on EINR (SINR). It may also be observed from the figures that for given reuse factor, outage is higher for EINR (SINR) as compared to EIR (SIR) which is because of considering and not considering the effect of noise. Further with the increase of reuse distance, the plots corresponding to EINR (SINR) changes very slowly as compared to the plots corresponding to EIR (SIR). This is because of the fact that while interference is affected by reuse distance, noise is not.

3.6 Conclusion

In this chapter, a new metric *EINR* is used to study the performance of interference limited asynchronized wireless networks. A modified network model is proposed to handle such interference limited asynchronous network. As the proposed *EINR* metric addresses the frame overlap among desired and interfering frames during reception, using this metric, interference can be estimated with fair amount of accuracy. This metric can be used to analyze both synchronized as well as asynchronized networks. Moreover, by classifying the interferers into type-1 and type-2 categories, additional insights are obtained regarding their individual effects on the desired frame. Taking MAC constraints into consideration, effective number of interferers is calculated and a closed form expression is found for the special case of $\eta_1 = \eta_2 = \eta$. Exposed node phenomenon is discussed from interference perspective. Use of two-slope path loss model, link probability based range and inclusion of MAC protocol as well as shadowing effect in interfering environment is found to provide better characterization of the network as compared to models that employ simple path loss conditions. In case of sensor network, using the proposed model for a given set of network parameters, the required number of active users satisfying specified performance criteria can be determined.

The work presented in this chapter, particularly deals with the composite fading scenario. For this case, accumulated interference may be assumed to be Gaussian distributed (as an approximation), but, we have followed a more general approach (GMM method) for mathematical analysis, which can handle non Gaussian cases also. Moreover, in case of composite fading, Gaussian assumption is reported not to be accurate [32, 108–110].

Therefore, an important outcome of this investigation is the formulation of an analytical framework for analyzing asynchronized wireless network in an interference limited environment. The investigation reported in this chapter can be useful in the analysis of large wireless networks where synchronization is not possible centrally among (groups of) user nodes.

4

BER Analysis of Asynchronous Interference Limited Wireless Network

Contents

The previous chapter dealt with outage performance of wireless networks considering asynchronized interference. Another important network performance evaluation parameter is the BER. This chapter introduces BER analysis of an asynchronized wireless network in the presence of i.n.i.d. interferers employing the BPSK scheme. For BER calculations, an alternate method/model is developed, since the model proposed in the previous chapter for outage analysis is an energy based model and it does not take sign of the interfering bit(s) into account (which is an essential factor to be considered in BER calculations). The *EINR* model is suitable for those approaches which does not take sign as a primary factor into consideration while quantifying interference, such as, energy (power) based methods.

In this chapter, a method is presented to calculate the index and the extent of overlap for the bit(s) of individual interfering signals. Taking into account the partial overlap of the bits, the pdf of effective signed fractional overlap variable is derived. The pdf of the resultant amplitude of asynchronized interfering signal is calculated using an amplitude metric based approach. A closed form expression for BER is also derived. While calculating the BER, the overlap of frames due to frequency reuse in the network is addressed carefully. The effect of the number of concurrent transmissions (active users), interference range factor and size of deployment area on the network performance is investigated. Analytical results are verified through simulation studies.

4.1 Introduction

We have previously discussed that in decentralised wireless networks, achieving synchronization is a difficult task. For such networks, as already mentioned, absence of the central entity leads to asynchronized transmission schedules resulting in random overlap of frames, if frequency reuse is employed. Such asynchronized transmissions can affect the performance of an individual node and the network as a whole, as shown in chapter 3. Due to broadcast nature of wireless channel, though it is not possible to completely remove the deleterious effects of interfering signals, however, such effects may be reduced to a considerable extent by adopting proper system design approach. Interference robust network design calls for proper insight into the interference mechanism which takes place in such asynchronized networks as well as accurate analysis and modeling of the same.

As discussed in chapter 2, several works [2, 55, 64–69] are available in literature which address different issues related to asynchronized transmissions in a network. However, most of them are

packet based approaches. and based on assumptions such as static channel, independent and identically distributed (i.i.d.) interferers. Effect of MAC protocol on over all interference in networks is also not investigated adequately.

While previous chapter analyzes outage performance for an interference limited asynchronized wireless network using an *EINR* parameter based model, this chapter analyzes the BER performance of such network. Typical networks which exhibit properties similar to one considered in this thesis may include the cases such as a large number of networks operating in close vicinity of each other resulting in inter-networks interference [8, 63], sensor network covering a large deployment area giving rise to intra-network asynchronized interference, cognitive radio networks where the secondary network is asynchronous with primary network [55, 56] etc. In the analysis presented in this chapter, an amplitude metric based approach [70, 111] is used to evaluate the BER performance. To improve the accuracy of the BER estimation as compared to the ones available in the existing literature, the effect of MAC protocol is included in the model also in the form of a guard zone around the communicating pair of nodes. Such a guard zone plays an important role in an interference limited environment. The effective number of interferers and hence, the amount of interference becomes dependent on the class of MAC protocol (class 1, 2 and 3, as in [30]) used. The effect of the guard zone on various network parameters is discussed in detail in the section 4.4. As before, the two-slope path-loss model is used so path loss variation over a large deployment area is reflected properly. Here, the pdf of the effective signed fractional overlap variable is calculated first as an intermediate step, then considering Rayleigh fading as a special case, pdf of the resultant amplitude of interference signal is calculated. Invoking the central limit theorem (CLT), closed form expression is derived for the BER taking into consideration the effects of various network parameters on the system performance. The theoretical BER performance is validated through simulation studies.

Main contributions of this chapter can be summarized as :

- ✎ This chapter proposes a method to calculate the index and the fractional overlap resulted due to a bit of interfering frame to a bit of desired frame in an asynchronous environment.
- ✎ Determines the pdf of asynchronous interference signal amplitude as a function of basic parameters of the network for a Rayleigh faded environment,
- ✎ Analyzes the effects of interference range along with other important network parameters on

the network performance.

4.2 System Model

The set-up of asynchronous network under consideration is same as presented in chapter 3. In such an asynchronous network, the desired frame may experience partial as well as complete overlap from the interfering frames resulting due to the random transmissions from other nodes in the network. Figure 4.1 shows the possible frames overlap in such an asynchronized network. It may be noted that this is a modified version of Figure 3.1 in chapter 3, where appropriate changes are made keeping in view the analytical approach followed in this chapter.. The terms T_f, T_b and N_b denote the frame duration, bit duration and the number of bits in a frame, respectively. For this analysis also, we assume that the frame size is same throughout the network. The upper row of numbers shown within the frame $(1, 2, ..., N_b)$ indicates the bit position and the lower row $(-1, +1, ..., -1)$ indicates the sign of that bit. As in chapter 3, framework presented in this chapter also, uses rectangular pulses for modelling purpose. To analyse the BER of such an asynchronous network, we propose a method for calculating the index(s) and the overlap(s) of interfering bit(s) in an accurate manner.

Those symbols used in the analysis carried out in this chapter are summarized in Table 4.1.

Table 4.1: Summary of Notations

Symbol	***Description***
I_{T_1}, I_{T_2}	number of type-1, type-2 interferers
I^*_{eff}	total number of effective interferers
$\alpha_{1\text{j}}$, $\alpha_{2\text{j}}$	relative position of the first bit of the desired frame to the last bit of the jth type-1, type-2 interferer frame
b_1^I, b_2^I	index (position) of the interfering bit 1, bit 2
$O_1^{\alpha_{1\text{j}}}$, $O_2^{\alpha_{1\text{j}}}$ ($O_1^{\alpha_{2\text{j}}}$, $O_2^{\alpha_{2\text{j}}}$)	amount of overlap of the ith desired bit due to two consecutive interfering bits of type 1 (type 2) jth interfering frame
$S_{b_1^I}$, $S_{b_2^I}$	sign of the first, second interfering bits
γ_j^{s,T_1}, γ_j^{s,T_2}	amount of the effective signed fractional overlap for type 1, type 2 interferers
G^I, G_n^I	Gaussian RV for noise free, noisy environment

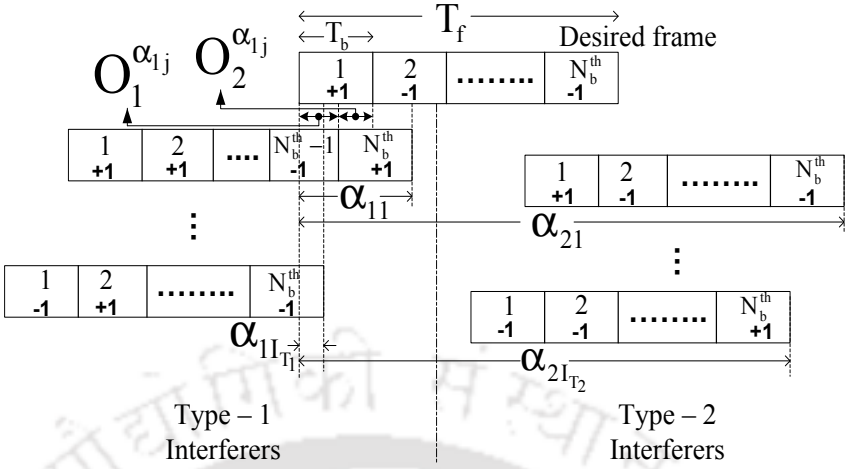

Figure 4.1: Random frames overlap in an asynchronized wireless network.

4.2.1 Statistics of the Proposed Model

As shown in Figure 4.1 and already mentioned in the previous chapter, the type-1 interferers refer to those ongoing transmissions which are not completed before the transmission of the first bit of the desired frame, while the type-2 interferers correspond to the transmissions which start when the desired frame is still getting transmitted. Assuming α_{1j} (α_{2j}) to represent the relative position of the first bit of the desired frame with respect to the last bit of the jth type -1 (type -2) interfering frame, the position (index) of the interfering bit(s) and the corresponding overlap(s) of the jth undesired frame for the ith[†] bit of the desired frame due the type-1 interferers can be written as (omitting the subscript $\{j, 1\}$ on α)

$$b_1^I \begin{cases} = i + N_b - \lceil \alpha \rceil & ; \quad \forall \quad i \leqslant \lceil \alpha \rceil \\ = 0 & ; \quad \text{otherwise} \end{cases} \tag{4.1}$$

$$O_1^{\alpha} = \alpha - \lfloor \alpha \rfloor \qquad ; \quad \forall \quad b_1^I \neq 0 \tag{4.2}$$

$$b_2^I \begin{cases} = i + N_b - \lfloor \alpha \rfloor & ; \quad \forall \quad i \leqslant \lfloor \alpha \rfloor \\ = 0 & ; \quad \text{otherwise} \end{cases} \tag{4.3}$$

$$O_2^{\alpha} = 1 - \alpha + \lfloor \alpha \rfloor \qquad ; \quad \forall \quad b_2^I \neq 0 \tag{4.4}$$

[†]Since we are considering one desired bit at a time, i is not considered as a part of the symbols to keep representation simple.

where b_1^I, O_1^α, b_2^I and O_2^α denote the position of the first interfering bit, its overlap with the desired bit, position of the second interfering bit and its overlap with the desired bit, respectively. Symbols $\lceil . \rceil$ and $\lfloor . \rfloor$ represent ceiling and flooring of the argument, respectively. The interfering bit(s) and corresponding overlap(s) for type-2 interferers can also be found from (4.1)-(4.4) with modified condition on i in (4.1) as $i > \lceil \alpha - N_b \rceil$ and in (4.3) as $i > \lfloor \alpha - N_b \rfloor$ for the interfering bits b_1^I and b_2^I, respectively. As mentioned in the previous chapter, in (4.1)-(4.4), α is a RV, uniformly distributed in the range $[0, 2N_b]$. The ranges of α corresponding to type -1 and type - 2 interferers are $[0, N_b)$ and $[N_b, 2N_b]$, respectively. It may be noted that for $\alpha_{1\mathrm{j}} \in I$, $b_1^I = b_2^I$ (shows complete overlap of desired bit by single interfering bit, similar to synchronous scenario) and $O_1^\alpha = 0$, $O_2^\alpha = 1$. For $\alpha_{1\mathrm{j}} \notin I$, any two consecutive bits (b_1^I, b_2^I) of interfering frame affect the ith bit of desired frame. The above observation is valid for $\alpha_{2\mathrm{j}}$ as well.

It is worth pointing out that unlike previous works in [66, 67, 70] where the overlap variable is assumed to be uniformly distributed in $[0, T_b]$, our proposed method calculates the explicit values of the overlap variable based on RV α.

For further analysis, same network model is considered as given in previous chapter, except for the shadowing effect to keep the analysis tractable. The average received power P_r at any node, taking two-slope path-loss model into account, is given by $P_r = P_T[K_o/(r^{\eta_1}(1 + \frac{r}{g})^{\eta_2})]$, symbols denote the same parameters as explained in Sec 3.2.3, chapter 3. Now, the (unfaded) average amplitude of the received signal can be written as $\sqrt{P_r}$.

For multipath fading environment, the received signal r during the ith bit of the desired frame, at the output of matched filter, can be modeled using the approach given in [112]. Therefore, after matched filtering operation, the received signal r during the ith bit of the desired frame in terms of weighted amplitude metric can be written as

$$r = h_o A_o + \sum_{j=1}^{I_{T_1}} h_j A_j + \sum_{k=1}^{I_{T_2}} h_k A_k + n \tag{4.5}$$

where $h_o(h_j, h_k)$, A_o, $A_j(A_k)$ and $I_{T_1}(I_{T_2})$ represent channel fading parameter of desired (type-1, type-2 interferers) bit (frame), received unfaded weighted amplitude of desired bit, effective amplitude of interference resulting due to type-1 (type-2) interferer frame and number of type-1 (type-2) interferers, respectively (effective amplitude will be described later). The term n represents additive white Gaussian noise (AWGN).

Our model can address the entire range of $\alpha_{1\mathrm{j}}$ ($\alpha_{2\mathrm{j}}$). However, here we present the case for type 1 interferers only, analysis for type 2 interferers follows the same steps. For the sake of clarity, first, we define individually the matched filter output for the desired as well as interfering signal. The unfaded weighted amplitude (weighted by $\sqrt{T_b}$) of the desired bit, after matched filtering can be written as [112]

$$A_o \;=\; S_o \sqrt{E_b} \;=\; S_o \sqrt{P_r\, T_b} =\; S_o\, A_o^{\mathrm{amp}} \tag{4.6}$$

where E_b, P_r and A_o^{amp} are the average received bit energy, average received power and unsigned weighted amplitude. S_o is the sign of received (weighted) amplitude. In case of BPSK, S_o takes values from the set $\{-1, 1\}$ with equal probability, depending upon whether the transmitted bit is $'-1'$ or $'+1'$ [58].

The interference created by the jth type-1 interferer's bit to the bit of desired frame at the output of matched filter in terms of weighted amplitude can be written as [70]

$$A_{b_1^I} \;=\; S_{b_1^I} \sqrt{E_{b_1^I}}\;\; O_1^{\alpha_{1\mathrm{j}}} \tag{4.7}$$

where $S_{b_1^I}$, $E_{b_1^I}$ and $O_1^{\alpha_{1\mathrm{j}}}$ are the sign, average received energy and fractional overlap of the first interfering bit of the jth interfering frame responsible for creating interference at the desired bit, respectively. Again, $S_{b_1^I}$ takes values from the set $\{-1, 1\}$ with equal probability, depending upon whether the interfering bit is $'-1'$ or $'+1'$ [58].

In an asynchronous environment, a bit of the desired frame can get affected by any two consecutive bits of the interfering frame. The position (index) of the bits of interfering frame can be calculated using (4.1) and (4.3). Therefore, after matched filtering, the effective amplitude of the interference experienced by the bit of desired frame can be expressed as

$$A_j \;=\; A_{b_1^I} \;+\; A_{b_2^I} \tag{4.8}$$

where $A_{b_2^I}$ is the interference caused by the other consecutive bit of jth type-1 interferer's frame. $A_{b_2^I}$ can be defined in the similar fashion as (4.7). Using (4.7), the effective amplitude of the interfering signal can further be written as (dropping the subscripts I and $\alpha_{1\mathrm{j}}$)

$$\begin{aligned} A_j \;&=\; S_{b_1} \sqrt{E_{b_1}}\;\; O_1 \;+\; S_{b_2} \sqrt{E_{b_2}}\;\; O_2 \\ &= S_{b_1} \sqrt{P_r^{\,b_1}\, T_b}\;\; O_1 \;+\; S_{b_2} \sqrt{P_r^{\,b_2}\, T_b}\;\; O_2 \end{aligned} \tag{4.9}$$

where S_{b_2}, E_{b_2} and O_2 are the sign, average energy and fractional overlap of the second interfering bit, respectively, the terms ${P_r}^{b_1}$ and ${P_r}^{b_2}$ are received powers of the two consecutive interfering bits of jth interfering frame. The amount of overlap of interfering bits O_1 and O_2 can be calculated using (4.2) and (4.4).

For further mathematical tractability, the received power can assumed to be constant during a particular frame reception. Therefore, by taking ${P_r}^{b_1} = {P_r}^{b_2} = P_r$, (4.9) can be further simplified as

$$A_j \;=\; \sqrt{P_r\; T_b}\;\; [S_{b_1} O_1 \;+\; S_{b_2}\, O_2\;] \tag{4.10}$$

where P_r is the average power received from the jth interfering frame.

4.2.2 Statistics of Effective Signed Fractional Overlap Variable

In (4.10), the terms in the bracket give the effective (resultant) fractional overlap with sign. Now, we introduce a term γ_j^{s,T_1} to represent the value of the entire term within the bracket in (4.10) and call it as the effective signed fractional overlap variable due to jth type-1 interferer. The pdf of RV γ_j^{s,T_1} can be calculated using the following procedure :

With the given range of $\alpha_{1\mathrm{j}}$ ($\alpha_{2\mathrm{j}}$) for type-1 (type-2) interferers, the ranges of variables O_1 and O_2 are $[\,0, 1)$ and $(0, 1]$, respectively. It may be observed that O_2 = 1- O_1.

Now, we consider a general case by assuming that a bit of the desired frame is overlapped by two consecutive bits of an interfering frame. In order to find the pdf of γ_j^{s,T_1}, we rewrite γ_j^{s,T_1} as follows

$$\begin{aligned} \gamma_j^{s,T_1} \;&=\; S_{b_1}\, O_1 \;+\; S_{b_2}\, O_2 \\ &= (S_{b_1} - S_{b_2})\, O_1 + \; S_{b_2}\,. \end{aligned} \tag{4.11}$$

The cdf of γ_j^{s,T_1} can be written as

$$\begin{aligned} F_{\gamma_j^{s,T_1}}\;(z) \;&=\; P\,[\,(S_{b_1} - S_{b_2})\, O_1 + S_{b_2} \;\le\; z\,] \\ &=\; P\,[\;1 \;\le\; z \mid S_{b_1} = 1,\; S_{b_2} = 1\;]\;\; P\,[S_{b_1} = 1]\, P\,[S_{b_2} = 1] \\ &\quad + P\,[\;2\; O_1 - 1 \;\le\; z\,|S_{b_1} = 1, S_{b_2} = -1\;]\;\; P\,[S_{b_1} = 1]\, P\,[S_{b_2} = -1] \\ &\quad + P\,[-2\; O_1 + 1 \;\le\; z\,|S_{b_1} = -1, S_{b_2} = 1\;]\;\; P\,[S_{b_1} = -1]\, P\,[S_{b_2} = 1] \\ &\quad + P\,[\;-1 \;\le\; z\,|S_{b_1} = -1, S_{b_2} = -1\;]\;\; P\,[S_{b_1} = -1]\, P\,[S_{b_2} = -1] \end{aligned} \tag{4.12}$$

which can be further simplified as

$$
\begin{aligned}
F_{\gamma_j^{s,T_1}}(z) \;= \tfrac{1}{4}\,[\,P[1 \le\; z \mid S_{b_1}=1,\; S_{b_2}=1\,] \\
+P[\,2\,O_1-1 \le\; z\,|S_{b_1}=1, S_{b_2}=-1\,] \\
+P[-2\,O_1+1 \le\; z\,|S_{b_1}=-1, S_{b_2}=1\,] \\
+\;P[\,-1 \le z\,|S_{b_1}=-1, S_{b_2}=-1\,]\,]
\end{aligned}
\tag{4.13}
$$

After simplifying the probability terms in (4.13) with the help of the pdf of the RV O_1 (details of the pdf of RV O_1 can be found in Appendix **??**), the cdf of γ_j^{s,T_1} takes the form

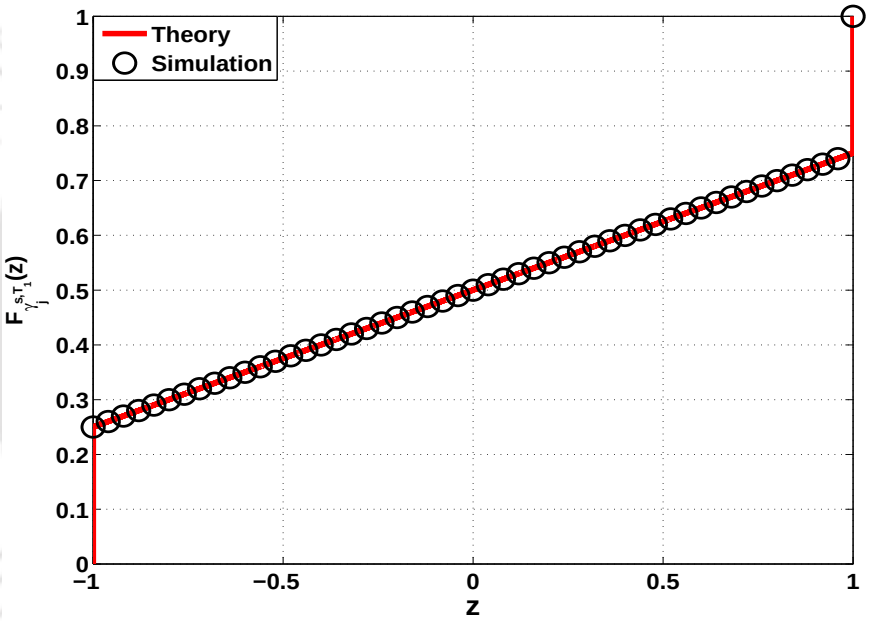

Figure 4.2: Cdf of the effective signed fractional overlap variable, γ_j^{s,T_1}.

$$
F_{\gamma_j^{s,T_1}}(z) \;=\; \frac{1}{4}\;[\;u(z+1)\;+\;1\;+\;z\;+\;u(z-1)\;]\,. \tag{4.14}
$$

where $u(.)$ is the unit step function. The cdf of γ_j^{s,T_1} is shown in Figure 4.2. The pdf of RV γ_j^{s,T_1} can be written after differentiating (4.14), as

$$
f_{\gamma_j^{s,T_1}}(z) \;=\; \frac{1}{4}\;[\;\delta(z+1)\;+\;1\;+\;\delta(z-1)\;]\,. \tag{4.15}
$$

Similar procedure can be used to obtain the pdf of γ_j^{s,T_2} with minor modifications. It may be

noted that unlike [69], the pdf in (4.15) is less complex and easier to obtain with the approach used. Moreover, the shape of the pdf of γ_j^{s,T_1} (γ_j^{s,T_2}) due to type -1 (type -2) interferers depends on which bit of the desired frame is considered for the calculation of interference, as shown in Figure 3.3, chapter 3.

With the representation described so far, (4.10) becomes

$$A_j = \sqrt{P_r\ T_b}\ \ \gamma_j^{s,T_1} = A_j^{\mathrm{m}}\ \gamma_j^{s,T_1} \tag{4.16}$$

Similarly, for type-2 interferers,

$$A_k = \sqrt{P_r\ T_b}\ \ \gamma_k^{s,T_2} = A_k^{\mathrm{m}}\ \gamma_k^{s,T_2} \tag{4.17}$$

where A_j^{m} (A_k^{m}) is the average weighted amplitude of jth (kth) interfering signal. Using (4.16) and (4.17), the final decision statistics (after matched filtering) can be rewritten as

$$r = S_o\, h_o\, A_o^{\mathrm{amp}} + \sum_{j=1}^{I_{T_1}} h_j\, A_j^{\mathrm{m}}\ \gamma_j^{s,T_1} + \sum_{k=1}^{I_{T_2}} h_k\, A_k^{\mathrm{m}}\ \gamma_k^{s,T_2} + n \tag{4.18}$$

The current form of (4.18) addresses the effect of all partial as well as full overlaps due to the interfering signals on the reception of the bit of desired frame in an asynchronous environment having i.n.i.d. interferers.

It may be noted that the expression for the received signal in (4.18) is derived using the amplitude based approach and does not include any phase term. Through simulation studies, we have found that inclusion of phase terms does not produce any significant difference in the BER performance. The comparison results are included in Appendix B.1 and some explanation is also provided why inclusion of phase terms becomes inconsequential particularly when number of interferers become large. Therefore, the rest of analysis presented in this chapter, does not consider the phased terms for a better mathematical tractability.

4.3 Error Analysis

For a given distribution of nodes ($\mathbf{d}$)[†], the average probability of bit error (P_e) becomes

$$P_e \;=\; P\left[r \underset{-1}{\overset{+1}{\lessgtr}} \beta\right] \tag{4.19}$$

where the elements of $\mathbf{d}$ represent the distances between the desired receiver with the interfering transmitters. β is the threshold for bit detection. Therefore, the conditional BER becomes

$$P_e \;=\; P\left[\left(S_o\, h_o\, A_o^{\text{amp}} \;+\; \sum_{j=1}^{I_{T_1}} h_j\, A_j^{\text{m}}\, \gamma_j^{s,T_1} + \sum_{k=1}^{I_{T_2}} h_k\, A_k^{\text{m}}\, \gamma_k^{s,T_2} + n\;\right) \underset{-1}{\overset{+1}{\lessgtr}} \beta\right] \tag{4.20}$$

For an interference dominated environment, when the effect of noise can be neglected [113,114], (4.20) can be written as

$$P_e \;=\; P\left[\left(\underbrace{S_o\, h_o\, A_o^{\text{amp}}}_{\text{first term}} + \underbrace{\sum_{j=1}^{I_{T_1}} h_j\, A_j^{\text{m}}\, \gamma_j^{s,T_1} + \sum_{k=1}^{I_{T_2}} h_k\, A_k^{\text{m}}\, \gamma_k^{s,T_2}}_{\text{second term}}\;\right) \underset{-1}{\overset{+1}{\lessgtr}} \beta\right] \tag{4.21}$$

The extension of the model which also includes noise, is discussed in Section 4.3.2. For simplifying the notations, we modify (4.21) as follows

$$P_e \;=\; P\left[\left(W_0 \;+\; \sum_{j=1}^{I^*_{\text{eff}}} W_j\right) \underset{-1}{\overset{+1}{\lessgtr}} \beta\right] \tag{4.22}$$

where

$$W_0 \;=\; S_o\, h_o\, A_o^{\text{amp}}$$

$$W_j \;=\; \begin{cases} h_j\, A_j^{\text{m}}\, \gamma_j^{s,T_1} & ;\; 1 \;<\; j \;\leqslant\; I_{T_1} \\ h_j\, A_j^{\text{m}}\, \gamma_j^{s,T_2} & ;\; I_{T_1} \;<\; j \;\leqslant\; I^*_{\text{eff}} \end{cases}$$

where I^*_{eff} is the total number of effective interferers i.e. $I^*_{\text{eff}} = (I_{T_1} + I_{T_2})$. The analytical expressions for the I^*_{eff}, I_{T_1} and I_{T_2} as a function of MAC protocol, guard zone, transmit power,

[†]As the focus of this thesis is the development of analytical models to quantify the asynchronous interference scenario for BER calculations, we assume that location of other nodes (interferers) can be obtained during the network set-up phase or before the starting of data communication by observing the received signal for considerable amount of time. For more advanced analytical modeling, which include the interferer-receiver distance as a random factor, method outlined in [30] can be utilized. In literature, authors have suggested some possible distributions also for interferer's location in deployment area, such as : Poisson Point Process (PPP) [39, 40], Binomial point process (BPP) [41] or Matern Point Process (MPP) [42,43]. However, distributions are unknown for interference calculations based on these point processes.

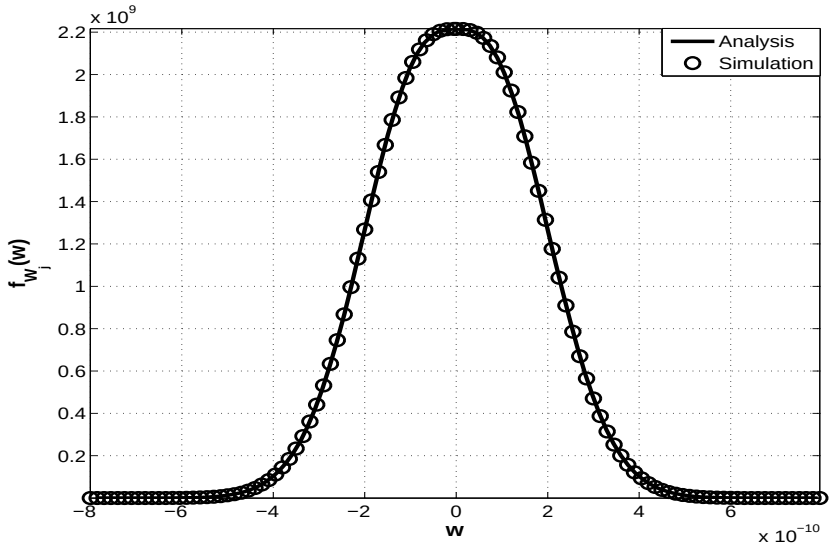

Figure 4.3: Pdf of the interfering signal (W_j) in the Rayleigh fading environment.

deployment area, signal wavelength and detection threshold can be obtained with the help of procedure outlined in chapter 3.

4.3.1 PDF of Interference Variable

To evaluate (4.22) further, the channel is assumed to be Rayleigh distributed. The terms h_o, h_j and h_m become Rayleigh RVs. Therefore, the first term of (4.21) is a weighted Rayleigh RV and the second term, which is a summation of $(I_{T_1} + I_{T_2})$ independent elements (not necessarily identical), contains Rayleigh distributed RVs weighted by random weights (not necessarily positive). The pdf of each interfering term W_j (4.22) can be written as

$$f_{W_j}(w) = \begin{cases} \frac{1}{4A_j^m\sigma_f}\left[\sqrt{\frac{\pi}{2}}\,\mathrm{erfc}\left(-\frac{w}{\sqrt{2}\,A_j^m\sigma_f}\right) - \frac{w}{A_j^m\sigma_f}\,\exp\left(-\frac{w^2}{2(A_j^m)^2\,\sigma_f^2}\right)\right] & w<0 \\ \frac{1}{4A_j^m\sigma_f}\left[\sqrt{\frac{\pi}{2}}\,\mathrm{erfc}\left(\frac{w}{\sqrt{2}\,A_j^m\sigma_f}\right) + \frac{w}{A_j^m\sigma_f}\,\exp\left(-\frac{w^2}{2(A_j^m)^2\,\sigma_f^2}\right)\right] & w>0 \end{cases} \tag{4.23}$$

Details of the derivation of the pdf expression in (4.23) can be found in Appendix B.2. Figure 4.3 shows the pdf of individual interfering signals in Rayleigh fading environment.

4.3.2 BER Expression

In order to evaluate the BER expression, we invoke the CLT for the interfering signal terms. It can be mentioned that although the CLT is generally applicable for the large number of summing

terms (which are interferers in the present scenario), in our case, the CLT can be used for the small number of interferers as well, taking the shape of the pdf of interfering term into the consideration [66]. For such scenarios, where the guard zone is assumed to be present, the received amplitude (power) of the desired signal is stronger than the amplitude (power) of a single interfering signal and hence, the dominant one. To apply the CLT on the second term of (4.22), we use a Gaussian RV G^I for the summation of the interfering terms, whose mean (m_{G^I}) and variance ($\sigma^2_{G^I}$) are given as follows :

$$m_{G^I} = \sum_{t=1}^{I^*_{\text{eff}}} m_t \lfloor \gamma_t^{s,T_q} \rceil \tag{4.24}$$

$$\sigma^2_{G^I} = \sum_{t=1}^{I^*_{\text{eff}}} \sigma_t^2 \lfloor \gamma_t^{s,T_q} \rceil \tag{4.25}$$

where m_t and σ_t^2 are the mean and variance of the individual interfering terms (in our case, the mean (m_{G^I}) evaluates to zero) and $q = 1$ for t $\in [1, I_{T_1}]$ and $q = 2$ for t $\in (I_{T_1}, I_{\text{eff}}]$. The notation $\lfloor . \rceil$ is defined as follows:

$$\begin{aligned} \lfloor \gamma_t^{s,T_q} \rceil &= 1, \quad \gamma_t^{s,T_q} \neq 0 \\ &= 0, \quad \gamma_t^{s,T_q} = 0 \end{aligned} \tag{4.26}$$

After applying the CLT, (4.22) becomes

$$P_e = P\left[(W_0 + G^I) \underset{-1}{\overset{+1}{\lessgtr}} \beta \right] \tag{4.27}$$

Without loss of generality, the threshold for detection (β) is set to 0 and the desired transmitted bit to $'+1'$ ($S_o = +1$). For this specific case, (4.27) reduces to

$$P_e = P\left[(W_0 + G^I) < 0 \right] \tag{4.28}$$

The conditional BER becomes

$$\begin{aligned} P_e | W_o &= \int_{-\infty}^{-W_o} \frac{1}{\sqrt{2\pi}\sigma_{G^I}} \exp\left(-\frac{g^2}{2\sigma^2_{G^I}} \right) dg \\ &= \frac{1}{2} - \frac{1}{2} \operatorname{erf}\left(\frac{W_o}{\sqrt{2}\sigma_{G^I}} \right) \end{aligned} \tag{4.29}$$

After removing the condition and using simple modifications, the expression for the BER comes out to be

$$
\begin{aligned}
P_e &= \int_0^{\infty} P_e|\, W_o \; f_{W_o}(w) \; dw \\
&= \frac{1}{2} - \frac{A_o^{\text{amp}}\, \sigma_{\text{f}}}{2\sqrt{\sum_{t=1}^{I_{\text{eff}}^*} \sigma_t^2 \lfloor \gamma_t^{s,T_q} \rceil + \left(A_o^{\text{amp}}\, \sigma_{\text{f}}\right)^2}}
\end{aligned} \tag{4.30}
$$

where $f_{W_o}(w)$ is the pdf of the RV W_o, which can be calculated by performing the pdf transformation [104] using (4.22). It may be noted that in [66], an expression for the computation of the average bit error probability has been derived. However, the expression given in [66] is more complex than (4.30) and requires the use of numerical method for the evaluation of the BER. Additionally, the expression in [66] is based on the assumption of i.i.d. interferers and it does not includes the effects of MAC protocol, interference range and distance dependent path-loss exponent also.

4.3.2.1 BER Expression : with Noise Considered

The study presented here can easily be extended for the analysis of the noisy environment as well. In (4.20), the term n represents the AWGN, which can be easily included in the second term of (4.21) while invoking the CLT. Therefore, in noisy environment, the variance $\sigma^2_{G_n^I}$ of the Gaussian RV G_n^I is now given by $(\sigma^2_{G^I} + \sigma_n^2)$, where, the term $\sigma^2_{G^I}$ and σ_n^2 represent the variance sum of interfering terms for the noise free environment and the variance of Gaussian noise, respectively. It may be easily figured out that after considering noise, the performance further degrades as compared to the noise free environment, since $\sigma^2_{G_n^I} \geq \sigma^2_{G^I}$. However, the extent of degradation varies for different basic parameters, as discussed in Section 4.4.3.

4.4 Results

Simulations are carried out considering the same network model as considered in chapter 3 except for the shadowing effects. The complete network is simulated using the parameters given in Table 4.2. It includes the generation of K homogeneous nodes distributed randomly over an area of $A_r \times A_r$ m^2. Pairing of randomly selected K_s transmitter nodes with receiver nodes based on reception range criteria. Guard zone as a function of I_{RF} is formed around communicating pairs as per class - 2 MAC protocol.

Along with the average BER (ABER), average number of successfully received bits by a user

Table 4.2: Simulation parameters

Parameter	***Value***
Number of nodes (K)	1000
Area ($A_r \times A_r$)	$1000 \times 1000\ m^2$ $2000 \times 2000\ m^2$ $3000 \times 3000\ m^2$
Transmission power (P_T)	0 dBm
Transmission range	200 m
Frame length (B/F)	1024 bits
Bandwidth	4 MHz
Path loss exponents (η_1, η_2)	(2, 3); (3, 4)
Threshold (β)	0
Interference range factor (I_{RF})	1, 1.25, 1.5, 2, 2.5, 3, 3.5

and the behaviour of the average interference variance sum (AIVS) as a function of increasing number of concurrent transmissions and as a function of the I_{RF} is also evaluated.

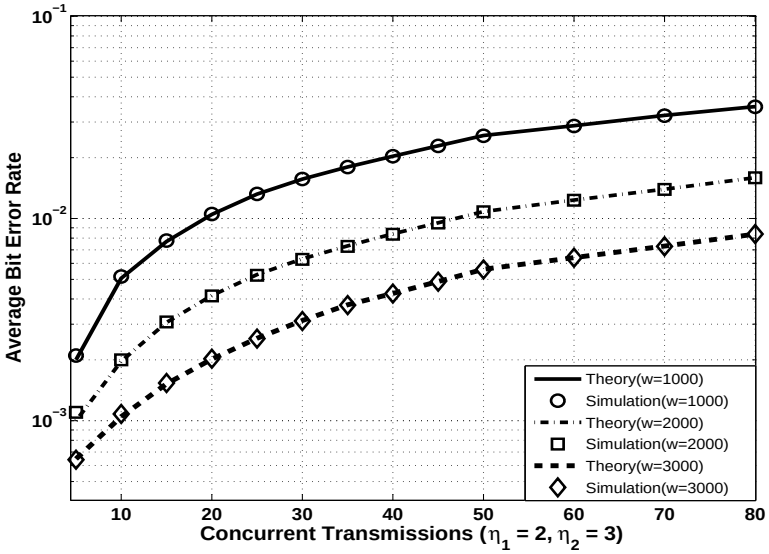

Figure 4.4: ABER in an asynchronous wireless network in the presence of i.n.i.d. interferers for $I_{RF} = 1.25$, (w = width of deployment area (m)).

4.4.1 Effect of the Number of Interferers

Figure 4.4 shows the variation of ABER as a function of increasing number of concurrent transmissions from i.n.i.d. interfering users in an asynchronous wireless network. The variation of the ABER is shown for three different deployment areas. Along with the increment in the

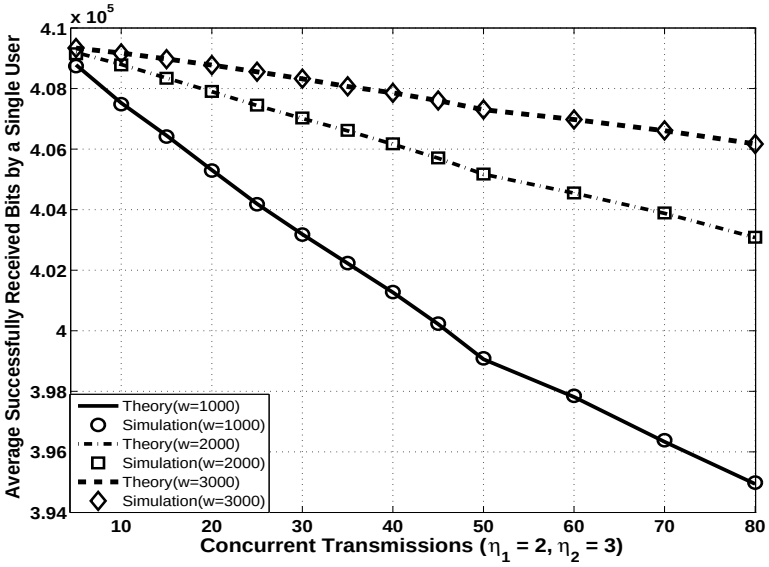

Figure 4.5: Average number of successfully received bits by a user node in an asynchronous wireless network in the presence of i.n.i.d. interferers.

ABER with the increasing number of interferers (transmissions), it can also be observed that the ABER decreases with an increment in the deployment area, but the ABER does not decrease at a constant rate as the deployment area decreases. It can be observed from Figure 4.4 that $ABER_{w=1000} - ABER_{w=2000} > ABER_{w=2000} - ABER_{w=3000}$. As pointed out in the previous chapter and it is worth mentioning here also that in practical scenarios, the actual value of ABER will be even less than that is shown in the plots, as some of the interferers will be further barred by the other transmitters as well.

The average number of successfully received bits by a user as a function of increasing number of interferers are shown in Figure 4.5. The effect of deployment area on successful reception can be observed in this plot also. The shape of plots is in accordance with the ABER plots variation as shown in Figure 4.4. Higher the value of ABER, lower will be the number of successfully received bits.

The variation of the AIVS for different deployment areas and path-loss environment is shown in Figure 4.6. Again, the effect of increasing the width of deployment area on the AIVS can be observed. AIVS is less for high path-loss exponent environment as the average received power from distant interferers reduce with an increment in path-loss exponent.

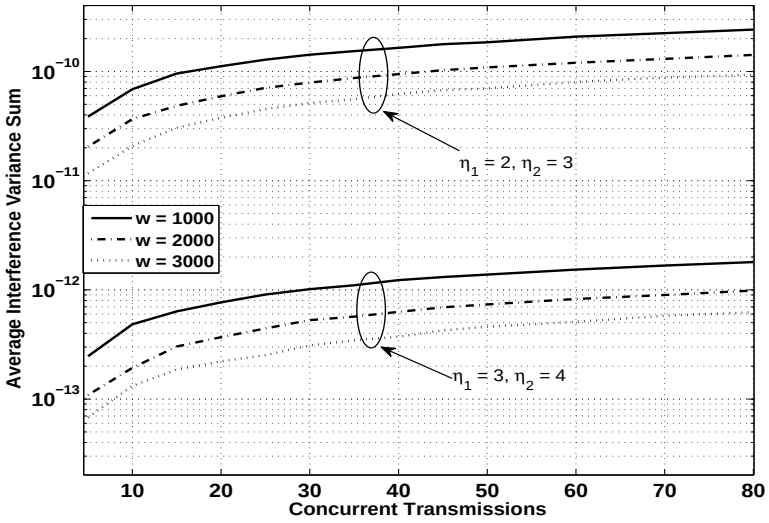

Figure 4.6: AIVS in an asynchronous wireless network.

4.4.2 Effect of the Interference Range

Figure 4.7 shows the average bit success rate (ABSR = 1-ABER) for different deployment areas and the number of i.n.i.d. interferers as a function of the interference range factor (I_{RF}). Here, we define I_{RF} as the ratio of the interference range R_I and the reception range R_{Rx}, i.e.

$$I_{RF} = \frac{R_I}{R_{Rx}} \tag{4.31}$$

Larger the interference range, smaller will be the number of effective interferers. Therefore, larger values of I_{RF} result in higher bit success probability, as shown in Figure 4.7.

Figure 4.8 shows the variation of the AIVS with I_{RF}. As stated earlier, for a given number of nodes, the effective number of interferers reduces with an increment in the interference range (factor), hence, the AIVS also decreases. Further, for large deployment areas, the effect of distant interferers is not as prominent as in the smaller one, hence, for the larger areas, smaller AIVS can be observed upto a certain value of I_{RF} from the plots in Figure 4.8. However, above a certain value of I_{RF} , the effect of increment in I_{RF} is more evident for smaller deployment areas. Due to high density of nodes in smaller areas, more number of nodes get restricted with high I_{RF}, hence, lower AIVS.

Figure 4.9 gives the variation of the successfully received bits by a user with respect to I_{RF}.

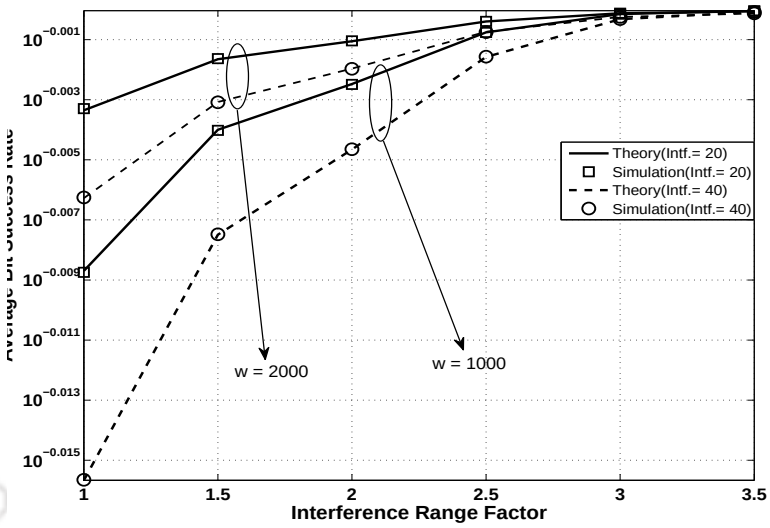

Figure 4.7: ABSR in an asynchronous wireless network.

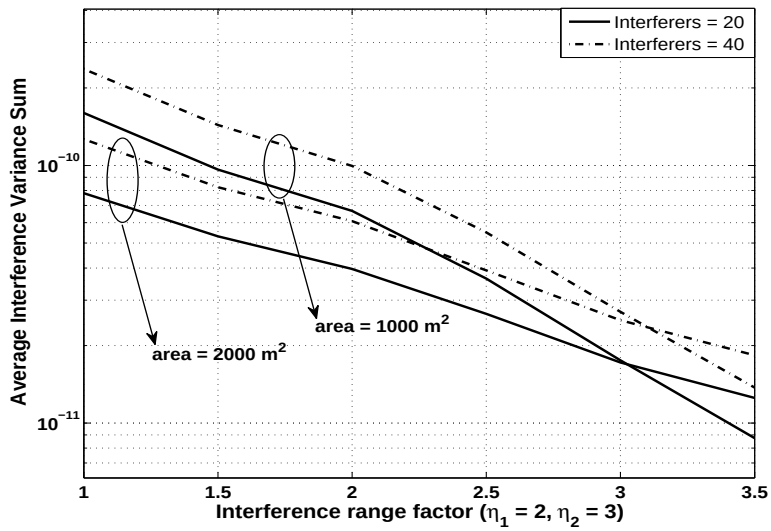

Figure 4.8: AIVS in an asynchronous wireless network.

The increment in the successfully received bits by a user can be explained by the fact that an increment in the I_{RF} results in the low values of the AIVS and high ABSR (as shown in Figure 4.7, Figure 4.8). Again, the effect of large deployment area on the successfully received bits wanes for high values of I_{RF}.

It can be noted that the improvement in the performance of a user, in term of the ABSR, AIVS and average successfully received bits, on increasing the value of I_{RF} comes at the cost of reduction

in the network throughput (not shown in the plots). More number of interfering nodes, which are otherwise user nodes in the network, will be barred from the transmission due to the higher value of the I_{RF} and hence, overall network throughput gets degraded.

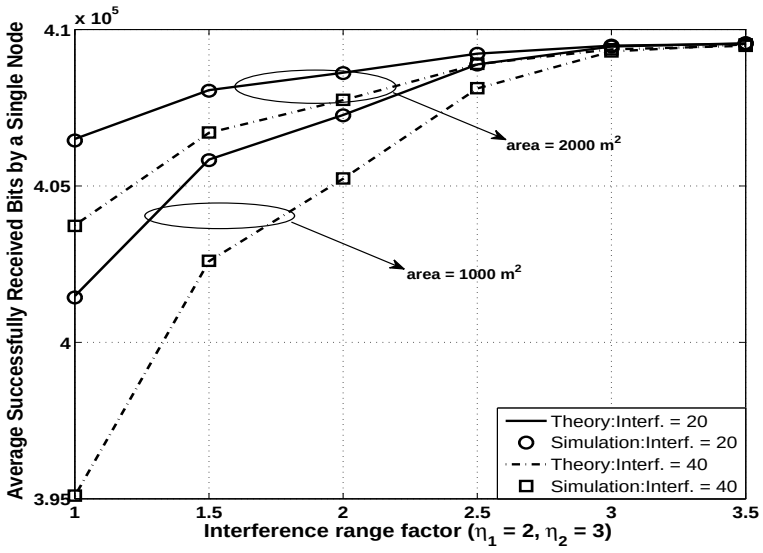

Figure 4.9: Average successfully received bits by a user node Vs interference range factor.

4.4.3 Performance With Noise Included

Figure 4.10 shows the simulation results for the ABER† with respect to increasing number of concurrent transmissions from i.n.i.d. interfering users after considering the effect of noise. The variation in the ABER performance with the noise included (ABER_N) is different for the different basic parameters. The behaviour of the ABER plot follows the same reasoning as given in Figure 4.7. The inclusion of the noise degrades the ABER performance with the number of concurrent transmissions. However, the difference in the performance between ABER_N and ABER vanishes slowly with increasing the number of concurrent transmissions because the higher values of the concurrent transmissions keep on making the effective interfering signal considerably stronger.

Figure 4.11 gives the simulation results for the ABER with respect to the I_{RF} with noise considered. In case of the variation of the ABER with I_{RF}, the change in the ABER_N plot occurs slowly as compared to the ABER plot at higher values of I_{RF}, because of the fact that noise (which remains unaffected by the increment in I_{RF} values) becomes dominant factor after a certain value of I_{RF}.

†ABER gives the average BER performance without considering the effect of noise.

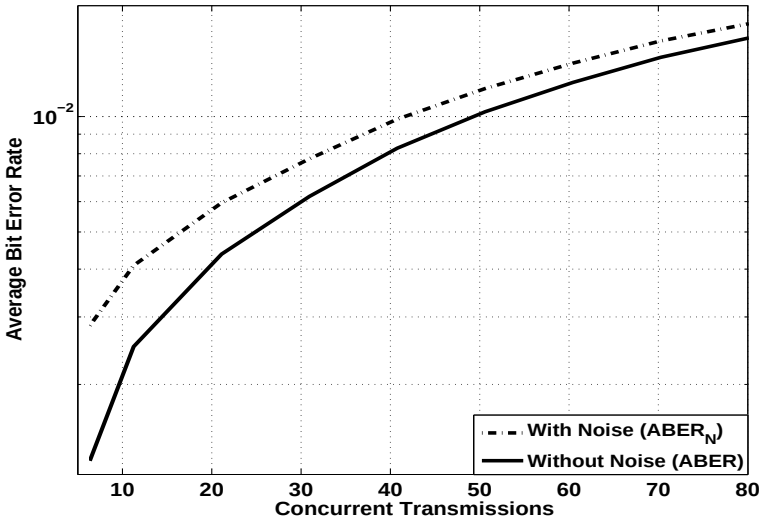

Figure 4.10: ABER Vs concurrent transmissions considering noise (w = 2000 m, $\eta_1 = 2$, $\eta_2 = 3$).

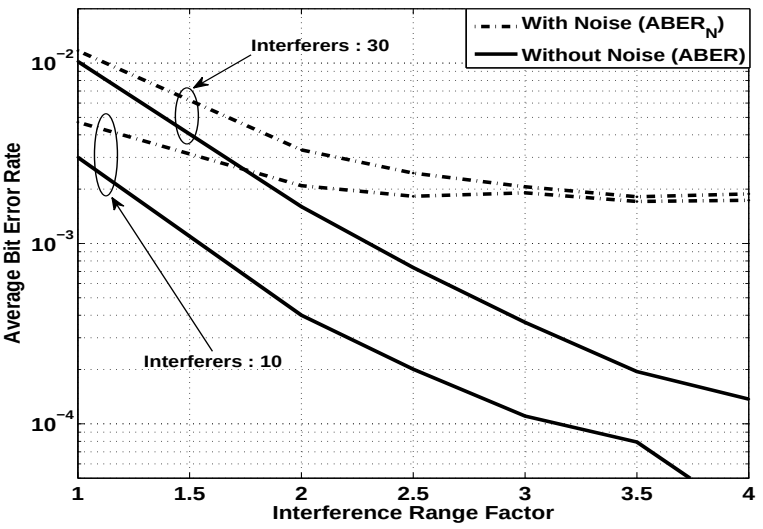

Figure 4.11: ABER Vs interference range factor considering noise (w = 2000 m, $\eta_1 = 2$, $\eta_2 = 3$).

Results obtained analytically by using appropriate approximation closely follow the simulation results in all the cases. It may be noted that while the use of the monte-carlo simulation method might be more accurate, the simulation set-up is usually computationally intensive and requires long time to get the accurate results without simplified assumptions. The analytical formulae derived here give results close to the simulation results with small amount of computational requirement. The simple closed form of the BER expression gives several additional insights into the

network performance. A useful relationship between the ABER and the number of effective i.n.i.d. interferers, MAC protocol, distance dependent path-loss exponent etc. can be inferred from the ABER expression in (4.30).

4.5 Conclusion

In this chapter, a method is proposed to calculate the index (position) of interfering bit(s) and the extent of their individual overlaps as well as effective overlap offered to the bit of the desired frame in an asynchronized wireless network. A model for the BER calculation using the amplitude metric based approach has been developed for such network. The model presented here is general enough to address the cases like partial overlap of interfering bits and interferers with unequal weights etc. The model is then used to find the pdf of signed fractional overlap variable using the proposed approach, which gives an easier way to calculate the same. The closed form expression for the pdf of the resultant amplitude of interfering term has also been derived. Based on the nature of the pdf, a closed form expression has been obtained for the ABER in a Rayleigh fading environment in the presence of i.n.i.d. interferers, as a special case by invoking the CLT. The analytical results have been validated through extensive simulations. Using this model, the effect of increasing the number of concurrent transmissions and the effect of MAC protocol on the ABER has been analysed in detail for an asynchronous environment having i.n.i.d. interferers. The effect of phase terms of interfering signals on system performance has also been discussed.

The analysis carried out in this chapter can be useful to find the active number of users for a given BER based on a specific QoS requirement. Also, a suitable interference range can be found out for a given set of network parameters.

5

Interference Management in Heterogeneous Wireless Network

Contents

This chapter introduces interference analysis and management in heterogeneous/overlaid wireless networks. After analyzing various aspects of interference in asynchronized wireless networks in previous chapters, here we focus on interference management. As discussed earlier, harmful effects of interference can not be eliminated completely due to the broadcast nature of wireless medium, but the same may be reduced to a considerable extent by adopting proper strategies for dealing with interference. Interference management is equally important for smooth and efficient functioning of various wireless networks. Out of various existing interference management approaches/methods, we take optimum subband selection for further investigation here. Many advanced devices nowadays come with the functionality of choosing a proper subband for communication purposes. Example of some such devices are sensor motes and transceivers in OFDMA based femtocells. Given the environmental conditions, such as subband availability, fading and interference statistics, these devices can choose suitable subband out of available ones. By selecting suitable subband, detrimental effects of environmental conditions can be minimized. For addressing various aspects of subband selection method further, here we consider heterogeneous/overlaid wireless networks such as OFDMA based femtocell-macrocell cellular network, as a representative case.

In this chapter, the subband allocation for femtocells in the presence of asynchronous CCI in OFDMA based cellular network is investigated in detail. Using an energy based approach, synchronized as well as asynchronized arrival of interfering frames are addressed in the analysis carried out for subband selection. For this work also, two-slope model is used to account for path loss. Channel effects are also embodied into the analytical framework. Two methods are presented here to find the subband least affected by interference and this subband is then used for communication within femtocells. Analytical and simulation results are in good agreement and they provide insight into various parameters, which can be adjusted to optimize the performance of the femtocell and cellular network as well.

5.1 Introduction

Integration of femtocells in OFDMA based cellular network is being considered as a reliable solution for achieving improved indoor coverage and higher data rates [115]. Keeping in view the continuously growing demand for the network capacity, incorporation of various FFR schemes in

the network operation is useful as a capacity improvement solution [35]. But the amelioration in capacity due to frequency reuse comes at the cost of increased CCI [3]. Interference mitigation in wireless networks may be possible to an extent by proper system design. In OFDMA based wireless networks, such as LTE and WIMAX (IEEE-802.16), interference might be alleviated by exploiting flexible orthogonal frequency band allocations possible due to FFR [73, 116].

Some works analyzing interference in OFDM/OFDMA based cellular networks can be found in [87,117,118]. But, very limited works are available in literature analyzing interference considering timing asynchronization issues that often occur due to propagation delays and timing offsets among various users within the network [33, 34]

Mitigation of deleterious effects of CCI through proper system design requires a detailed model incorporating asynchronous interference present in such wireless networks. Further, various impairments like multipath and doppler shift affect the signal reception through wireless channel. In such scenarios, femtocells must perform reallocation of optimum subband often (in some situations periodically) for proper spectrum usage [85, 119, 120].

In this work, we present an analysis to find a suitable subband which is least affected by the CCI received at a femtocell in an OFDMA network. While addressing the timing asynchronization issues due to timing offsets and propagation delays, our methods make use of an energy based metric. Two approaches are presented here for the subband selection analysis. The first approach makes use of CLT as an approximation for the calculation of pdf of summation of individual interfering signals. The second approach suggests a suitable approximation to the pdf of the individual interfering signal in order to obtain a closed form solution for the optimum subband selection.

Main contributions of this chapter can be summarized as :

- ✎ This chapter addresses the asynchronous interference issues in heterogeneous/overlaid wireless networks,
- ✎ Investigates some important interference management schemes for heterogeneous networks,
- ✎ Proposes a method to find the optimum subband for communication purposes in femtocell taking asynchronous nature of interference into account.

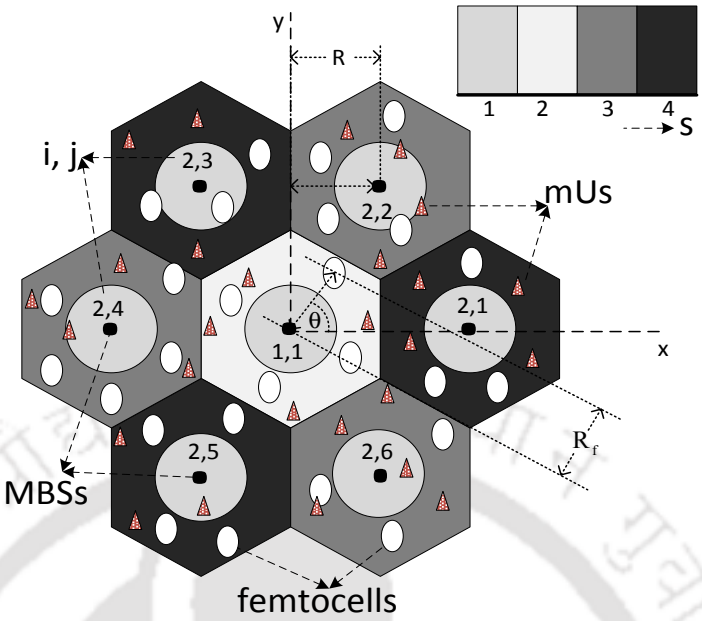

Figure 5.1: Cellular model based on FFR with femtocells.

5.2 System Description

Figure 5.1 shows the cellular structure of macrocells under consideration. Each macrocell consists of a base station (MBS) at the center and random number of mobile users (mUs) and femtocells distributed uniformly. Each femtocell has a base station (FBS) and limited number of users (fUs) uniformly located within a small area ($10 \sim 30$ meter) [14]. Femtocell may choose a subband which is least affected by the interference. Multipath and distance dependent path loss effects are used to model the interfering signal received at the femtocell. It is assumed that channel remain constant during a frame reception. Two-slope path loss model is used to address the distance dependency of average received signal from co-channel interferers located in nearby as well as distant tiers. All femtocell transmitters are assumed to be working with same transmit power. Rayleigh fading is considered to model the small scale variations. Shadowing and ACI are not included in the analysis to keep computational requirements low, however, modeling is general enough and it can be extended to accommodate the same.

5.2.1 Frequency Subband Selection Strategy

There are various FFR techniques available in literature [87, 116, 121]. For analysis purpose, FFR technique given in [87] is used here. Generally, in a FFR technique, the total system bandwidth

is partitioned into N subbands. This work analyses a special case with $N = 4$. Overall bandwidth is divided into 4 subbands, where each subband is denoted by B_s, $s = 1, 2, 3, 4$. Interior part of macrocells is assigned a common subband and allocation to the exterior part is based on the reuse factor ($\Re = 1/3$). The subband assignment is such that the interference among nearby cell users as well as interior and exterior users of the same cell is minimized.

In general, femtocells are configured to work in two modes : co-channel deployment and separate channel deployment [16]. The co-channel deployment mode might be efficient from the scarce spectrum perspective but produces considerable amount of interference within the cell. On the other hand, based on reuse factor, a subband might be selected as a separate channel assignment by the femtocell which reduces the interference at the cost of spectrum [3]. It might be emphasized that a proper subband selection by femtocell should fulfill the QoS parameters requirement whichever deployment mode it chooses.

Table 5.1: List of Interfering Macrocells From Different Tiers in Various Subbands

sth subband	***jth macrocell ;ith tier***		***Total Interferers***
2	j = 1	; i = 1	13
	j = 2, 4, 6, 8, 10, 12	; i = 3	
	j = 1, 4, 7, 10, 13, 16	; i = 4	
3	j = 1, 3, 5	; i = 2	12
	j = 3, 7, 11	; i = 3	
	j = 2, 6, 8, 12, 14, 18	; i = 4	
4	j = 2, 4, 6	; i = 2	12
	j = 1, 5, 9	; i = 3	
	j = 3, 5, 9, 11, 15, 17	; i = 4	

5.3 Interference Analysis and Modeling

CCI resulting due to frequency reuse is one of the main factors for the performance degradation in a subband. Quantifying the effect of CCI before subband selection is therefore imperative. Let, the position of a randomly located femtocell is denoted by (R_f, θ) in the polar coordinates, as shown in Figure 5.1. Tier two onwards, the positions of MBSs are given by $(R_i\ cos(\frac{\pi}{3}(m_{ij} - 1)), R_i\ sin(\frac{\pi}{3}(m_{ij} - 1)))$ where i and j are the tier and corresponding macrocell indices, respectively and $m_{ij} = 1, 2, 3...$. Let M_{ij} denotes the jth interfering macrocell from ith tier, then interfering

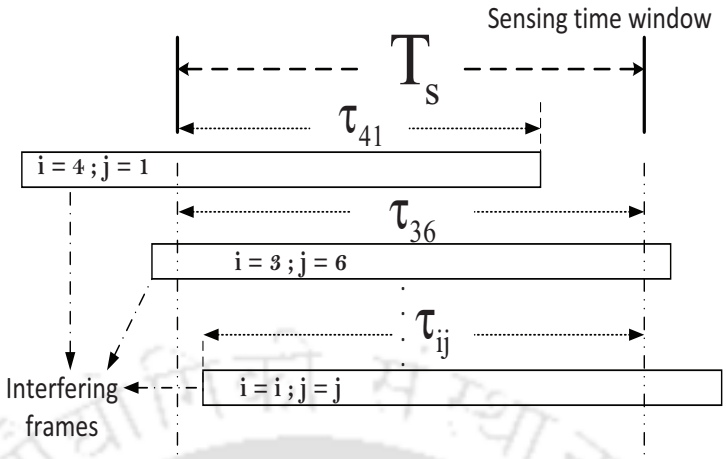

Figure 5.2: Interfering signals arrival with timing offsets during sensing time window T_s.

macrocell for different subbands B_s can be listed as given in Table 5.1, where $j = 1; i = 1$ show the macrocell 1 in the center (tier 1). Subband $s = 1$ is not included in Table 5.1 and in the analytical framework because this subband is expected to have the maximum level of interference due to being assigned to the interior users of each macrocell.

The delay differences for different paths and imperfect timing synchronization (TS) among different users give rise to timing offset (TO) which results in interfering frames arriving with different delays [34]. Some of the interfering frames may have their end parts and some of them may have the starting parts within the sensing time window (T_s) during which a femtocell senses a particular subband in terms of interference level. Due to the various levels of partial overlapping [33], T_s may not be completely overlapped by a single interfering frame originating from different MBSs, mUs and femtocells as shown in Figure 5.2. It can be noted that T_s for a network depends upon the protocol/technolgy used. Due to different deployment locations of various femtocells, each femtocell is supposed to find the suitable subband independently as each of them experiences substantially dissimilar strength of interfering signals.

To address the partial overlap scenario with respect to T_s, we follow the energy based approach (as proposed in earlier chapters) and introduce a parameter τ, distributed uniformly in $(0, 1]$ denoting the effective overlap of interfering frames within T_s. The value $\tau = 1$ represents the full overlap case, whereas fractional values $(0, 1)$ denote the partial (overlap) contribution of interfering frames. Using two-slope path loss model, the interference energy received at the fth femtocell in sth subband from M_{ij} macrocell can be written as

$$\begin{aligned} E_{Iij}^{fs} &= P_{r_{ij}}\, \tau_{ij}\, T_s \\ &= \frac{K_o P_{T_{ij}}\, |h_{f,ij}|^2}{d_{f,ij}^{\eta_1}\left(1+\frac{d_{f,ij}}{g}\right)^{\eta_2}}\ \tau_{ij}\, T_s \end{aligned} \tag{5.1}$$

where E_{Iij}^{fs}, $P_{r_{ij}}$, $P_{T_{ij}}$, τ_{ij} and T_s represent the interference energy at fth femtocell in sth subband, received power, transmitted power, fractional contribution from ij indexed macrocell and the sensing time. Term $h_{f,ij}$ denotes the channel coefficient between fth femtocell and M_{ij} indexed macrocell. The distance between fth femtocell and M_{ij} indexed macrocell is denoted by $d_{f,ij}$ and calculated as $(R_f^2 + R_i^2 - 2R_f R_i\ cos(\theta - \frac{\pi}{3}(m_{ij}-1)))^{1/2}$. Terms K_o, g and λ are the system dependent parameter, turning point of the attenuation curve is given by $g = (4h_T h_R)/\lambda$, where h_T and h_R are the heights of MBS (mU) transmitter and FBS (fU) receiver antennas and the signal wavelength, respectively [10]. Two path loss exponents are denoted by η_1 ($\approx 2 \sim 3$) and η_2 ($\approx 2 \sim 6$), respectively.

Considering additive model of interference, total interference energy can be written as the summation of all individual interference energies, given by (5.1). The total interference energy comes out to be

$$E_{TI}^{fs} = \sum_i \sum_j U_j\ E_{Iij}^{fs} \tag{5.2}$$

where the first summation is over the tiers and the second summation covers the cells of the ith tier of cellular network. The term E_{TI}^{fs} includes the effect of interference due to the downlink transmissions from MBSs. Term U_j denotes the number of uplink interferers in the jth macrocell in the analysis of the effect of interference due to uplink transmissions. In the uplink case, the total interference due to the uplink interferers in the jth macrocell can be approximated as the interference generated by a interferer at the center of the same cell scaled by U_j. Thus, (5.2) can be used to analyze the interference due to the downlink as well as the uplink interferers. As this work deals with the downlink interferers, hence $U_j = 1$ for the remaining part of the analysis.

The downlink transmissions from MBSs, uplink transmission from mUs and a nearby femtocell operating on the same subband can be the primary sources of interference. However, contribution of femtocells in overall interfering signal will be very less as femtocells operate at very low transmission power ($\approx 10 \sim 100mW$). Therefore, effect of interference from femtocells is neglected in the

analysis. Since, in this paper, we are considering interference from MBSs, the proposed framework is likely to be equally applicable for closed and open access type femtocells, therefore, any explicit assumption is not being made for the type of femtocell.

5.3.1 Statistics of Aggregated Interference Signal

For a given deployment scenario, assuming no power control protocol, (5.1) can be written as

$$E_{Iij}^{fs} = \frac{K_o P_T \, T_s}{d_{f,ij}^{\eta_1}\left(1+\frac{d_{f,ij}}{g}\right)^{\eta_2}} |h_{f,ij}|^2 \, \tau_{ij} = W_{ij} \, \tau_{ij} \tag{5.3}$$

where the product of two RVs namely, W_{ij} and τ_{ij} denote the interference energy term E_{Iij}^{fs}. The term W_{ij} is a weighted exponential RV with modified (rate) parameter λ_W given as λ_o/K, where λ_o is the parameter corresponding to the exponential RV $|h_{f,ij}|^2$ and K is the (conditional) term given by $[(K_o P_{T_{ij}} T_s)/(d_{f,ij}^{\eta_1}(1+\frac{d_{f,ij}}{g})^{\eta_2})]$.

The pdf of the term W_{ij} can be calculated using the pdf transformation method [104] as

$$f_{W_{ij}}(w) = \frac{\lambda_o}{K} \exp\left(-\frac{\lambda_o}{K} w\right) \tag{5.4}$$

With the pdf of W_{ij} and τ_{ij} known, the pdf of individual interference term E_{Iij}^{fs} can be found as

$$\begin{aligned} f_{E_{Iij}^{fs}}(\xi) &= \int_{\tau} \tfrac{1}{\tau_{ij}} \, f_{W_{ij}}\left(\tfrac{\xi}{\tau}\right) f_{\tau_{ij}}(\tau) \, d\tau \\ &= -\lambda_W \, \mathrm{Ei}(-\lambda_W \xi) \end{aligned} \tag{5.5}$$

where $f_{\tau_{ij}}(\tau)$ and Ei(.) are the pdf of RV τ and exponential integral (EI), defined as $\mathrm{Ei}(\Delta) = -\int_{-\Delta}^{\infty} \frac{\exp(-t)}{t} dt$, respectively.

5.3.2 Analysis Under Approximation

Further calculations which are required to obtain the statistics (cdf/pdf) of aggregated interference term E_{TI}^{fs}, are not easily tractable with the pdf of E_{Iij}^{fs} as given in (5.5). Therefore, in order to obtain a simplified analytical method for optimum subband selection, two approaches can be adopted which are presented in the following subsections.

5.3.2.1 First Approach : Using CLT

In first proposed approach towards solving the subband selection problem, we use the CLT for the resultant interference term[†]. The pdf of resultant sum of all interfering signals is approximated by invoking CLT. Therefore, application of CLT on the summing terms RV E_{TI}^{fs} in (5.2) makes the distribution of total interference energy term for the sth subband as Gaussian. The E_{TI}^{fs} is now denoted by the term G_{TI}^{fs} having mean (m_{G^s}) and variance ($\sigma_{G^s}^2$) as follows

$$\begin{aligned} m_{G^s} &= \sum_{k=1}^{N_I} m_k \\ \sigma_{G^s}^2 &= \sum_{k=1}^{N_I} \sigma_k^2 \end{aligned} \tag{5.6}$$

where m_k, σ_k^2 and N_I are the mean, variance of the individual interference term defined by (5.3) and the effective number of interferers. It should be noted that though, the accuracy of calculation of the interference energy depends on how many tiers of interferers are included, the effective contribution of interferers located in distant tiers may be considerably less[‡] [122].

The application of CLT to calculate the overall interference energy at the fth femtocell for all available subbands (four, $s = 1, 2, 3, 4$) results in four Gaussian RVs, namely $G_{TI}^{f1}, G_{TI}^{f2}, G_{TI}^{f3}$ and G_{TI}^{f4}. However, now onwards G_{TI}^{f1} is excluded from the analysis for the reasons already explained in Sec. 5.3. The selection of the suitable subband for the communication purposes can be carried out by solving following equations :

$$\psi_{23} = P(G_{TI}^{f2} < G_{TI}^{f3}) \tag{5.7}$$

$$\psi_{24} = P(G_{TI}^{f2} < G_{TI}^{f4}) \tag{5.8}$$

$$\psi_{34} = P(G_{TI}^{f3} < G_{TI}^{f4}) \tag{5.9}$$

Based on the subband availability, solving (5.7), (5.8) and (5.9) for the values of ψ_{23}, ψ_{24} and ψ_{34} lead to the knowledge of the suitable subband.

Further, (5.7), (5.8) and (5.9) can be modified as

[†]It may be noted that, since individual interference terms are assumed to be independent but not identically distributed, the Lyapunov CLT [123] is being used here instead of classical CLT.

[‡]In carrying out the analysis with fewer tiers ($i \leq 3$), use of *T distribution* may be appropriate.

$$\psi_{23} = P(G_{TI}^{f23} < 0) \tag{5.10}$$

$$\psi_{24} = P(G_{TI}^{f24} < 0) \tag{5.11}$$

$$\psi_{34} = P(G_{TI}^{f34} < 0) \tag{5.12}$$

where G_{TI}^{f23}, G_{TI}^{f24} and G_{TI}^{f34} are the Gaussian RVs with modified means as $m_{G^{23}} = m_{G^2} - m_{G^3}$, $m_{G^{24}} = m_{G^2} - m_{G^4}$, $m_{G^{34}} = m_{G^3} - m_{G^4}$ and variances $\sigma^2_{G^{23}} = \sigma^2_{G^2} + \sigma^2_{G^3}$, $\sigma^2_{G^{24}} = \sigma^2_{G^2} + \sigma^2_{G^4}$, $\sigma^2_{G^{34}} = \sigma^2_{G^3} + \sigma^2_{G^4}$. Values of m_{G^s} and $\sigma^2_{G^s}$, $s = 2, 3, 4$ can be obtained from (5.6).

Further, solving (5.10), (5.11) and (5.12) for ψ_{23}, ψ_{24} and ψ_{34} give us

$$\psi_{23} = \frac{1}{2}\,\mathrm{erfc}\left(\frac{m_{G^{23}}}{\sqrt{(2)}\,\sigma_{G^{23}}}\right) \tag{5.13}$$

$$\psi_{24} = \frac{1}{2}\,\mathrm{erfc}\left(\frac{m_{G^{24}}}{\sqrt{(2)}\,\sigma_{G^{24}}}\right) \tag{5.14}$$

$$\psi_{34} = \frac{1}{2}\,\mathrm{erfc}\left(\frac{m_{G^{34}}}{\sqrt{(2)}\,\sigma_{G^{34}}}\right) \tag{5.15}$$

For this CLT based approach, it is found that for having closer match between the analytical results and the simulation results, appropriate weighting factors need to be introduced for the mean and variance of Gaussian RV (5.6) obtained through the use CLT[†]. Therefore, though the use of CLT gives an easy way of determining the resultant pdf of total interference but requirement of appropriate weighting factors results in added complexity. Keeping this in mind, we propose a second approach to solve the subband selection problem.

5.3.2.2 Second Approach : PDF approximation

This approach is based on using approximations for the pdf of individual interfering signals, unlike the first approach, where resultant pdf of interference is approximated. For Rayleigh fading environment, the pdf of E_{Iij}^{fs} in (5.5) is approximated by an exponential pdf $f_{E_{Iij}^{fs}}^{e}$ with modified

[†]Results obtained using this approach are discussed in Sec. 5.4.1.

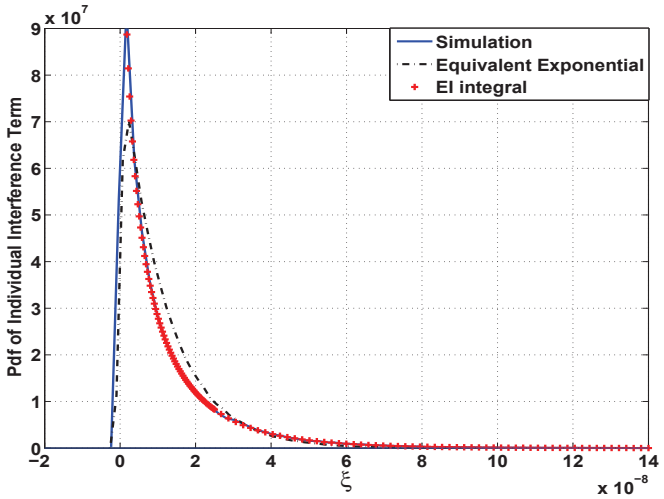

Figure 5.3: Comparison of the original pdf in (5.5), simulated pdf and approximated exponential pdf (second approach).

parameter $\lambda^e = \lambda_o/(m_{W_{ij}} m_{\tau_{ij}})$, where $m_{W_{ij}}$ and $m_{\tau_{ij}}$ are the mean of W_{ij} and τ_{ij}, respectively. A comparison among actual pdf in (5.5), simulated pdf and approximated exponential pdf is shown in Figure 5.3.

After approximating E_{Iij}^{fs} as an exponential RV E_{Iij}^{efs}, the evaluation of cdf (pdf) of E_{TI}^{fs} requires the summation of i.n.i.d. exponential RVs. The interfering signals received at the femtocell are i.n.i.d as they are received from MBSs and mUs located in different tiers and likely to have different average values.

Moreover, the symmetrical deployment of macrocells results in few similar values of λ_e. By defining $\lambda_1^e = \lambda_2^e = ... = \lambda_{r1}^e = \beta_1$, $\lambda_{r_1+1}^e = \lambda_{r_1+2}^e = ... = \lambda_{r_1+r_2}^e = \beta_2$,..., $\lambda_{r_1+r_2+..+r_{a-1}+1}^e = ... = \lambda_{r_1+r_2+...r_n}^e = \beta_a$, where $r_i \geq 1$ and $\sum_i r_i = n$ (total number of interferers), the cdf of summation of such i.n.i.d. exponential RVs can be found by using the method given in [124]. Therefore, cdf of summation of exponential RVs can be written as

$$F_{E_{TI}^{efs}}(z) = 1 - \left(\prod_{j=1}^{a} \beta_j^{r_j}\right) \sum_{k=1}^{a} \sum_{l=1}^{r_k} \frac{\psi_{k,l}(-\beta_k)\, z^{r_k-l} \exp(-\beta_k z)}{(r_k-l)!\ (l-1)!} \tag{5.16}$$

where $\psi_{k,l}(t) = -\frac{\partial^{l-1}}{\partial t^{l-1}} \left\{ \prod_{j=0, j\neq k}^{a} (\beta_j + t)^{-r_j} \right\}$, $r_o = 1$ and $\beta_o = 0$. Similarly, cdf can be calculated for other subbands also. With the cdfs known for all subbands, the optimum subband (s_{optimum}) will be the one having maximum cdf value for a given threshold. Therefore, optimum

subband can be found as

$$s_{\text{optimum}} \;=\; s \;;\quad \text{for which}\;\; F_{E_{TI}^{efs}}(z) \text{ is maximum for } \forall\;\; s. \tag{5.17}$$

where threshold may be the function of minimum detectable signal energy, channel conditions etc.

5.4 Results and Discussions

Simulation studies are carried out to verify the performance of the proposed methods for the network configuration shown in Figure 5.1. Network performance is simulated with the parameters given in Table 5.2. Four tiers of cellular network are considered with MBSs located at the center of the each cell. Every cell consists of uniformly distributed mUs. Femtocells are uniformly distributed within the cell region. Each femtocell consists of a FBS and few fUs. FBS and fUs can also be randomly located within the femtocell region. For our simulation, the various locations for positioning of the femtocell are considered within the cellular cell with index {i, j} = {1, 1}.

5.4.1 Results : First Approach

While verifying the accuracy of the CLT based first proposed analytical framework through simulations, it is found that by appropriately weighting the mean and variance values of the Gaussian RVs (5.6) obtained through the application of CLT, a good match can be achieved between the analytical results and the results obtained through the simulation studies carried out for the system under consideration. The weight factors take into account the variation of the average interference

Table 5.2: Simulation parameters

Parameter	***Symbol***	***Value***
MBS transmission power	$P_{T_{ij}}$	20 watt
Macrocell radius	R	1000 meter
MBS antenna height	h_T	32 meter
fBS (fU) antenna height	h_R	1.5 meter
Path loss exponents	η_1, η_2	(2, 3)
Sensing time	T_s	1 ms
Frequency subbands	B_s	5.18, 5.20, 5.22, 5.24 (GHz)
(Rate) parameter for exponential RV	λ_o	1

energy with the relative location of femtocell in a macrocell as some locations of femtocell result in relatively higher interference contribution from some of the interferers.

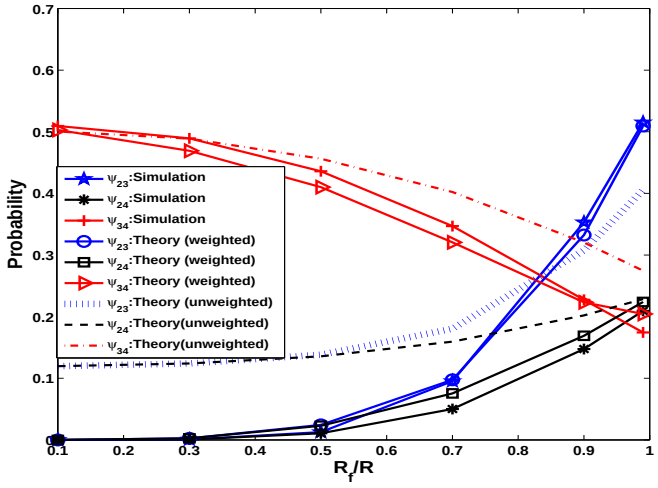

Figure 5.4: R_f/R Vs $\psi_{23}, \psi_{24}, \psi_{34}$ for $\eta_1 = 2$, $\eta_2 = 3$ and $\theta = 0$.

The effect of use of weighting factors on the variation of ψ_{23}, ψ_{24} and ψ_{34} for various values of R_f/R with $\theta = 0$ is shown in Figure 5.4, for the path loss environment, $\eta_1 = 2, \eta_2 = 3$. Figure 5.4 shows that the subband 3 has the highest probability of getting selected for $R_f \leq .2R$, while for $R_f \geq .2R$ subband 4 is least affected by the interference.

Table 5.3: Conditions for subband selection

Selected Subband	***Condition***
s = 2	$\psi_{23} > 0.5$ and $\psi_{24} > 0.5$
s = 3	$\psi_{23} < 0.5$ and $\psi_{34} > 0.5$
s = 4	$\psi_{24} < 0.5$ and $\psi_{34} < 0.5$

It may be observed that the plots obtained through the use of weighted and unweighted CLT approach in Figure 5.4 follow the same slope. Heuristically, the suitable weight factors are found as $¥_{m_{Gs}} = -0.5(R_f/R) + 1.15$ and $¥_{\sigma^2_{Gs}} = 0.05(R_f/R) + 0.1$.

Variation of Gaussian RVs (corresponding to different subbands) with θ and R_f/R is shown in Figure 5.5, Figure 5.6 and Figure 5.7. Based on the results obtained, it may be noted that for the lower values of R_f/R, satisfying the condition of Table 5.3, a subband may be optimal, while for the higher values of R_f/R another subband may have to be selected.

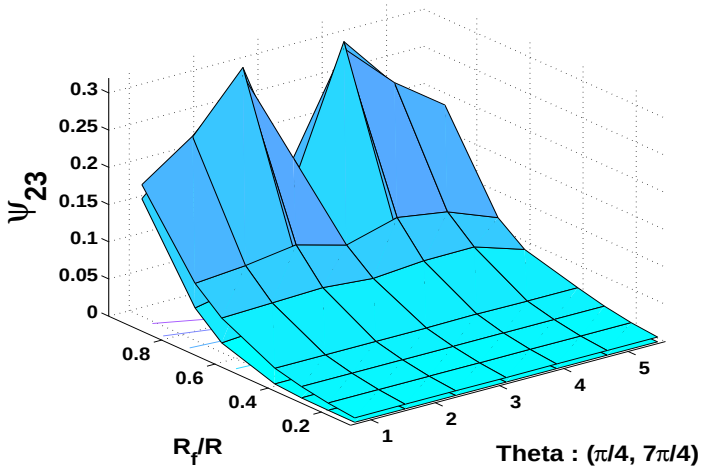

Figure 5.5: R_f/R and theta Vs subband 2 and 3 Gaussian RV ψ_{23}.

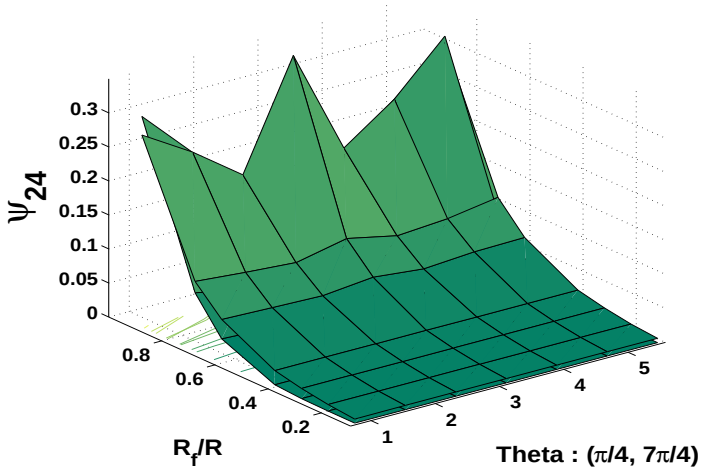

Figure 5.6: R_f/R and theta Vs subband 2 and 4 Gaussian RV ψ_{24}.

It is worth mentioning here that one of the possible reasons for the high values of the ψ_{23}, ψ_{24} and ψ_{34} obtained in the results (Figure 5.4) through the application of (unweighted) CLT is the presence of distant interferers in higher tiers that results in the relatively larger differences in means and variances of the interfering signals. However, plots obtained through the application of CLT in this case also, follow almost the same slope (as compared to the simulation results) and results in the same optimum subband because interferers of same tiers may possibly be approximated as i.i.d. RVs. Further, by using appropriate weight factors with mean and variance values corresponding

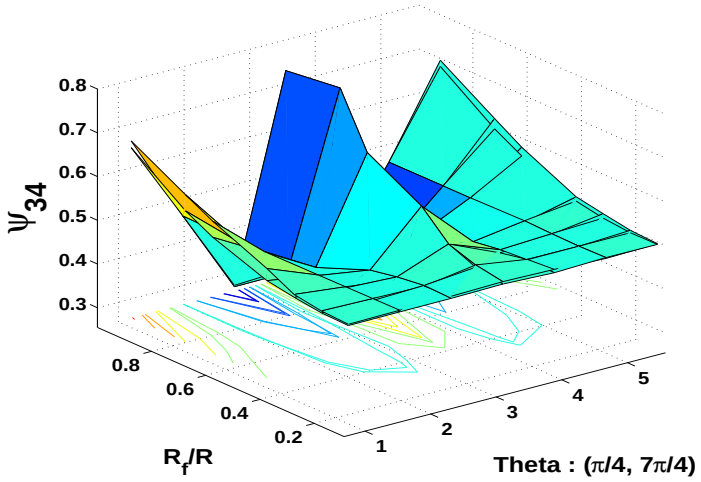

Figure 5.7: R_f/R and theta Vs subband 3 and 4 Gaussian RV ψ_{34}.

to CLT, values of ψ_{23}, ψ_{24} and ψ_{34} might have been obtained sufficiently close to the simulation results. Results may be further improved by making use of the separate weight factors for each subband at the cost of increased computational complexity.

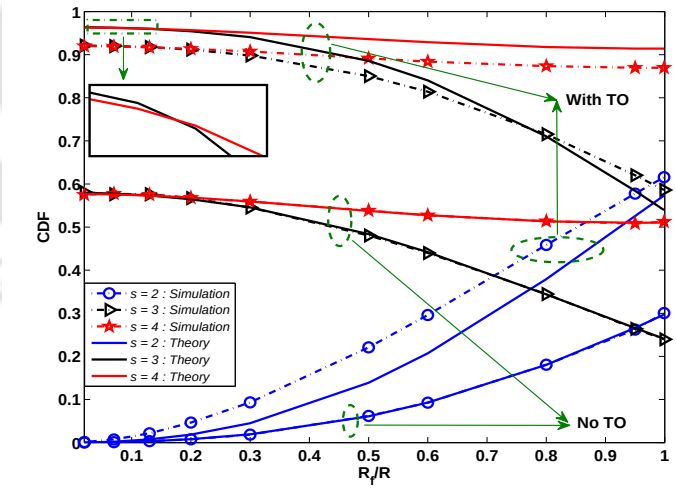

Figure 5.8: R_f/R Vs cdf (with/without TO cases) for $\theta = 0$.

5.4.2 Results : Second Approach

Based on the values of τ, two possible scenarios are discussed here in order to verify the performance of second proposed method. The values of τ taken from the set $\{0, 1\}$ lead to the perfect

TS (without TO) case, in which, either the entire transmission of a particular interferer lies within the T_s ($\tau = 1$) or it remains completely outside ($\tau = 0$). For the other possible case of imperfect TS (with TO), τ takes values from the set $(0, 1)$.

Figure 5.8 shows the cdf of with/without TO scenarios for different values of R_f/R with $\theta = 0$. It may be observed that for lower values of R_f/R ($\lesssim .2$), subband 3 has the highest probability (maximum cdf values) of getting selected (crossing point of subband 2 and subband 3 is emphasized separately in Figure 5.8). For the values of $R_f/R \gtrsim .2$, subband 4 becomes the optimum choice for femtocell communication. Variation of cdf of different subbands with R_f/R and θ is shown in Figure 5.9, Figure 5.10 and Figure 5.11.

Theory and simulation results are in perfect match for the case when there is no timing offset. The E_{TI}^{fs} term in this case constitutes the sum of exponential RVs. Therefore, cdf can be calculated by (5.16) with a fair amount of accuracy. Analysis where TO is included has E_{TI}^{fs} which comprises of sum of RVs having EI pdf (5.5), the EI pdf is further approximated by exponential pdf, which may have resulted in the marginal difference between analysis and simulation results.

The substantial difference in the cdf values for the cases of with and without TO indicates the considerable difference in the total interference energy sum among various subbands, which is essentially due to the inclusion of asynchronization effects into the analysis. While asynchronous interference does not effect subband selection considerably, the large differences in total interference energy among various subbands which arise for considering asynchronous interference, can have significant impact on proper selection of parameters in the network design phase.

5.4.3 Some More Observations

It may be observed from the results obtained that the subband 2 is not suitable for any position of the femtocell in a cellular cell with index $\{\mathrm{i},\ \mathrm{j}\} = \{1,\ 1\}$ (as $\psi_{24} < 0.50$ for first approach and subband 2 has the minimum cdf for the second approach). It can be justified by the fact that the subband 2 is also used by the MBS for mUs located in the outer ring of the cellular cell with index $\{\mathrm{i},\ \mathrm{j}\} = \{1,\ 1\}$, therefore, MBS acts as the strongest contributor to the aggregate interference for subband 2. Thus, the overall interference level in subband 2 remains considerably high for almost all the locations of femtocell. However, if femtocell is allowed to choose only between subband 2 and 3 (in case subband 4 is unavailable), subband 2 may be an optimal choice for very high values of $R_f/R \gtrsim .96$ (near the cell boundary).

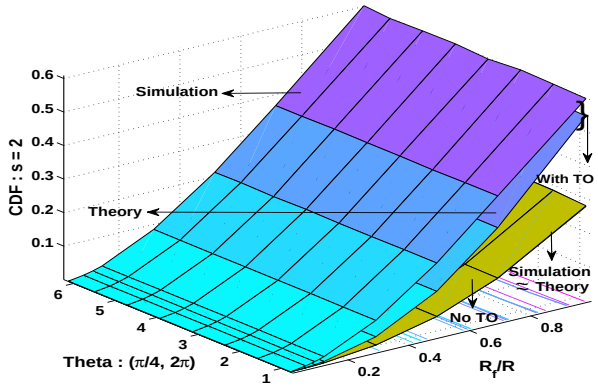

Figure 5.9: R_f/R and Theta (θ) Vs cdf of subband 2.

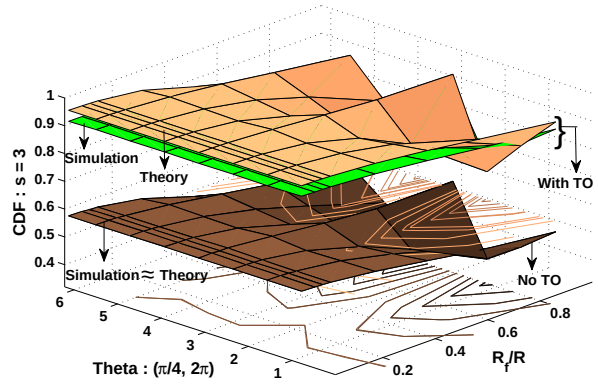

Figure 5.10: R_f/R and Theta (θ) Vs cdf of subband 3.

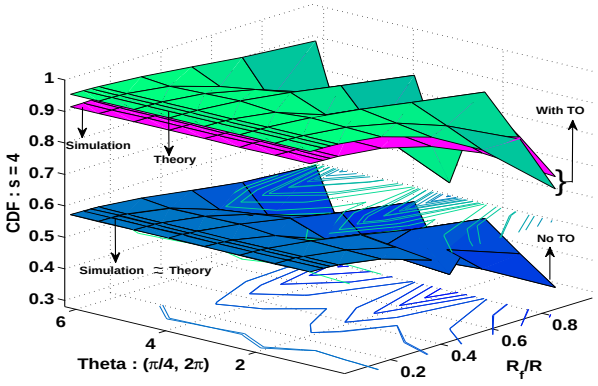

Figure 5.11: R_f/R and Theta (θ) Vs cdf of subband 4.

Analytical results and simulation results are in good match for all the cases. The symmetrical behaviour can be observed with respect to θ. It may be noted that a subband which becomes an optimal choice for communication for lower values of R_f/R may not remain as an optimal choice for higher values of R_f/R.

5.5 Conclusion

In this chapter, analytical methods of optimum subband selection for femtocells in OFDMA based cellular network have been presented. The proposed method is general enough to address the scenarios like signals with and without TO and various types of interferers (uplink/downlink) as well. Using appropriate approximations, closed form solutions are obtained while addressing the effect of CCI in the analysis of subband selection. Moreover, this is an energy based approach and points out the effect of asynchronization (which results due to propagation delays and TO in the network) on the system parameters to be considered while designing the practical network. While the first approach is independent of specific cases and applicable over almost all kind of interference scenarios, second approach is scenario specific. However, the first approach using Gaussian approximation requires the use of heuristic weights, which need to be calculated for different locations of femtocells to optimize the network performance.

It may be noted that the performance improvement or the network designing advantage gained by choosing the subband least affected by the interference comes at the cost of reduced network throughput, as the femtocells have to sense the environment on a regular basis, based on the network settings. Therefore, it becomes imperative to choose the T_s very carefully to achieve an optimal trade-off between performance and throughput. This analytical framework can be useful for subband and optimum values of system parameter selection in a large practical cellular network which is based on OFDMA (OFDM) technique.

6

Discussion and Future Work

Contents

In this thesis, we address issues concerning modeling and analysis of interference in an asynchronous environment. We propose models and methods to quantify the asynchronous interference. Moreover, this thesis discusses an crucial issue of interference management in heterogeneous/overlaid wireless networks. This chapter presents the summary of the thesis and also discusses some of the possible future directions of extension of the research works reported in this thesis. The main contributions of this thesis are summarized in Section 6.1 and possible future extension of the work are outlined in Section 6.2.

6.1 Summary of Contributions and Discussions

In this section, we briefly summarize and discuss our contributions and findings during this thesis work. This thesis presents :

- ✔ **Comprehensive review of Various Aspects of Interference in an Asynchronous Environment** :

  Issues related to interference in un-coordinated networks have been discussed in detail. Various available models/approaches to quantify the interference have been discussed thoroughly and their shortcomings while addressing interference in asynchronous environment have been pointed out. Some asynchronous interference modeling aspects which are not well addressed in the literature have also been discussed.

- ✔ **Outage Analysis of an Asynchronous network Using Proposed Model** :

  We proposed a model to calculate the effective overlap experienced by the bit of desired frame due to the bit(s) of interfering frame. Also, we introduced a metric *EINR* to quantify ratio of the desired energy to interference energy plus noise spectral density ratio. Effective number of interferers, taking MAC protocol into account, is calculated. Using the *EINR* metric, outage performance has been analyzed to observe the effects of i.n.i.d. interferes on wireless network performance. Apart from outage probability, some other parameters such as performance of individual node in terms of total successfully received bits, total successful receptions throughout the network, average interference energy are also investigated. To observe the effect of antenna height on network performance in an interference limited environment, some simulation results has been presented.

✔ **BER Analysis of an Asynchronous network** :

In order to quantify the effects of interference on network performance, we have evaluated the BER in the presence of i.n.i.d. interferers employing the BPSK scheme. A method is proposed to find the (partial) overlap and index of bit(s) of interfering frame. To calculate the BER, overlap of frames is addressed carefully using the proposed method. Pdf of effective signed fractional overlap variable is calculated taking partial overlap into account. Using an amplitude metric approach, pdf of resultant amplitude of effective interference has been calculated. By applying appropriate approximations, closed form expression for the BER is also derived. Along with BER variation w.r.t number of i.n.i.d. interferers, several other performance measures have also been investigated, such as, variation of number of successfully received bits by a single user and average variance sum w.r.t. i.n.i.d. interferers as well as interference range factor. Average bit success rate and interference variance sum are investigated w.r.t. interference range factor. Inconsequentialness of phase terms, associated with interfering signals, in the presence of large number of interferers are also pointed out.

✔ **Investigation of Interference Management methods for Heterogeneous/Overlaid networks** :

In this part of work, we have discussed management of interference in heterogeneous/overlaid wireless networks. Some existing methods of interference management have been investigated. Interference management by subband allocation has been discussed in detail. For illustrating the concept of interference management in an overlaid network, a two-tier OFDMA based femtocell-cellular network combination has been taken as an example. An analytical framework has been proposed to find the optimum subband for communication purposes in femtocells.

6.2 Suggestions for Future Work

In this thesis we have addressed some of the basic issues related to interference analysis and management for multi-user environment. We classify some possible directions in which the present work can be extended into two parts, as outlined below:

a) Direct Extension of the Current Work :

While carrying out the research work presented in this thesis, we have taken some assumptions

in order to reduce the computational complexities. Replacing those assumptions with more practical constraints may bring some additional insight to the system performance. Therefore, the work presented here can be directly extended by incorporating practical conditions in place of assumptions taken. This sub-section talks about some such possibilities :

- ✎ In outage analysis, to calculate the mean and variance of sum of log normal RVs, Wilkinson's approach has been used. Some other robust methods such as Schwartz and Yeh's, cumulants Matching Method may be used to obtain better accuracy. However, it may incur calculation burden.
- ✎ For BER calculations, system is assumed to be utilizing BPSK modulation scheme. Work can be extended for MPSK schemes. It can also be extended for other modulation schemes as well.
- ✎ An uncoded system is assumed for this work. Study of coded systems may be a possible area of extension.
- ✎ BER and subband selection investigations may be extended by including shadow effects for a better characterization of fading environment.
- ✎ Users with unequal frame lengths and effects of ACI may be taken into account for modeling of a relatively general scenario.

b) Extension in Other Possible Directions :

Apart from the possibilities described above, some other potential directions in which, this work can be extended are as follows :

- ✎ Recent literature shows that various interactions among independent nodes, interference and resource conflict scenarios in wireless networks may be efficiently modeled as a game by using a set of tools offered by *game theory*. We envisage that analysing interference limited networks with help of game theory may be an efficient and interesting way to model complex scenarios.
- ✎ The analysis presented in this thesis does not consider any user cooperation. Interference analysis of a co-operative system can also be carried out.

A

Outage Performance

Contents

A.1 Calculations for Special Case ($\eta_1 = \eta_2 = \eta$) of $P^i_{r_z,Rx}$

Considering the special case, $\eta_1 = \eta_2 = \eta$, we make the following assumptions

$$\begin{aligned} r\left(1+\frac{r}{g}\right) &\approx M_1\, r \qquad ; \text{for} \quad r < g \\ r\left(1+\frac{r}{g}\right) &\approx M_2\, \frac{r^2}{g} \qquad ; \text{for} \quad r \geqslant g \end{aligned} \tag{A.1}$$

where M_1 and M_2 are constants to be defined later. It can be noted that accuracy of assumptions made decreases as r lies in the vicinity of g. $P^i_{r_{zRx}}$ in (3.21) can be written as

$$P^i_{r_{zRx}} = \frac{1}{2\left(\sqrt{2}A_r - \lambda_o\right)} \left[\int_{\lambda_o}^{g} P\left[i \in r_{zRx} | \, r\right] \, dr + \int_{g}^{\sqrt{2}A_r} P\left[i \in r_{zRx} | \, r\right] \, dr\right] \tag{A.2}$$

Now, with some calculations using above assumptions, $P^i_{r_{zRx}}$ for this case can be written as

$$\begin{aligned} P^i_{r_{zRx}}\big|_{\eta_1=\eta_2=\eta} = \frac{1}{2\left(\sqrt{2}A_r - \lambda_o\right)} \times \\ \Big[\Big\{ f\left(r, m_1, n_1\right)|_{r=g} + f\left(r, m_2, n_2\right)|_{r=\sqrt{2}A_r} + f\left(r, m_3, n_3\right)|_{r=\lambda_o} + f\left(r, m_4, n_4\right)|_{r=g} \Big\} \\ - \Big\{ f\left(r, m_1, n_1\right)|_{r=\lambda_o} + f\left(r, m_2, n_2\right)|_{r=g} + f\left(r, m_3, n_3\right)|_{r=g} + f\left(r, m_4, n_4\right)|_{r=\sqrt{2}A_r} \Big\} \Big] \end{aligned} \tag{A.3}$$

where, $f(r, m_i, n_i)$ is given by

$$f\left(r, m_i, n_i\right) = (r)\, \mathrm{erf}\left(m_i - n_i \log_{10} r\right) - 10^{\frac{4 m_i n_i + \log 10}{4 {n_i}^2}} \mathrm{erf}\left(m_i - n_i \log_{10} r + \frac{\log 10}{2 n_i}\right) \quad ; i = 1, 2, 3, 4 \tag{A.4}$$

Constants m_{1-4} and n_{1-4} are given by

$$\begin{aligned} m_1 &= \left(\frac{P_T}{\Psi P_{th}}\bigg|_{dB} - \eta 10 \log_{10} M_1\right) \Big/ \sqrt{2}\sigma \\ m_2 &= m_1|_{M_1 -> (M_2/g)} \\ m_3 &= \left(-\eta 10 \log_{10} M_1\right) \Big/ \sqrt{2}\sigma \\ m_4 &= m_3|_{M_1 -> (M_2/g)} \\ n_1 &= n_3 = (\eta 10) \Big/ \sqrt{2}\sigma \\ n_2 &= n_4 = (\eta 20) \Big/ \sqrt{2}\sigma \end{aligned} \tag{A.5}$$

Heuristically, we found that $M_1 = 1 + \eta/7$ and $M_2 = 1 + \eta/10$ gives better agreement with simulation results.

A.2 Comment on Replacement in Equation 3.38

In asynchronized environment, it is difficult to calculate analytically the absolute values of effective number of interferers (type-1, type-2) with independently scheduled transmission slots. Therefore, simulations have been carried out, with expected as well as absolute values of I_{T_1} and I_{T_2}. We have observed that error induced for using expected values of I_{T_1} and I_{T_2} in place of their absolute values is not significant as long as the total number of interferers I^*_{eff} are same for both the cases. For the sake of completeness, we performed the simulation for outage analysis considering both the cases as shown in Figure A.1. The classification of interferers as type-1 and type-2 is based on the starting point of the transmission rather then received energy (power), therefore, it does not make any significant difference in calculation of total received interfering energy as far as total interferers are same.

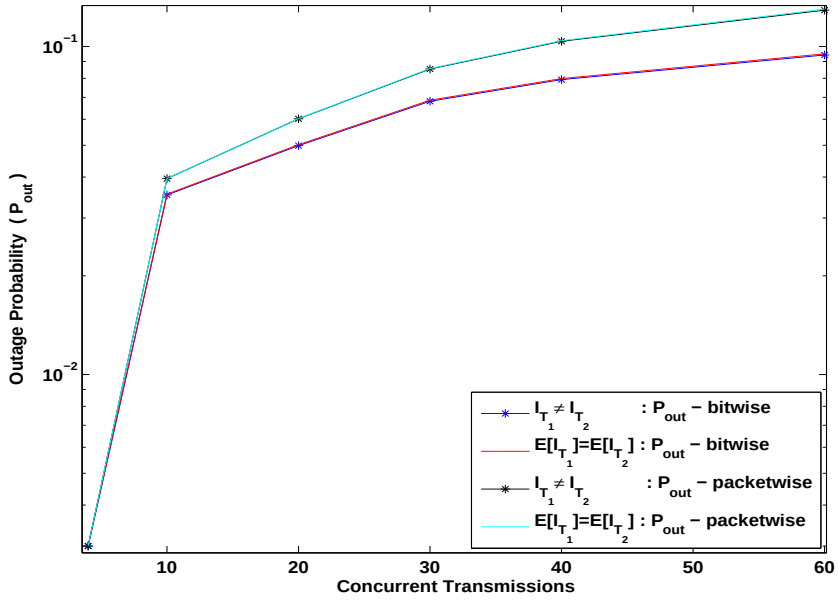

Figure A.1: Outage probability with $I_{T_1} \neq I_{T_2}$ and $E(I_{T_1}) = E(I_{T_2})$.

A.3 GMM method : Mean and Variance Calculation of $\hbar$

To calculate the mean ($m_\hbar$) and variance ($\sigma_\hbar$) of Gaussian RV $\hbar$, we use Wilkinson's approach [4], [9] in generalized form [31]. Some important calculation steps are as follows :

Wilkinson's approach calculates the mean and variance of $\hbar$ by matching the first and second moments of both side of (3.41), i.e.

$$E\left[\Upsilon_o e^{-\lambda\varepsilon} + \sum_{j=1}^{I_{eff}} \Upsilon_{ij}\; e^{\lambda(\varepsilon_j-\varepsilon)}\right] = E\left[e^{\lambda\hbar}\right] \tag{A.6}$$

$$E\left[\left(\Upsilon_o e^{-\lambda\varepsilon} + \sum_{j=1}^{I_{eff}} \Upsilon_{ij}\; e^{\lambda(\varepsilon_j-\varepsilon)}\right)^2\right] = E\left[e^{2\lambda\hbar}\right] \tag{A.7}$$

The above equations are different from traditional ones due to weighting factors Υ_o and Υ_j (infact in [31] also, due to SIR consideration only, Υ_o is neglected). For any integer n, using $E\left[e^{n\hbar}\right] = \exp\left(nm_\hbar + \frac{1}{2}n^2\sigma_\hbar^2\right)$ and with some modifications, final expressions of mean ($m_\hbar$) and variance ($\sigma_\hbar$) for Gaussian RV $\hbar$, can be written as

$$m_\hbar = (1/\lambda)\left(2\ln(¥_1) - \frac{1}{2}\ln(¥_2)\right) \tag{A.8}$$

$$\sigma_\hbar^2 = (1/\lambda^2)\left(\ln(¥_2) - 2\ln(¥_1)\right) \tag{A.9}$$

where $¥_1$ is given by

$$¥_1 = \Upsilon_o\, e^{-m_{t_o}+\frac{1}{2}\sigma_{t_o}^2} + \sum_{j=1}^{I_{eff}} E\left[\Upsilon_j\right] e^{-m_{\hat{t}_j}+\frac{1}{2}\sigma_{\hat{t}_j}^2} \tag{A.10}$$

where $t_o = \lambda\varepsilon$ and $\hat{t}_j = \lambda(\varepsilon_j - \varepsilon)$ and $\mathrm{E}[\Upsilon_j]$ is given by

$$\begin{aligned} E\left[\Upsilon_j\right] &= E\left[\left(\frac{r}{r_j}\right)^{\eta_1}\right] E\left[\left(\frac{g+r}{g+r_j}\right)^{\eta_2}\right] E\left[|a_{jd}|^2\right] E\left[\tau_{ij}^{T_1} + \tau_{ij}^{T_2}\right] \\ &= \frac{r^{\eta_1}\left[\left(\sqrt{2}A_r\right)^{\eta_1-1} - (\lambda_o)^{\eta_1-1}\right]}{(\eta_1-1)\left(\sqrt{2}A_r - \lambda_o\right)\left(\sqrt{2}A_r\lambda_o\right)^{\eta_1-1}} \frac{(g+r)^{\eta_2}\left[\left(\sqrt{2}A_r + g\right)^{\eta_2-1} - (\lambda_o + g)^{\eta_2-1}\right]}{(\eta_2-1)\left(\sqrt{2}A_r - \lambda_o\right)\left(\sqrt{2}A_r + g\right)^{\eta_2-1}(\lambda_o + g)^{\eta_2-1}} \\ &\quad \times \left[E\left[\tau_{ij}^{T_1}\right] + E\left[\tau_{ij}^{T_2}\right]\right] \end{aligned} \tag{A.11}$$

Further, $E[\tau_{ij}^{T_1}]$ and $E[\tau_{ij}^{T_2}]$ in (A.11) can be found from (3.11) and (3.17), respectively.

In addition, $¥_2$ is

$$¥_2 \;=\; ¥_{21} \,+ ¥_{22} \,+ ¥_{23} \tag{A.13}$$

where $¥_{21} = \Upsilon_o^2 \exp\left(-2\, m_{t_o} \,+\, 2\,\sigma_{t_o}^2\right)$ and $¥_{22}$ and $¥_{23}$ are given by following equations :

$$¥_{22} \;=\; \sum_{j=1}^{I_{eff}} E\left[\Upsilon_j^2\right] \exp\left(2\, m_{\hat{t}_j} \,+\, 2\,\sigma_{\hat{t}_j}^2\right) + 2 \sum_{j=1}^{I_{eff}-1} \sum_{k=j+1}^{I_{eff}} E\left[\Upsilon_j\right] E\left[\Upsilon_k\right] \exp\left(\left(m_{\hat{t}_j} + m_{\hat{t}_k}\right) + \frac{1}{2}\left(\sigma_{\hat{t}_j}^2 + \sigma_{\hat{t}_k}^2\right)\right) \tag{A.14}$$

$$¥_{23} \;=\; \Upsilon_o \exp\left(-m_{t_o} + \frac{1}{2}\,\sigma_{t_o}^2\right) \sum_{j=1}^{I_{eff}} E\left[\Upsilon_j\right] \exp\left(m_{\hat{t}_j} + \frac{1}{2}\,\sigma_{\hat{t}_j}^2\right) \tag{A.15}$$

B

BER Performance

Contents

B.1 ABER Analysis with Phase Considered

The modeling in chapter 4 is carried out using an amplitude based metric, which does not take phase of the interfering signals into account. It may be interesting to figure out the differences in ABER values which may occur when phase is also taken into consideration. Here, we analyze the effect of inclusion of phase on ABER with the help of simulation and compare the results of two cases, namely, ABER with phase and without phase (amplitude based metric).

To observe the effects of phase term on ABER values, we consider an individual jth interfering signal as follows :

$$I_j^{phase} = \sqrt{P_r\ T_b}\ h_j\ cos(\theta_j)\ (S_{b_1}\, O_1 + S_{b_2}\, O_2) \tag{B.1}$$

where θ_j is assumed to be uniformly distributed in $[0, 2\pi]$. For comparison purpose, following jth interfering signal based on amplitude metric without taking phase term into account is considered :

$$I_j = \sqrt{P_r\ T_b}\ h_j\ \ (S_{b_1}\, O_1 + S_{b_2}\, O_2) \tag{B.2}$$

Figure B.1 shows the simulation results for the ABER_p[†] with respect to increasing number of concurrent transmissions from i.n.i.d. interfering users after considering the effect of phase term.

Result shows that inclusion of phase term does not affect the overall system performance considerably in terms of ABER. However, difference in ABER values for the two cases is more prominent at small number of concurrent transmissions and this difference vanishes as the number of concurrent transmissions increases. One intuitive explanation of this result comes from the fact that as an additive term, resultant interference gives randomness to the desired signal component. This additional randomness in the desired signal component results in (bit) error. Considering the phase term ($\cos(\theta)$) for each interfering signal component further increases the randomness of the overall signal, which can be the possible reason of higher BER at small number of interferers. Now, as the number of interferers increases, the randomness (variance) of resultant interfering signal reduces considerably due to law of large numbers. Therefore, the phase term loses its effect in terms of added randomness which reduces in the presence of large number of interferers and hence, ABER

[†] ABER_p gives the average BER performance after considering the effect of phase term.

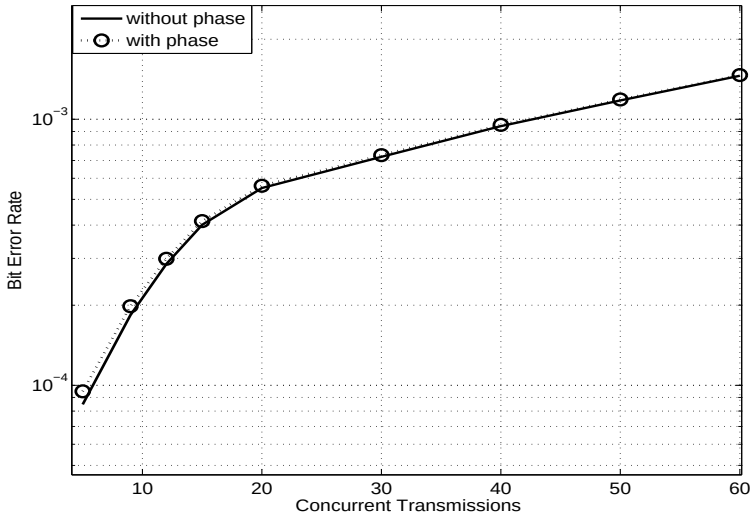

Figure B.1: ABER in an asynchronous wireless network in the presence of i.n.i.d. interferers (w = 2000 m., $I_{RF} = 2.5$.

and ABER_p approach toward almost the similar values. Therefore, this result shows that inclusion of phase terms, associated with interfering signals, is inconsequential for a interference limited environment. The result obtained here is supported by some of the previous works [64, 67] also.

B.2 Details of Derivation of the PDF of RV W_j (4.23)

First, we define a new RV $\xi_j = A_j^{\text{m}}\ \gamma_j^{s,T_1}$. With the pdf of γ_j^{s,T_1} calculated in (4.15), the pdf of RV ξ_j can be easily calculated and we represent the same pdf by $f_{\xi_j}(\xi)$. The range of the new RV ξ_j becomes $[-A_j^{\text{m}}, A_j^{\text{m}}]$. Now, we provide some of the important steps needed to find the pdf of the effective interference term W_j as follows :

After some simplification, the pdf of W_j conditioned on ξ_j can be written as

$$f_{W_j}\left(w\,|\xi_j\right) \;=\; \frac{1}{\xi_j}\, f_{h_j}\left(\frac{w}{\xi_j}\right) \tag{B.3}$$

where $f_{h_j}(.)$ is the pdf of channel fading parameter corresponding to the jth effective interfering term. Removing the condition on ξ_j, we can write

$$f_{W_j}\left(w\right) \;=\; \int_{-A_j^m}^{A_j^m} \frac{1}{\xi_j} f_{h_j}\left(\frac{w}{\xi_j}\right)\; f_{\xi_j}\left(\xi\right)\, d\xi \tag{B.4}$$

For $\xi_j \in [-A_j^{\text{m}}, 0]$, w requires to be less than zero to make the argument of the pdf of channel

fading parameter positive. Therefore, for $w < 0$,

$$f_{W_j}(w)|_{\xi_j<0} = \int_{-A_j^m}^{0} \frac{-1}{\xi_j} f_{h_j}\left(\frac{w}{\xi_j}\right) f_{\xi_j}(\xi)\, d\xi \tag{B.5}$$

Eq. (B.5) can be further written as

$$\begin{aligned} f_{W_j}(w)|_{\xi_j<0} &= -\int_{-A_j^{\mathrm{m}}}^{0} \frac{w}{\xi^2\sigma_f^2} \exp\left(-\frac{w^2}{2\xi^2\sigma_f^2}\right)\left[\frac{\delta\left(\xi+A_j^{\mathrm{m}}\right)}{4} + \frac{1}{4A_j^{\mathrm{m}}}\right] d\xi \\ &= \sqrt{\frac{\pi}{2}}\frac{1}{4A_j^{\mathrm{m}}\sigma_f}\operatorname{erfc}\left[-\frac{w}{\sqrt{2}\,A_j^{\mathrm{m}}\sigma_f}\right] - \frac{w}{4(A_j^{\mathrm{m}})^2\sigma_f^2}\exp\left[-\frac{w^2}{2(A_j^{\mathrm{m}})^2\sigma_f^2}\right] \end{aligned} \tag{B.6}$$

For $\xi_j \in [0, A_j^{\mathrm{m}}]$, w has to be greater than zero to make the argument of the pdf of channel fading parameter positive. Therefore, for $w > 0$ also, we have

$$\begin{aligned} f_{W_j}(w)|_{\xi_j>0} &= \int_{0}^{A_j^{\mathrm{m}}} \frac{w}{\xi^2\sigma_f^2} \exp\left(-\frac{w^2}{2\xi^2\sigma_f^2}\right)\left[\frac{\delta\left(\xi-A_j^{\mathrm{m}}\right)}{4} + \frac{1}{4A_j^{\mathrm{m}}}\right] d\xi \\ &= \sqrt{\frac{\pi}{2}}\frac{1}{4A_j^{\mathrm{m}}\sigma_f}\operatorname{erfc}\left[\frac{w}{\sqrt{2}\,A_j^{\mathrm{m}}\sigma_f}\right] + \frac{w}{4(A_j^{\mathrm{m}})^2\sigma_f^2}\exp\left[-\frac{w^2}{2(A_j^{\mathrm{m}})^2\sigma_f^2}\right] \end{aligned} \tag{B.7}$$

Eq. (B.6) and (B.7) jointly describe the complete pdf of the effective interfering term W_j, as given in (4.23).

Bibliography

[1] P. Cardieri, "Modeling interference in wireless ad hoc networks," *Communications Surveys Tutorials, IEEE*, vol. 12, no. 4, pp. 551 –572, quarter 2010.

[2] A. Stranne, O. Edfors, and B. Molin, "Energy-based interference analysis of heterogeneous packet radio networks," *Communications, IEEE Transactions on*, vol. 54, no. 7, pp. 1299 –1309, july 2006.

[3] T. Zahir, K. Arshad, A. Nakata, and K. Moessner, "Interference management in femtocells," *Communications Surveys Tutorials, IEEE*, vol. 15, no. 1, pp. 293–311, 2013.

[4] A. Abu-Dayya and N. Beaulieu, "Outage probabilities in the presence of correlated lognormal interferers," *Vehicular Technology, IEEE Transactions on*, vol. 43, no. 1, pp. 164 –173, feb 1994.

[5] T. S. Rappaport, *Wireless Communications*, 2nd ed. NJ, USA: Prentice-Hall, 2002.

[6] U. Schilcher, G. Brandner, and C. Bettstetter, "Diversity schemes in interference-limited wireless networks with low-cost radios," in *Wireless Communications and Networking Conference (WCNC), 2011 IEEE*, march 2011, pp. 707 –712. doi: 10.1109/WCNC.2011.5779249

[7] P. Gupta and P. Kumar, "The capacity of wireless networks," *Information Theory, IEEE Transactions on*, vol. 46, no. 2, pp. 388 –404, mar 2000.

[8] I. Krikidis, J. Thompson, and S. McLaughlin, "Relay selection issues for amplify-and-forward cooperative systems with interference," in *Wireless Communications and Networking Conference, 2009. WCNC 2009. IEEE*, 2009, pp. 1–6.

[9] P. Cardieri and T. Rappaport, "Statistics of the sum of lognormal variables in wireless communications," in *Vehicular Technology Conference Proceedings, 2000. VTC 2000-Spring Tokyo. 2000 IEEE 51st*, vol. 3, 2000, pp. 1823 –1827 vol.3. doi: 10.1109/VETECS.2000.851587

[10] M.-S. Alouini and A. Goldsmith, "Area spectral efficiency of cellular mobile radio systems," in *Vehicular Technology Conference, 1997 IEEE 47th*, vol. 2, may 1997, pp. 652 –656 vol.2. doi: 10.1109/VETEC.1997.600409

[11] G. Peng, T. Guofang, F. Yuan, and L. Shuangchun, "The analysis of the interference between wcdma and wimax systems," in *Communications Technology and Applications, 2009. ICCTA '09. IEEE International Conference on*, Oct 2009, pp. 180–184. doi: 10.1109/ICCOMTA.2009.5349215

[12] H. Zhang, N. Mehta, A. Molisch, J. Zhang, and H. Dai, "Asynchronous interference mitigation in cooperative base station systems," *Wireless Communications, IEEE Transactions on*, vol. 7, no. 1, pp. 155–165, Jan 2008.

[13] M. Park, K. Ko, H. Yoo, and D. Hong, "Performance analysis of ofdma uplink systems with symbol timing misalignment," *Communications Letters, IEEE*, vol. 7, no. 8, pp. 376–378, Aug 2003.

[14] V. Chandrasekhar, J. Andrews, and A. Gatherer, "Femtocell networks: a survey," *Communications Magazine, IEEE*, vol. 46, no. 9, pp. 59–67, 2008.

[15] D. Calin, H. Claussen, and H. Uzunalioglu, "On femto deployment architectures and macrocell offloading benefits in joint macro-femto deployments," *Communications Magazine, IEEE*, vol. 48, no. 1, pp. 26–32, January 2010.

[16] N. Saquib, E. Hossain, L. B. Le, and D. I. Kim, "Interference management in ofdma femtocell networks: issues and approaches," *Wireless Communications, IEEE*, vol. 19, no. 3, pp. 86–95, June 2012.

[17] K. Hamdi, "Precise interference analysis of ofdma time-asynchronous wireless ad-hoc networks," *Wireless Communications, IEEE Transactions on*, vol. 9, no. 1, pp. 134–144, January 2010.

[18] F. Babich and M. Comisso, "Theoretical analysis of asynchronous multi-packet reception in 802.11 networks," *Communications, IEEE Transactions on*, vol. 58, no. 6, pp. 1782–1794, June 2010.

[19] R. Rom and M. Sidi, *Multiple Access Protocols*. Springer-Verlag, 1989.

[20] A. Krishna and R. O. LaMaire, "A comparison of radio capture models and their effect on wireless lan protocols," in *Universal Personal Communications, 1994. Record., 1994 Third Annual International Conference on*, Sep 1994, pp. 666–672.

[21] A. Iyer, C. Rosenberg, and A. Karnik, "What is the right model for wireless channel interference?" *Wireless Communications, IEEE Transactions on*, vol. 8, no. 5, pp. 2662 –2671, may 2009.

[22] A. Behzad and I. Rubin, "On the performance of graph-based scheduling algorithms for packet radio networks," in *Global Telecommunications Conference, 2003. GLOBECOM '03. IEEE*, vol. 6, Dec 2003, pp. 3432–3436 vol.6. doi: 10.1109/GLOCOM.2003.1258872

[23] A. Gore, A. Karandikar, and S. Jagabathula, "On high spatial reuse link scheduling in stdma wireless ad hoc networks," in *Global Telecommunications Conference, 2007. GLOBECOM '07. IEEE*, Nov 2007, pp. 736–741. doi: 10.1109/GLOCOM.2007.143

[24] A. Bertossi, C. Pinotti, and R. Tan, "Channel assignment with separation for interference avoidance in wireless networks," *Parallel and Distributed Systems, IEEE Transactions on*, vol. 14, no. 3, pp. 222–235, March 2003.

[25] S. Vakil and B. Liang, "Cooperative diversity in interference limited wireless networks," *Wireless Communications, IEEE Transactions on*, vol. 7, no. 8, pp. 3185 –3195, august 2008.

[26] J. Andrews, F. Baccelli, and R. Ganti, "A tractable approach to coverage and rate in cellular networks," *Communications, IEEE Transactions on*, vol. 59, no. 11, pp. 3122–3134, November 2011.

[27] M. Win, P. Pinto, and L. Shepp, "A mathematical theory of network interference and its applications," *Proceedings of the IEEE*, vol. 97, no. 2, pp. 205 –230, feb. 2009.

[28] A. El-Hoiydi, "Interference between bluetooth networks-upper bound on the packet error rate," *Communications Letters, IEEE*, vol. 5, no. 6, pp. 245 –247, june 2001.

[29] K. Gulati, B. Evans, J. Andrews, and K. Tinsley, "Statistics of co-channel interference in a field of poisson and poisson-poisson clustered interferers," *Signal Processing, IEEE Transactions on*, vol. 58, no. 12, pp. 6207 –6222, dec. 2010.

[30] R. Hekmat and P. Mieghem, "Interference power statistics in ad-hoc and sensor network," *Wireless Networks*, vol. 14, no. 5, pp. 591 –599, Jan. 2007.

[31] M. Pratesi, F. Santucci, and F. Graziosi, "Generalized moment matching for the linear combination of lognormal rvs: application to outage analysis in wireless systems," *Wireless Communications, IEEE Transactions on*, vol. 5, no. 5, pp. 1122 –1132, may 2006.

[32] F. Graziosi and F. Santucci, "On sir fade statistics in rayleigh-lognormal channels," in *Communications, 2002. ICC 2002. IEEE International Conference on*, vol. 3, 2002, pp. 1352 – 1357 vol.3. doi: 10.1109/ICC.2002.997071

[33] P. Tarasak, T. Quek, and F. Chin, "Uplink timing misalignment in open and closed access ofdma femtocell networks," *Communications Letters, IEEE*, vol. 15, no. 9, pp. 926–928, 2011.

[34] K. Raghunath, Y. Itankar, A. Chockalingam, and R. Mallik, "Ber analysis of uplink ofdma in the presence of carrier frequency and timing offsets on rician fading channels," *Vehicular Technology, IEEE Transactions on*, vol. 60, no. 9, pp. 4392–4402, 2011.

[35] T. Novlan, R. Ganti, A. Ghosh, and J. Andrews, "Analytical evaluation of fractional frequency reuse for ofdma cellular networks," *Wireless Communications, IEEE Transactions on*, vol. 10, no. 12, pp. 4294–4305, 2011.

[36] T. Nandagopal, T. eun Kim, X. Gao, and V. Bharghavan, "Achieving mac layer fairness in wireless packet networks," in *Proc. ACM/IEEE MobiCom 2000*, Aug. 2000, pp. 87–98.

[37] J. Venkataraman, M. Haenggi, and O. Collins, "Shot noise models for the dual problems of cooperative coverage and outage in random networks," in *44th Annual Allerton Conf. Commun., Control, Comput.*, 2006.

[38] S. Lowen and M. C. Teich, "Power-law shot noise," *Information Theory, IEEE Transactions on*, vol. 36, no. 6, pp. 1302–1318, Nov 1990.

[39] D. J. Daley and D. Vere-Jones, *An Introduction to The Theory of Point Processes: Volume I: Elementry Theory and Methods*. Springer.

[40] H. Koskinen, T. Tirronen, and J. Virtamo, "Exact distribution of poisson shot noise with constant marks under power-law attenuation," *Electronics Letters*, vol. 42, no. 21, pp. 1237–1238, Oct 2006.

[41] D. Stoyan, W. S. Kendall, and J. Mecke, *Stochastic Geometry and its Applications*. John Wiley & Sons, 1995.

[42] A. Busson, G. Chelius, and J. M. Gorce, "Interference modeling in csma multi-hop wireless networks," INRIA, research Report 6624.

[43] F. Baccelli, B. Blaszczyszyn, and P. Muhlethaler, "A spatial reuse aloha mac protocol for multihop wireless mobile networks," INRIA, research Report 4955.

[44] D. B. West, *Introduction to Graph Theory*. Prentice-Hall, 1996.

[45] Y. Wang, X. Liu, J. Yin, and N. Jing, "Efficiently link scheduling in wireless sensor network," in *Pervasive Computing and Applications, 2006 1st International Symposium on*, Aug 2006, pp. 764–768. doi: 10.1109/SPCA.2006.297526

[46] W. Hale, "Frequency assignment: Theory and applications," *Proceedings of the IEEE*, vol. 68, no. 12, pp. 1497–1514, Dec 1980.

[47] Y. Gao, J. Hou, and H. Nguyen, "Topology control for maintaining network connectivity and maximizing network capacity under the physical model," in *INFOCOM 2008. The 27th Conference on Computer Communications. IEEE*, April 2008, pp. –. doi: 10.1109/INFOCOM.2008.155

[48] O. Dousse, F. Baccelli, and P. Thiran, "Impact of interferences on connectivity in ad hoc networks," in *INFOCOM 2003. Twenty-Second Annual Joint Conference of the IEEE Computer and Communications. IEEE Societies*, vol. 3, March 2003, pp. 1724–1733 vol.3. doi: 10.1109/INFCOM.2003.1209195

[49] K. Jain, J. Padhye, V. N. Padmanabhan, and L. Qiu, "Impact of interference on multi-hop wireless network performance," in *Proceedings of the 9th Annual International Conference on Mobile Computing and Networking*, ser. MobiCom '03. New York, NY, USA: ACM, 2003, pp. 66–80.

[50] F. Meyer auf de Heide, C. Schindelhauer, K. Volbert, and M. Grünewald, "Energy, congestion and dilation in radio networks," in *Proceedings of the Fourteenth Annual ACM Symposium on Parallel Algorithms and Architectures*, ser. SPAA '02. New York, NY, USA: ACM, 2002, pp. 230–237.

[51] P. von Rickenbach, S. Schmid, R. Wattenhofer, and A. Zollinger, "A robust interference model for wireless ad-hoc networks," in *Parallel and Distributed Processing Symposium, 2005. Proceedings. 19th IEEE International*, April 2005, pp. 8 pp.–. doi: 10.1109/IPDPS.2005.65

[52] M. Burkhart, P. von Rickenbach, R. Wattenhofer, and A. Zollinger, "Does topology control reduce interference?" in *Proceedings of the 5th ACM International Symposium on Mobile Ad Hoc Networking and Computing*, ser. MobiHoc '04. ACM, 2004, pp. 9–19.

[53] T. Johansson and L. Carr-Motyčková, "Reducing interference in ad hoc networks through topology control," in *Proceedings of the 2005 Joint Workshop on Foundations of Mobile Computing*, ser. DIALM-POMC '05. ACM, 2005, pp. 17–23.

[54] Y. chai Ko, M.-S. Alouini, and M. K. Simon, "Outage probability of diversity systems over generalized fading channels," *Communications, IEEE Transactions on*, vol. 48, no. 11, pp. 1783–1787, Nov 2000.

[55] C. Jang and J. H. Lee, "Outage probability analysis for asynchronous cognitive radio networks," in *Proc. 2014 Inf. Theory Appl. Workshop, San Diego, CA*, feb 2014.

[56] ——, "Outage probability of asynchronous cognitive dual-hop networks," in *Proc. ITC-CSCC 2013, Yeosu, Korea*, July 2013.

[57] M. Hellebrandt and R. Mathar, "Cumulated interference power and bit-error-rates in mobile packet radio," *Wirel. Netw.*, vol. 3, no. 3, pp. 169–172, Aug. 1997.

[58] S. Panichpapiboon, G. Ferrari, and O. Tonguz, "Optimal transmit power in wireless sensor networks," *Mobile Computing, IEEE Transactions on*, vol. 5, no. 10, pp. 1432 –1447, oct. 2006.

[59] J. Cheng and N. Beaulieu, "Accurate ds-cdma bit-error probability calculation in rayleigh fading," *Wireless Communications, IEEE Transactions on*, vol. 1, no. 1, pp. 3–15, Jan 2002.

[60] G. Ferrari and O. Tonguz, "Performance of ad hoc wireless networks with aloha and pr-csma mac protocol," in *Global Telecommunications Conference, 2003. GLOBECOM '03. IEEE*, vol. 5, Dec 2003, pp. 2824–2829 vol.5.

[61] M. R. McKay, A. Zanella, I. B. Collings, and M. Chiani, "Optimum combining of rician-faded signals: Analysis in the presence of interference and noise," in *Communications, 2007. ICC'07. IEEE International Conference on*. IEEE, 2007, pp. 1096–1101.

[62] M. Mckay, A. Zanella, I. Collings, and M. Chiani, "Error probability and sinr analysis of optimum combining in rician fading," *Communications, IEEE Transactions on*, vol. 57, no. 3, pp. 676 –687, march 2009.

[63] A. Lavric, V. Popa, I. Finis, A. Gaitan, and A. Petrariu, "Packet error rate analysis of ieee 802.15.4 under 802.11g and bluetooth interferences," in *Communications (COMM), 2012 9th International Conference on*, 2012, pp. 259–262. doi: 10.1109/ICComm.2012.6262616

[64] M. Chiani, "Performance of bpsk and gmsk with multiple cochannel interferers," in *Personal, Indoor and Mobile Radio Communications, 1996. PIMRC'96., Seventh IEEE International Symposium on*, vol. 3, oct 1996, pp. 833 –837 vol.3. doi: 10.1109/PIMRC.1996.568398

[65] K. Hamdi, "Interference analysis in unslotted packet radio networks employing bpsk modulation," in *Personal, Indoor and Mobile Radio Communications, 2000. PIMRC 2000. The 11th IEEE International Symposium on*, vol. 2, 2000, pp. 1155 –1159 vol.2. doi: 10.1109/PIMRC.2000.881601

[66] ——, "Exact probability of error of bpsk communication links subjected to asynchronous interference in rayleigh fading environment," *Communications, IEEE Transactions on*, vol. 50, no. 10, pp. 1577 – 1579, oct 2002.

[67] A. Giorgetti and M. Chiani, "Influence of fading on the gaussian approximation for bpsk and qpsk with asynchronous cochannel interference," *Wireless Communications, IEEE Transactions on*, vol. 4, no. 2, pp. 384–389, 2005.

[68] K. Hamdi, L. Pap, and E. Alsusa, "Accurate evaluation of packet error probabilities considering bit-to-bit error dependence," in *Global Telecommunications Conference, 2005. GLOBECOM '05. IEEE*, vol. 5, dec. 2005, pp. 5 pp. –2504. doi: 10.1109/GLOCOM.2005.1578212

[69] M. Chiani, "Analytical distribution of linearly modulated cochannel interferers," *Communications, IEEE Transactions on*, vol. 45, no. 1, pp. 73 –79, jan 1997.

[70] K. Sivanesan and N. Beaulieu, "Exact ber analyses of nakagami/nakagami cci bpsk and nakagami/rayleigh cci qpsk systems in slow fading," *Communications Letters, IEEE*, vol. 8, no. 1, pp. 45–47, Jan 2004.

[71] S. R. Saunders, S. Carlaw, A. Giustina, R. R. Bhat, V. S. Rao, and R. Siegberg, *FEMTOCELLS OPPORTUNITIES AND CHALLENGES FOR BUSINESS AND TECHNOLOGY*. U.K.: John Wiley and Sons, 2009.

[72] J. Zhang and G. de la Roche, *Femtocells: Technologies and Deployment*. Wiley, 2010.

[73] G. Gonzalez, M. Garcia-Lozano, S. BequE, M. A. Lema, and D. Lee, "Adapting fractional frequency reuse to realistic ofdma cellular networks," in *Wireless and Mobile Networking Conference (WMNC), 2013 6th Joint IFIP*. IEEE, 2013, pp. 1–8.

[74] R. Ghaffar and R. Knopp, "Fractional frequency reuse and interference suppression for ofdma networks," in *Modeling and Optimization in Mobile, Ad Hoc and Wireless Networks (WiOpt), 2010 Proceedings of the 8th International Symposium on*, 2010, pp. 273–277.

[75] I. Guvenc, M.-R. Jeong, F. Watanabe, and H. Inamura, "A hybrid frequency assignment for femtocells and coverage area analysis for co-channel operation," *Communications Letters, IEEE*, vol. 12, no. 12, pp. 880–882, December 2008.

[76] 3GPP TS 22.220 v. 9.0.0, March 2009.

[77] G. de la Roche, A. Valcarce, D. Lopez-Perez, and J. Zhang, "Access control mechanisms for femtocells," *Communications Magazine, IEEE*, vol. 48, no. 1, pp. 33–39, January 2010.

[78] A. Khandekar, N. Bhushan, J. Tingfang, and V. Vanghi, "Lte-advanced: heterogeneous networks," in *Wireless Conference (EW), 2010 European*. IEEE, 2010, pp. 978–982.

[79] A. Damnjanovic, J. Montojo, Y. Wei, T. Ji, T. Luo, M. Vajapeyam, T. Yoo, O. Song, and D. Malladi, "A survey on 3gpp heterogeneous networks," *Wireless Communications, IEEE*, vol. 18, no. 3, pp. 10–21, June 2011.

[80] A. Barbieri, P. Gaal, S. Geirhofer, T. Ji, D. Malladi, Y. Wei, and F. Xue, "Coordinated downlink multi-point communications in heterogeneous cellular networks," in *Information Theory and Applications Workshop (ITA), 2012*, Feb 2012, pp. 7–16.

[81] V. Chandrasekhar, J. Andrews, T. Muharemovict, Z. Shen, and A. Gatherer, "Power control in two-tier femtocell networks," *Wireless Communications, IEEE Transactions on*, vol. 8, no. 8, pp. 4316–4328, August 2009.

[82] H. S. Jo, J.-G. Yook, C. Mun, and J. Moon, "A self-organized uplink power control for cross-tier interference management in femtocell networks," in *Military Communications Conference, 2008. MILCOM 2008. IEEE*, Nov 2008, pp. 1–6.

[83] D. Choi, P. Monajemi, S. Kang, and J. Villasenor, "Dealing with loud neighbors: The benefits and tradeoffs of adaptive femtocell access," in *Global Telecommunications Conference, 2008. IEEE GLOBECOM 2008. IEEE*, Nov 2008, pp. 1–5.

[84] V. Chandrasekhar and J. Andrews, "Spectrum allocation in tiered cellular networks," *Communications, IEEE Transactions on*, vol. 57, no. 10, pp. 3059–3068, October 2009.

[85] J. Y. Lee, S. J. Bae, Y. M. Kwon, and M. Y. Chung, "Interference analysis for femtocell deployment in ofdma systems based on fractional frequency reuse," *Communications Letters, IEEE*, vol. 15, no. 4, pp. 425–427, 2011.

[86] W. S. Jeon, J. Kim, and D. G. Jeong, "Downlink radio resource partitioning with fractional frequency reuse in femtocell networks," *Vehicular Technology, IEEE Transactions on*, vol. 63, no. 1, pp. 308–321, Jan 2014.

[87] S.-E. Elayoubi, O. Ben Haddada, and B. Fourestie, "Performance evaluation of frequency planning schemes in ofdma-based networks," *Wireless Communications, IEEE Transactions on*, vol. 7, no. 5, pp. 1623–1633, 2008.

[88] A. Salati, M. Nasiri-kenari, and P. Sadeghi, "Distributed subband, rate and power allocation in ofdma based two-tier femtocell networks using fractional frequency reuse," in *Wireless Communications and Networking Conference (WCNC), 2012 IEEE*, April 2012, pp. 2626–2630.

[89] W. Li, W. Zheng, W. Xiangming, and T. Su, "Dynamic clustering based sub-band allocation in dense femtocell environments," in *Vehicular Technology Conference (VTC Spring), 2012 IEEE 75th*, May 2012, pp. 1–5.

[90] L. Li, C. Xu, and M. Tao, "Resource allocation in open access ofdma femtocell networks," *Wireless Communications Letters, IEEE*, vol. 1, no. 6, pp. 625–628, December 2012.

[91] P. Tarasak, T. Quek, and F. Chin, "Closed access ofdma femtocells under timing misalignment," in *Global Telecommunications Conference (GLOBECOM 2010), 2010 IEEE*, 2010, pp. 1–5. doi: 10.1109/GLOCOM.2010.5683959

[92] H. Huang, G. Hu, F. Yu, and Z. Zhang, "Energy-aware interference-sensitive geographic routing in wireless sensor networks," *Communications, IET*, vol. 5, no. 18, pp. 2692 –2702, 16 2011.

[93] H. Li and P. Mitchell, "Full interference model in wireless sensor network simulation," in *Wireless Communication Systems, 2009. ISWCS 2009. 6th International Symposium on*, sept. 2009, pp. 647 –651. doi: 10.1109/ISWCS.2009.5285349

[94] C.-K. Toh, V. Vassiliou, G. Guichal, and C.-H. Shih, "March: a medium access control protocol for multihop wireless ad hoc networks," in *MILCOM 2000. 21st Century Military Communications Conference Proceedings*, vol. 1, 2000, pp. 512 –516 vol.1. doi: 10.1109/MILCOM.2000.905007

[95] W. Ye, J. Heidemann, and D. Estrin, "An energy-efficient mac protocol for wireless sensor networks," in *INFOCOM 2002. Twenty-First Annual Joint Conference of the IEEE Computer and Communications Societies. Proceedings. IEEE*, vol. 3, 2002, pp. 1567 – 1576 vol.3. doi: 10.1109/INFCOM.2002.1019408

[96] P. Harley, "Short distance attenuation measurements at 900 mhz and 1.8 ghz using low antenna heights for microcells," *Selected Areas in Communications, IEEE Journal on*, vol. 7, no. 1, pp. 5 –11, jan 1989.

[97] C. Comaniciu and H. Poor, "On the capacity of mobile ad hoc networks with delay constraints," *Wireless Communications, IEEE Transactions on*, vol. 5, no. 8, pp. 2061 –2071, aug. 2006.

[98] L. Ong and M. Motani, "On the capacity of the single source multiple relay single destination mesh network," *Ad Hoc Networks*, vol. 5, no. 6, pp. 786 – 800, 2007.

[99] R. Hekmat and P. Van Mieghem, "Degree distribution and hopcount in wireless ad-hoc networks," in *Networks, 2003. ICON2003. The 11th IEEE International Conference on*, sept.-1 oct. 2003, pp. 603 – 609. doi: 10.1109/ICON.2003.1266257

[100] A. Safak, "Statistical analysis of the power sum of multiple correlated log-normal components," *Vehicular Technology, IEEE Transactions on*, vol. 42, no. 1, pp. 58 –61, feb 1993.

[101] C.-L. Ho, "Calculating the mean and variance of power sums with two log-normal components," *Vehicular Technology, IEEE Transactions on*, vol. 44, no. 4, pp. 756 –762, nov 1995.

[102] S. Schwartz and Y. Yeh, "On the distribution function and moments of power sums with lognormal components," *Bell Syst. Tech. J.*, vol. 61, pp. 1441 – 1462, Sept 1982.

[103] L. Fenton, "The sum of log-normal probability distributions in scatter transmission systems," *Communications Systems, IRE Transactions on*, vol. 8, no. 1, pp. 57 –67, march 1960.

[104] A. Papoulis, *Probability, Random Variables and stochastic process*, 3rd ed. New York: McGraw - Hills, 1991.

[105] A. Jeffrey and H. Dai, *Handbook of Mathematical Formulas And Integrals*, 4th ed. New York: Elsevier, 2008.

[106] D. Tse and P. Viswanath, *Fundamental of Wireless Communication*, 1st ed. New York: Cambridge University Press, 2005.

[107] R. Prasad and M. Ruggieri, *Technology Trends in Wireless Communications*. USA: Universal Personal Communications, 2003.

[108] J. H. Kim and J. K. Lee, "Capture effects of wireless csma/ca protocols in rayleigh and shadow fading channels," *Vehicular Technology, IEEE Transactions on*, vol. 48, no. 4, pp. 1277–1286, Jul 1999.

[109] J.-P. Linnartz, "Exact analysis of the outage probability in multiple-user mobile radio," *Communications, IEEE Transactions on*, vol. 40, no. 1, pp. 20–23, Jan 1992.

[110] R. Prasad and J. Arnbak, "Effects of rayleigh fading on packet radio channels with shadowing," in *TENCON '89. Fourth IEEE Region 10 International Conference*, Nov 1989, pp. 546–548.

[111] M. Hanif, N. Beaulieu, and D. Young, "Two useful bounds related to weighted sums of rayleigh random variables with applications to interference systems," *Communications, IEEE Transactions on*, vol. 60, no. 7, pp. 1788 –1792, july 2012.

[112] S. Panichpapiboon, G. Ferrari, and O. K. Tonguz, "Connectivity of ad hoc wireless networks: an alternative to graph-theoretic approaches," *Wireless Networks*, vol. 16, no. 3, pp. 793–811, 2010.

[113] G. Wang, D. Yue, and B. Feng, "System performance analysis of mrc with unequal power co-channel interference over nakagami fading channel," in *Wireless, Mobile and Multimedia Networks, 2006 IET International Conference on*, 2006, pp. 1–4.

[114] J. Arnbak and W. van Blitterswijk, "Capacity of slotted aloha in rayleigh-fading channels," *Selected Areas in Communications, IEEE Journal on*, vol. 5, no. 2, pp. 261 – 269, feb 1987.

[115] F. Mhiri, K. Sethom, and R. Bouallegue, "A survey on interference management techniques in femtocell self-organizing networks," *Journal of Network and Computer Applications*, vol. 36, no. 1, pp. 58–65, 2013.

[116] R. Ghaffar and R. Knopp, "Fractional frequency reuse and interference suppression for ofdma networks," in *Modeling and Optimization in Mobile, Ad Hoc and Wireless Networks (WiOpt), 2010 Proceedings of the 8th International Symposium on*, May 2010, pp. 273–277.

[117] A. Hosseinzadeh-Salati and M. Nasiri-Kenari, "Aggregate interference modelling and static resource allocation in closed and open access femtocells," *Communications, IET*, vol. 8, no. 7, pp. 1007–1016, May 2014.

[118] Y. Zhou and N. Zein, "Simulation study of fractional frequency reuse for mobile wimax," in *Vehicular Technology Conference, 2008. VTC Spring 2008. IEEE*, 2008, pp. 2592–2595. doi: 10.1109/VETECS.2008.569

[119] Y.-Y. Li, M. Macuha, E. Sousa, T. Sato, and M. Nanri, "Cognitive interference management in 3g femtocells," in *Personal, Indoor and Mobile Radio Communications, 2009 IEEE 20th International Symposium on*, 2009, pp. 1118–1122. doi: 10.1109/PIMRC.2009.5450030

[120] A. Adhikary, V. Ntranos, and G. Caire, "Cognitive femtocells: Breaking the spatial reuse barrier of cellular systems," in *Information Theory and Applications Workshop (ITA), 2011*, 2011, pp. 1–10. doi: 10.1109/ITA.2011.5743563

[121] R. Giuliano, C. Monti, and P. Loreti, "Wimax fractional frequency reuse for rural environments," *Wireless Communications, IEEE*, vol. 15, no. 3, pp. 60–65, June 2008.

[122] A. K. Dinnis and J. Thompson, "The effects of including wraparound when simulating cellular wireless systems with relaying," in *Vehicular Technology Conference, 2007. VTC2007-Spring. IEEE 65th*, 2007, pp. 914–918. doi: 10.1109/VETECS.2007.197

[123] A. Spanos, *Probability Theory and Statistical Inference: Econometric Modeling with Observational Data*. UK: Cambridge University Press, 1999.

[124] S. Amari and R. Misra, "Closed-form expressions for distribution of sum of exponential random variables," *Reliability, IEEE Transactions on*, vol. 46, no. 4, pp. 519–522, Dec 1997.